SECTION EDITOR: W. RICHARD GREEN, MD

Silicone Oil Egressing Through an Inferiorly Implanted Ahmed Valve

Silicone oil use as an adjunct to complicated vitreoretinal surgery is becoming more frequent. Refractory glaucoma in these patients is common. Isolated reports have mentioned the possibility of silicone oil migrating and/or obstructing the tube in the anterior chamber of Molteno implants (IOP, Costa Mesa, Calif).[1,2] This report describes a case of intraocular silicone oil egressing through an Ahmed implant (New World Medical, Rancho Cucamonga, Calif), impairing the functioning of the tube and requiring replacement of the implant plus oil removal. We present photographic documentation of the oil progressing through the tube and histopathologic analysis of the orbital tissue surrounding the extruded silicone oil.

Report of a Case. A 69-year-old white man lost his left eye to trauma at age 12 years. In September 2000, blunt trauma resulted in a lacerated eyebrow, scleral rupture, uveal prolapse, extrusion of his crystalline lens, retinal detachment, and suprachoroidal hemorrhage in his right eye. A limited anterior chamber washout was performed at the time of the primary repair. Ten days later, he underwent pars plana vitrectomy, silicone oil injection, and a scleral buckle. A pars plana vitrectomy revision with endolaser, membrane stripping, and silicone oil reinjection were performed 1 month later for a recurrent retinal detachment.

In January 2001, glaucoma surgery was needed to control elevated intraocular pressure (IOP). The eye was aphakic and had total traumatic aniridia. An Ahmed valve was implanted inferonasally in an attempt to avoid the silicone oil bubble (**Figure 1** and **Figure 2**). The patient's IOP responded well initially but rose subsequently to 30 mm Hg. A bubble of silicone oil was wrapping the tip of the tube (**Figure 3**). Silicone oil could be seen migrating through the Ahmed tube (**Figure 4** and **Figure 5**) and the bleb over the implant progressively enlarged and appeared encapsulated during the next few months. A glistening material was noted in cystic spaces overlying the Ahmed implant under the conjunctiva. An inferior ectropion that progressed gradually was also

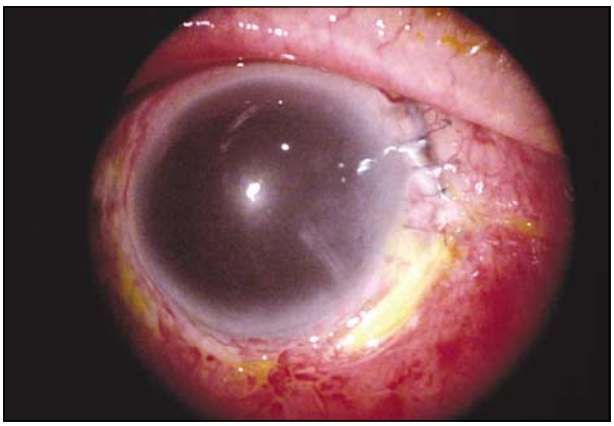

Figure 1. Slitlamp photograph showing the Ahmed tube inferonasally short after implantation. Notice total traumatic aniridia and superotemporal paralimbal scleral wound with interrupted sutures.

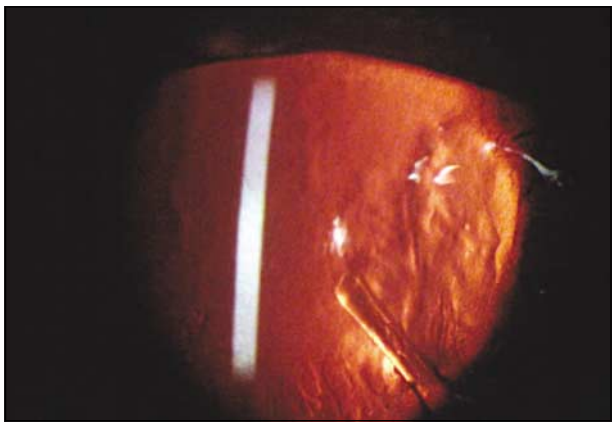

Figure 2. Retroillumination photograph showing a patent Ahmed tube.

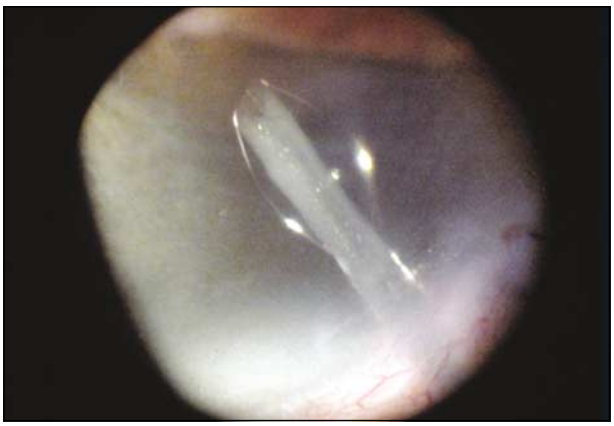

Figure 3. Slitlamp photograph showing "candle wax" appearance of the silicone oil wrapped around the tip of the Ahmed tube.

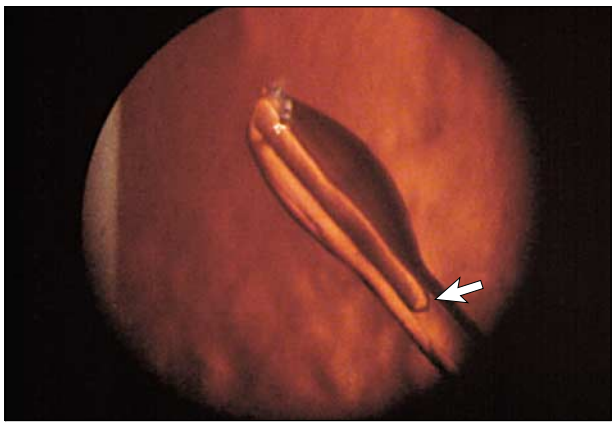

Figure 4. Retroillumination photograph showing a level of silicone oil (arrow) inside the Ahmed tube.

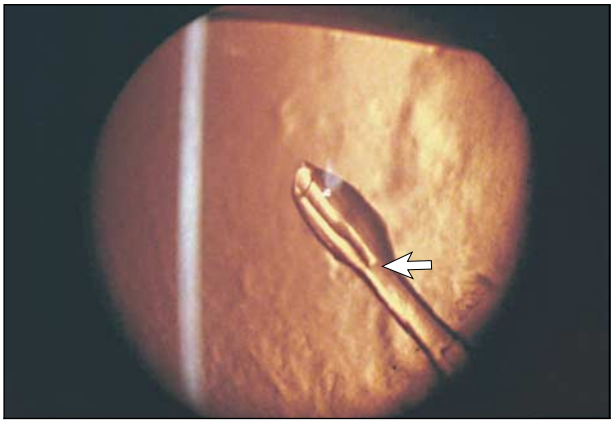

Figure 5. Retroillumination photograph taken on a different day shows a different level of silicone oil (arrow) inside the Ahmed tube.

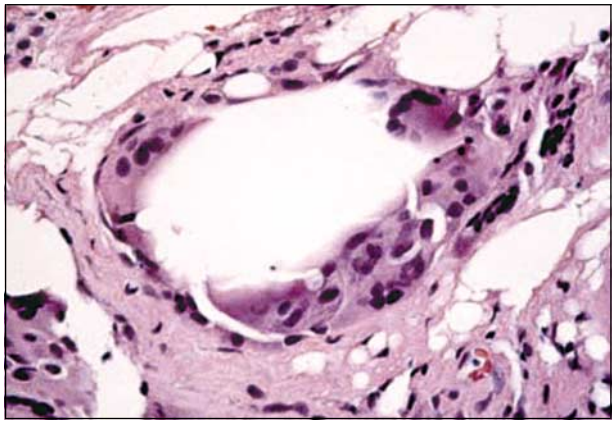

Figure 6. Histopathologic examination of orbital tissue excised during removal of valve shows empty vacuoles consistent with silicone oil and larger deposit of oil surrounded by epithelioid histiocytes and foreign body giant cells (hematoxylin-eosin, original magnification ×200).

noted. The volume of the silicone bubble in the vitreous cavity decreased from an estimated 85% fill to an estimated 50% fill. Ectropion repair was necessary in June 2001.

Owing to persistently elevated IOP measurements, transcorneal removal of the silicone oil combined with replacement of the Ahmed implant was performed. Multiple silicone oil–filled conjunctival cysts were found surrounding the Ahmed plate. A tissue sample was taken inferotemporally from a thick capsule surrounding the Ahmed implant. Histopathologic analysis of the tissue surrounding the plate demonstrated fibroconnective tissue with numerous small vacuoles. Surrounding this tissue were numerous foreign-body giant cells and histiocytes (**Figure 6**).

Comment. To our knowledge, this is one of the first documented cases of silicone oil exiting the eye through an Ahmed implant. Review of the literature yielded 2 previous reports, both involving Molteno implants in aphakic patients[1,2] and 1 recent report involving an Ahmed implant.[3] Minckler[4] describes adhesion of the silicone oil to the anterior chamber portion of the drainage tube, resembling candle wax, without lumen obstruction. He recommends placing the tube in an inferior location to minimize the chance of oil-tube obstruction. In our case, the inferior location of the tube did not prevent the migration of the silicone oil through the Ahmed implant. The inflammatory reaction observed in the periocular tissues, apparently caused by the silicone oil, has been documented before.[1,2] This contrasts with no observed clinical reaction in intraocular tissues, although histopathologically foreign-body granulomas have been documented in intraocular tissues.

The silicone oil did impair the drainage of aqueous through the implant as evidenced by the elevated IOPs. Encapsulation of the bleb might also have contributed to the obstruction of the implant. The photographs (Figures 3 and 4), showing oil at different levels of the tube, demonstrate the progression of the silicone oil through the tube of the Ahmed implant. We believe that aphakia with total aniridia resulted in an anatomic situation (a truly unicameral eye) that favored the anterior migration of the silicone oil when the patient inadvertently assumed a supine position. This was probably favored by the well-known physical attraction of the silicone tube toward the silicone oil. Once an oil bubble made it to the entrance of the tube, the combined effect of capillary action with elevated IOP may have facilitated the migration of the oil to the subconjunctival space. The patient's IOP has been under control since replacement of the Ahmed implant and removal of the silicone oil. His last corrected visual acuity was 20/50 OD.

It seems that a "unicameral" eye with silicone oil, particularly with significant iris defects, is a poor candidate for successful IOP control with a seton in a 1-stage procedure. In our case, the inferior location of the implant did not prevent silicone oil movement out of the eye with secondary impairment of IOP control. Silicone oil removal needs to be considered prior to implantation of a seton in such cases. If silicone oil removal is not an option, diode laser cyclophotocoagulation is another alternative for IOP control.

Jose Morales, MD
Michel Shami, MD
Geert Craenen, MD
Thom F. Wentlandt, CRA
Lubbock, Tex

Corresponding author: Jose Morales, MD, Texas Tech University Health Sciences Center, Department of Ophthalmology and Visual Sciences, 3601 Fourth St, STOP 7217, Lubbock, TX 79430-7217 (e-mail: jose.morales@ttuhsc.edu).

1. Hyung SM. Min JP. Subconjunctival silicone oil drainage through the Molteno implant. *Kor J Ophthalmol.* 1998;12:73-75.
2. Senn P, Buchi ER, Daicher B, Schipper I. Bubbles in the bleb: troubles in the bleb? molteno implant and intraocular tamponade with silicone oil in an aphakic patient. *Ophthalmic Surg.* 1991; 26:379-382.
3. Nazemi PP, Chong LP, Varma R, Burnstine MA. Migration of intraocular silicone oil into the subconjunctival space and orbit through an Ahmed glaucoma valve. *Am J Ophthalmol.* 2001;132: 929-931.
4. Minckler D. Silicone oil glaucoma: cases in controversy. *J Glaucoma.* 2001;10:51-54.

Lens Dislocation in Marfan Syndrome: Potential Role of Matrix Metalloproteinases in Fibrillin Degradation

Marfan syndrome is an autosomal dominant disorder with pleiotropic manifestations that involve the ocular, cardiovascular, and skeletal systems. Marfan syndrome remains primarily a clinical diagnosis with a frequency of 2 to 3 individuals per 10000. Patients with this disorder may have a variety of ocular complaints, most commonly, subluxation of the lens, which occurs in more than 60% of patients.[1] Several studies have identified the *FBN1* fibrillin gene located on chromosome 15 as defective in this syndrome.[2]

Matrix metalloproteinases (MMPs) are proteolytic enzymes important in physiological and pathological remodeling, the activity of which is stringently controlled by a family of natural antagonists, the tissue inhibitors of MMPs (TIMPs). Both MMPs and TIMPs are present in the aqueous humor in normal and inflamed eyes,[3] resulting in their interaction with the lens zonules.

We describe a patient with Marfan syndrome lens subluxation associated with positive MMP expression and no TIMP immunoreactivity within the lens zonule. To our knowledge, this is the first report of MMP staining associated with lens zonules in a patient with Marfan syndrome. Understanding the role these proteases play may lead to the development of novel therapies to reduce the progressive nature of Marfan syndrome lens subluxation.

Report of a Case. A 43-year-old woman diagnosed with Marfan syndrome in 1980 was referred to the Ophthalmology Clinic at Prince of Wales Hospital (Sydney, Australia) in 1999. The patient described deterioration of her vision occurring throughout a 9-month period. Her medical history included mitral valvuloplasty in 1997, paroxysmal atrial fibrillation, scoliosis, and hypertension controlled with 50 mg of atenolol administered daily. The patient's grandfather, cousin, and mother also had Marfan syndrome. Her mother developed bilateral lens subluxation and glaucoma. A systemic examination revealed arachnodactyly and a high arched palate. Ophthalmologic examination revealed a best-corrected visual acuity of 20/220 OD and 20/120 OS. The right eye had an intraocular pressure of 19 mm Hg; and the left eye, 18 mm Hg. Goldmann visual fields were normal. Slitlamp examination confirmed bilateral superonasal lens subluxation that was worse in the right eye than in the left (**Figure**). The fundus was normal, with cup-disc ratios of 0.2 for each eye. The ocular examination was otherwise normal. Because of the advanced zonular dialysis, bilateral intracapsular lens extractions were performed with a cryoprobe and without α-chymotrypsin. The lenses were so mobile that they were expressed from the eye by injecting viscoelastic inferiorly and posteriorly (in front of the vitreous face), and scleral fixated posterior chamber intraocular lenses were sutured into position with standard techniques.

Both crystalline lenses from the patient were immediately formalin fixed. Lenses from corneal donor postmortem eyes (n=8) were enucleated 4 to 8 hours after the time of death and were also immediately fixed in formalin. The 10 lenses were paraffin embedded, and 4-µm sections were placed on slides coated with 3-amino propyltriethoxy triethoxysilane (TES) for immunohistochemical analysis using a panel of monoclonal antibodies directed against MMP-1, MMP-2, MMP-3, MMP-9, and TIMP-1, TIMP-2, and TIMP-3. Matrix metalloproteinases seem to be stable for as long as 24 hours in harvested ocular tissue.[4]

Sections were deparaffinized in xylene, rehydrated through decreasing graded ethanol, followed by two 5-minute washes in 0.05mM of Tris-buffered saline (10× stock Tris-buffered saline contains 0.25M Tris base, 0.25M Tris-hydrochloride, and 8.5% sodium chloride, with a pH of 7.6). Antigen retrieval method was not necessary. Endogenous peroxidase was quenched with 3% hydrogen peroxide/methanol for 5 minutes, and then washed in Tris-buffered saline. The sections were incubated with a 1:5 dilution of preimmune serum from the secondary host species. Tissue sections were incubated with 1:100 goat primary polyclonal antifibrillin antibody (Santa Cruz Biotechnology, Santa Cruz, Calif) and 1:100 mouse primary monoclonal anti-MMP–1, anti-MMP–2, anti-MMP–3, anti-MMP–9 (ICN Pharmaceuticals, Costa Mesa, Calif), 1:100 TIMP-1, TIMP-2 (ICN), and 1:100 TIMP-3 (Calbiochem, San Diego, Calif) overnight at 4°C. The sections were then washed in 0.05M Tris-buffered saline (pH, 7.6) before the addition of a biotinylated rabbit antigoat secondary antibody (for fibrillin) and biotinylated goat anti-mouse secondary antibody (for MMPs and TIMPs). The antibodies directed against human antigens display no cross-reactivity and are all IG_1 subclass antibodies. Sections were again washed, incubated for 1 hour with horseradish peroxidase–conjugated streptavidin (Dako, Carpinteria, Calif), and the immunoreactivity was revealed by adding 3-amino-9-ethylcarbazole (Sigma, Sydney, Australia). Control reactions were included, incubating sections with an isotype antibody and omitting the primary antibody or adding preimmune serum. Sections were counterstained with hematoxylin, viewed by light microscopy, and photographed with Spot Version 2.2 for Windows (Diagnostic Instruments Inc, Sterling Heights, Mich).

Macroscopically, both the Marfan lenses appeared normal. Microscopically, both Marfan lens capsules appeared thickened, with the germinative zone smaller than that of the normal lens. Immunohistochemical analysis revealed specific localization of MMP-1 (Figure, A), MMP-3 (Figure, C), and MMP-9 (Figure, D) in the Marfan lens zonules, with relatively little or no MMP-2 (data not shown) and no TIMP-1, TIMP-2, or TIMP-3 immunoreactivity (Figure, L-N). In contrast, no MMP-1 or MMP-3 staining was observed in the zonules of normal lenses (Figure, E and F) but TIMP-1, TIMP-2, and TIMP-3 were detected in the zonules of the normal lenses (Figure, H-J). On all lens sections, more than 1 zonular site

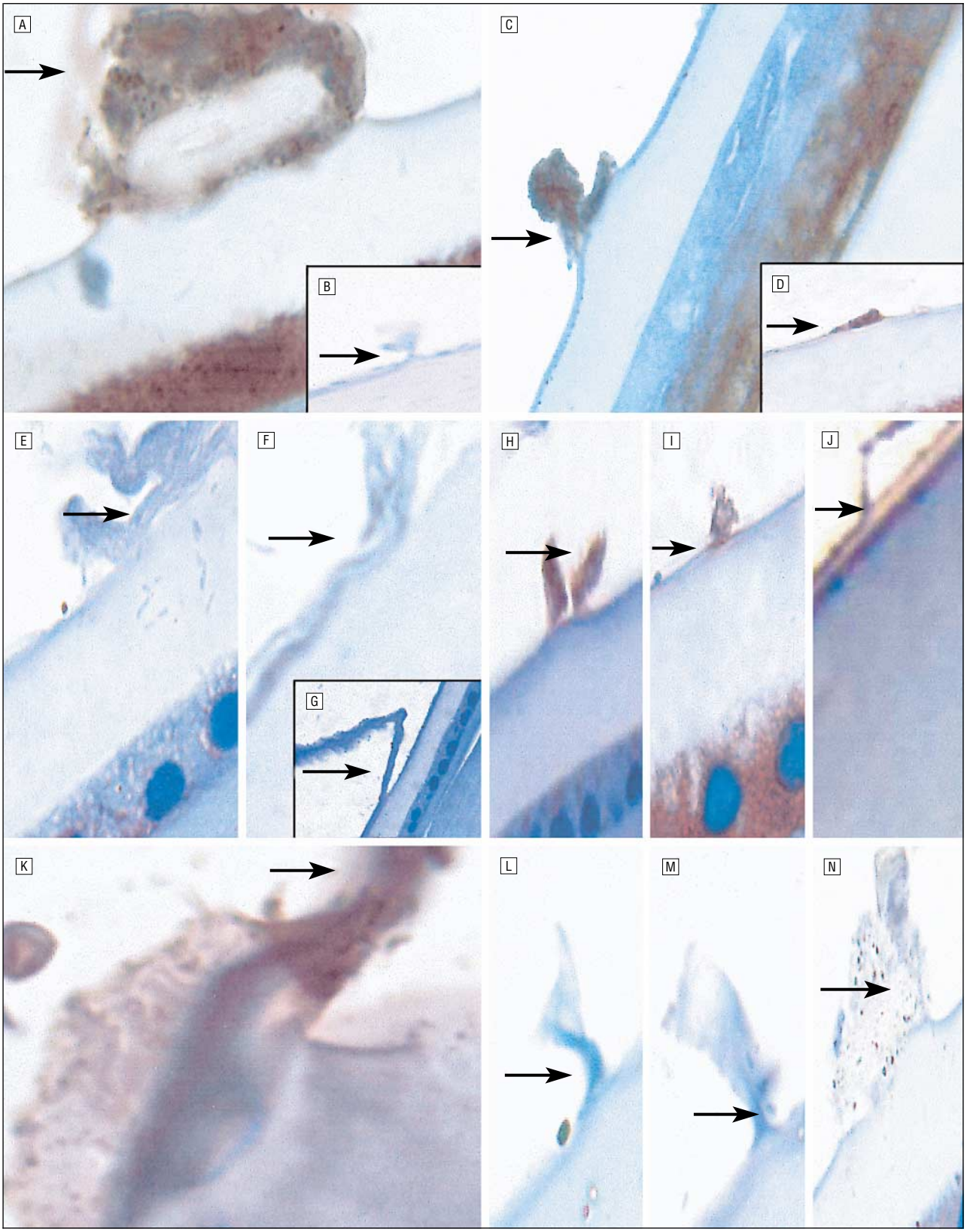

Immunohistochemistry of normal and Marfan syndrome lenses revealed positive immunoreactivity for matrix metalloproteinases (MMP)–1, MMP-3, and MMP-9 (A, C, and D) on Marfan lens zonules, with no tissue inhibitors of MMPs (TIMP)–1, TIMP-2, or TIMP-3 (L-N) immunoreactivity. The arrows indicate the zonule. When the primary antibody was omitted, no immunoreactivity could be detected in the Marfan lens (B) or the normal lens (G). In contrast, no MMP-1 (E) or MMP-3 (F) staining was observed in the zonule of normal lenses, but TIMP-1, TIMP-2, and TIMP-3 (H-J) was detected (original magnification ×125). A fibrillin monoclonal antibody was included to identify the lens zonule in the Marfan lens (K) (original magnification ×250).

contained MMP or TIMP activity. A fibrillin monoclonal antibody was included to identify the lens zonule in the Marfan lens (Figure, K). Sections incubated with isotype control antibodies demonstrated no reactivity in either the Marfan (Figure, B) or normal lenses (Figure, G).

Comment. This is the first case report, to our knowledge, describing zonule-associated staining of MMPs in Marfan syndrome lens subluxation. We hypothesize that the product of the defective *FBN1* gene in Marfan syndrome is more prone to degradation by MMPs as compared with normal fibrillin. It is also possible that dysregulation of MMPs and TIMPs results in the progressive destruction of lens zonules and subsequent lens subluxation.

The lens zonule consists of a series of fibers composed of microfibrils that are 8 to 12 nm in diameter. The fibrils consist largely of a cysteine-rich microfibrillar component of the fibrillin elastin system. In other tissues, fibrillin provides a template for elastin deposition.[5] Genetic linkage between the fibrillin gene and the Marfan phenotype has been established, and the gene mapped to the same chromosomal position as the disease locus.[6] Understanding of the functions of the fibrillin-containing microfibrils is still incomplete, and correspondingly, no comprehensive theory of the pathogenesis of Marfan syndrome has emerged to date.

Both fibrillin molecules and fibrillin-rich microfibrils are susceptible to degradation by serine proteases, and amino acid substitutions (as found in Marfan syndrome) change the fragmentation patterns.[7] Fibrillin degradation products generated by MMP activity provide conclusive evidence that these enzymes cause specific changes to assembled microfibrils.[7] As most of the mutations in fibrillin-1 are found within epidermal growth factor–like motifs and are predicted to disrupt calcium binding, it has been suggested that these mutations render fibrillin-1 more susceptible to proteolytic cleavage.[8] Previous investigators have demonstrated structural modifications in fibrillin-rich microfibrils during aging of human ciliary zonules.[9] These age-related changes may account for the increased incidence of ocular disease observed in older patients with Marfan syndrome.

If the proposed hypothesis regarding the role of MMPs in Marfan-associated lens subluxation is correct, then the development of matrix metalloproteinase inhibitors may be of potential therapeutic value in the treatment of progressive lens subluxation and other complications of Marfan syndrome.[10]

Nitin H. Sachdev, MBChB
Nick Di Girolamo, PhD
Peter J. McCluskey, FRACO, FRACS
Angela V. Jennings, MBBS
Roger McGuinness, FRACO, FRACS
Denis Wakefield, FRCPA
Minas T. Coroneo, FRACO, FRACS, MD
Sydney, Australia

The authors have no proprietary interests in any of the products or companies mentioned in this article.

Corresponding author: Minas T. Coroneo, FRACO, FRACS, MD, Department of Ophthalmology, Prince of Wales Hospital, University of New South Wales, Randwick, Sydney, Australia (e-mail: m.coroneo @unsw.edu.au).

1. Maumenee IH. The eye in the Marfan syndrome. *Trans Am Ophthalmol Soc*. 1981;79:684-733.
2. Sarfarazi M, Tsipouras P, Del Mastro R, et al. A linkage map of 10 loci flanking the Marfan syndrome locus on 15q: results of an International Consortium study. *J Med Genet*. 1992; 29:75-80.
3. Di Girolamo N, Verma MJ, McCluskey PJ, et al. Increased matrix metalloproteinases in the aqueous humor of patients and experimental animals with uveitis. *Curr Eye Res*. 1996;15: 1060-1068.
4. Kamei M, Hollyfield JG. TIMP-3 in Bruch's membrane: changes during aging and in age-related macular degeneration. *Invest Ophthalmol Vis Sci*. 1999;40:2367-2375.
5. Robinson PN, Godfrey M. The molecular genetics of Marfan syndrome and related microfibrillopathies. *J Med Genet*. 2000;37:9-25.
6. Maslen CL, Glanville RW. The molecular basis of Marfan syndrome. *DNA Cell Biol*. 1993; 12:561-572.
7. Ashworth JL, Murphy G, Rock MJ, et al. Fibrillin degradation by matrix metalloproteinases: implications for connective tissue remodelling. *Biochem J*. 1999;340(pt 1):171-181.
8. Reinhardt DP, Ono RN, Sakai LY. Calcium stabilizes fibrillin-1 against proteolytic degradation. *J Biol Chem*. 1997;272:1231-1236.
9. Hanssen E, Franc S, Garrone R. Fibrillin-rich microfibrils: structural modifications during ageing in normal human zonule. *J Submicrosc Cytol Pathol*. 1998;30:365-369.
10. Boyle JR, McDermott E, Crowther M, et al. Doxycycline inhibits elastin degradation and reduces metalloproteinase activity in a model of aneurysmal disease. *J Vasc Surg*. 1998;27:354-361.

Histopathological Changes Following Photodynamic Therapy in Human Eyes

To identify histopathological changes induced by photodynamic therapy (PDT), 2 human eyes received PDT using verteporfin 1 week before enucleation for large malignant melanoma. Two light doses, 50 and 100 J/cm^2, were applied to unaffected chorioretinal areas and the optic disc using the standard procedure recommended for patients with age-related macular degeneration (ARMD).

Characteristic hypofluorescence following PDT was documented angiographically 1 week later. The enucleated globes were processed for standard light and electron microscopy.

The PDT-treated areas revealed uniform occlusion of the choriocapillary layer. Vascular endothelial cells were swollen, detached from the basement membrane, and showed rupture and fragmentation to complete degeneration. Capillary lumina were filled with cell debris, fibrin, and thrombocytes. Remaining intact endothelial cells seemed to generate novel vascular channels by recanalization of the obliterated lumen. The overlying retinal pigment epithelium (RPE) showed no significant alteration. Photoreceptors and optic nerve exposed to verteporfin and 100 J/cm^2 of light were structurally unremarkable.

Photodynamic therapy induces at a dosage used clinically in the treatment of ARMD a selective destruction of vascular endothelial cells within the choriocapillary layer. Recanalization of the physiological choroid is observed as early as 1 week following PDT. Neural structures, photoreceptors, and RPE remained intact.

The therapeutic benefit of PDT using verteporfin in the treatment of predominantly classic choroidal neovascularization (CNV) has introduced a novel strategy into the management of exudative ARMD. A prospective, randomized, double-masked clinical trial[1] demonstrated that verteporfin PDT reduces the risk of severe visual loss, preserves contrast sensitivity, and may even im-

prove visual acuity in a subgroup of patients. The results of the Treatment of Age-Related Macular Degeneration With Photodynamic Therapy Study Group provided the rationale for the recent approval of the method by the health authorities. Meanwhile, thousands of patients with neovascular ARMD received PDT following the guidelines of the Treatment of Age-Related Macular Degeneration With Photodynamic Therapy trial.

The characteristic features observed in patients undergoing PDT seem to be well characterized: clinical exudation of serous fluid, blood, and lipids is halted; and retinal edema resolves.[2] By angiography, cessation of leakage from classic CNV is documented,[3] which usually recurs and requires repeated treatment applications to achieve long-term absence of exudative activity.[4] However, despite thorough clinical and angiographic evaluation, the knowledge of the photodynamic effects on human ocular structures is limited and mostly based on observation of the secondary phenomena induced by PDT than a revelation of primary mechanisms.

A histopathological evaluation from animal studies has detected changes within the physiological choroid and the RPE and laser-induced CNV.[5,6] In patients, PDT-associated findings seem to be contradictory: retinal function is maintained or improved, while homogeneous choroidal hypofluorescence seen angiographically may be consistent with choroidal nonperfusion.[7]

To identify the structural effects induced by PDT, intact retinal, RPE, and choroidal layers of human eyes that were scheduled for enucleation were exposed to verteporfin therapy. Light and electron microscopic evaluation was performed, with particular emphasis on photoreceptor, RPE, and choriocapillary alterations.

Patients and Methods. The study protocol was compiled using the Declaration of Helsinki, and approved by the institutional ethics committee. Informed consent was obtained from each patient, specifically indicating the scientific nature of the photodynamic procedure with no therapeutic relevance in respect to the underlying malignancy.

Patients. Two eyes of 2 patients received PDT. Both organs were scheduled for enucleation because of malignant melanoma of the uvea too large for conservative management. Tumors were located anteriorly so that the posterior pole was accessible ophthalmoscopically and for photosensibilization. Patient 1 was a 72-year-old man who had a large tumor reaching the ciliary body in the supranasal quadrant, with a tumor base of 35 mm radially and 36 mm at the equator and a height of 12 mm. Patient 2, an 85-year-old woman, was seen with a prominent tumor mass located superiorly at the 12-o'clock position. The tumor size was 24 mm vertically and 23 mm horizontally, and it reached 12 mm in height. Localized exudative retinal detachments were associated with the malignancies. Both eyes showed mild age-related degenerative changes of the macular area with some scattered drusen.

Photodynamic Therapy. Photodynamic therapy using verteporfin was applied 7 days before the scheduled enucleation. Retinochoroidal areas without involvement by the tumor or the accompanying serous detachment were selected by ophthalmoscopy and angiography. The procedure was performed according to the approved treatment recommendations for patients with ARMD. Verteporfin was administered intravenously by infusion of 6 mg of drug per square meter of body surface area over 10 minutes. Photoactivation was started 5 minutes after the completion of the administration, with light at a wavelength of 689 nm delivered by a diode laser and a laser-link slit-lamp (Coherent Inc, Palo Alto, Calif). Two areas per eye were treated subsequently, a first one with a total light dose of 50 J/cm^2 followed by a second one with application of a light dose of 100 J/cm^2, both at an irradiance constant of 600 mW/cm^2. Exposures are shown schematically in **Figure 1** A and B. In eye 1, the 100-J/cm^2 spot had a diameter of 5000 µm and was positioned superiorly to the optic nerve, including the disc (Figure 1A). The 50-J/cm^2 spot with a diameter of 3000 µm was directed onto the retina below the optic nerve head. In eye 2, the area receiving 50 J/cm^2 was located central to the temporal inferior vascular arcade, while the 100-J/cm^2 spot was placed below the vascular arcade (Figure 1B).

Clinical Documentation. Visual acuity was examined before, 1 day after, and 1 week after PDT, and was unchanged, with 20/400 in patient 1 and 20/100 in patient 2. No additional field defects were described by the patients. Ophthalmoscopically, no change in the clinical appearance of the retina, the RPE, or the choroid was noted; treated areas were indistinguishable from the surrounding retina. Fluorescein angiography (FA) and indocyanine green angiography (ICGA) were performed to localize and quantify the vascular effects before and 1 week after PDT.

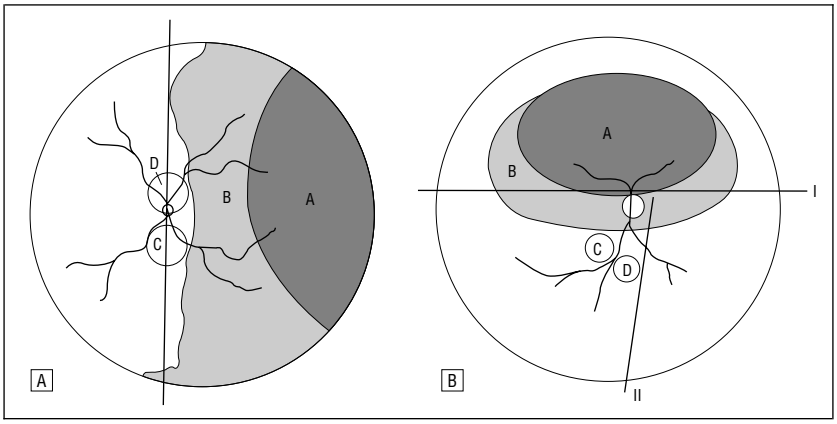

Figure 1. Eye 1 (A) and eye 2 (B) showing the location of the tumor (A), the associated retinal detachment (B), and the laser spots exposed to 50 J/cm^2 (C) and 100 J/cm^2 (D) of light. Treatment spots were placed on areas without involvement of the tumor or detachment. Globe 1 was bisected vertically through the laser spots. Globe 2 was first bisected horizontally, followed by a vertical section adjacent to laser spot D.

Histopathological Evaluation. Immediately after surgical removal, the globes were fixed in a combination of 4% paraformaldehyde and 1% glutaraldehyde in a 0.1M phosphate buffer for 5 days and processed for routine paraffin embedding. A macroscopic examination and transillumination were performed, and the tumor dimensions were measured. Angiographic images were used to locate PDT-treated areas before dissection of the posterior pole. Globe 1 was bisected along the laser spots and processed for light and transmission electron microscopy. Globe 2 was reembedded from paraffin into epoxy resin for electron microscopy.

For light microscopy, 8-µm-thick paraffin sections were stained with hematoxylin-eosin and periodic acid–Schiff. For electron microscopy, tissue specimens containing the choroid and retina of the PDT-treated areas and untreated control areas were postfixed in 2% buffered osmium tetroxide and embedded in epoxy resin (Epon) according to the standard method. Semithin sections (1 µm) were stained with toluidine blue O; ultrathin sections (0.2 µm) were stained with uranyl acetate–lead citrate and examined with an electron microscope (LEO 906E; Zeiss, Oberkochen, Germany).

Results. *Angiography*. By FA, light-exposed areas revealed homogeneous hypofluorescence characteristic for PDT, with no difference in fluorescence intensity between the 2 different light doses. Indocyanine green angiography provided a more detailed image of the choroidal vasculature and the extent of vaso-occlusion. In patient 1, the image taken 1 week after PDT was partially obscured by the bullous serous detachment associated with the tumor located in the nasal periphery. However, a round hypofluorescent area with a sharp demarcation during early ICGA was documented in the 50- and the 100-J/cm^2 spot (**Figure 2**A). Retinal perfusion was not compromised with the higher-dose treatment, including the optic nerve. In late ICGA, hypofluorescence was still present, with scattered areas of leakage from larger choroidal vessels (Figure 2B). No pathologic exudation was seen from the vasculature of the optic nerve.

In patient 2, the central spot that illuminated with 50 J/cm^2 of light showed absence of the choriocapillary background fluorescence but maintenance of the vascular pattern of medium- and larger-caliber vessels without any reduction in fluorescent demarcation of these vessels during early ICGA (Figure 2C). The area that had received 100 J/cm^2 of light demonstrated choriocapillary loss combined with a marked decrease in the overall density of choroidal vessels. Late-phase ICGA showed the persistence of hypofluorescence in both areas, with exudation from the margins and the remaining patent vessels within the lesions (Figure 2D).

Light Microscopy. In globe 1, PDT-treated areas were identified superior and inferior to the optic nerve. Complete occlusion of the choriocapillary vascular lumina was noted in these areas. Vascular channels were blocked by swollen endothelial cells that enclosed red blood cells and fibrin. In some segments, the lumen was completely obliterated, while others demonstrated a residual small opening. Occlusion was seen throughout the dimensions of the treatment spot and reached a depth of approximately 150 µm below the Bruch membrane. Small deeper vessels were also clogged, while larger choroidal vessels showed open lumina with intact, not deformed, erythrocytes. Areas adjacent to the photosensitized spot exhibited a regular choroidal vascular structure with open capillary channels and larger choroidal vessels.

Intact choroidal sections taken from control areas appeared less condensed and thicker than PDT-treated sections. Retinal pigment epithelial cells were attached and showed only minor age-related changes, with vacuolization in the treatment zone and in control areas. Photoreceptors were artificially detached in some areas, but did not show any structural changes. Capillaries of the optic nerve head were open and lined with intact endothelial cells. Neural structures, such as ganglion cells and axons, showed no evidence of structural alteration, histologic signs related to ischemia, or infiltration of the nerve.

Choroidal vascular changes seen in globe 2 were identical to findings observed in globe 1. An occlusion of capillaries of the choroid was seen only in PDT-exposed areas (**Figure 3**A). Endothelial cells were swollen, detached from the basement membrane, and partially ruptured. Large-caliber vessels appeared to be regular and perfused. However, the RPE and the Bruch membrane were unchanged. Untreated areas showed vascular channels with intact endothelial lining (Figure 3B).

Electron Microscopy. Photodynamic therapy–treated areas showed occlusion and degenerative changes of the choriocapillaris (**Figures 4**A, B, and D, **5**A-F, and **6**B-D) compared with untreated areas with wide open lumina, several rows of loosely organized erythrocytes, and intact fenestrated endothelia of the capillaries (Figures 4C and E, 5G, and 6A). Vascular alterations in the treated areas comprised swelling of endothelial cells and a few pericytes leading to narrowed, compressed, capillary lumina with densely packed deformed erythrocytes immured between the endothelial lining (Figures 4D and 6B). Alterations further comprised endothelial shrinkage, ruptures, fragmentations, and the detachment of cells from their basement membrane up to complete degeneration of the endothelial lining, leaving denuded vascular basement membranes (Figures 5A and B and 6C). Finally, complete occlusion of capillary lumina by fibrin, platelets, and cellular debris derived from endothelial cells, macrophages, and granulocytes was frequently observed (Figures 4A and B and 5C and D). Erythrocytes in the affected capillaries were often degenerative, appearing as ghost cells. Granulocytes accumulated in the lumina of affected capillaries and macrophages seemed to gather in the periphery of degenerated vessels. Extravasation of erythrocytes and migration of inflammatory cells into the extracellular space could often be observed (Figure 5B). In case of advanced endothelial degeneration, the original vessel outline was occasionally delineated by erythrocyte configurations or by electron-dense blood-plasma accumulations (Figure 6C

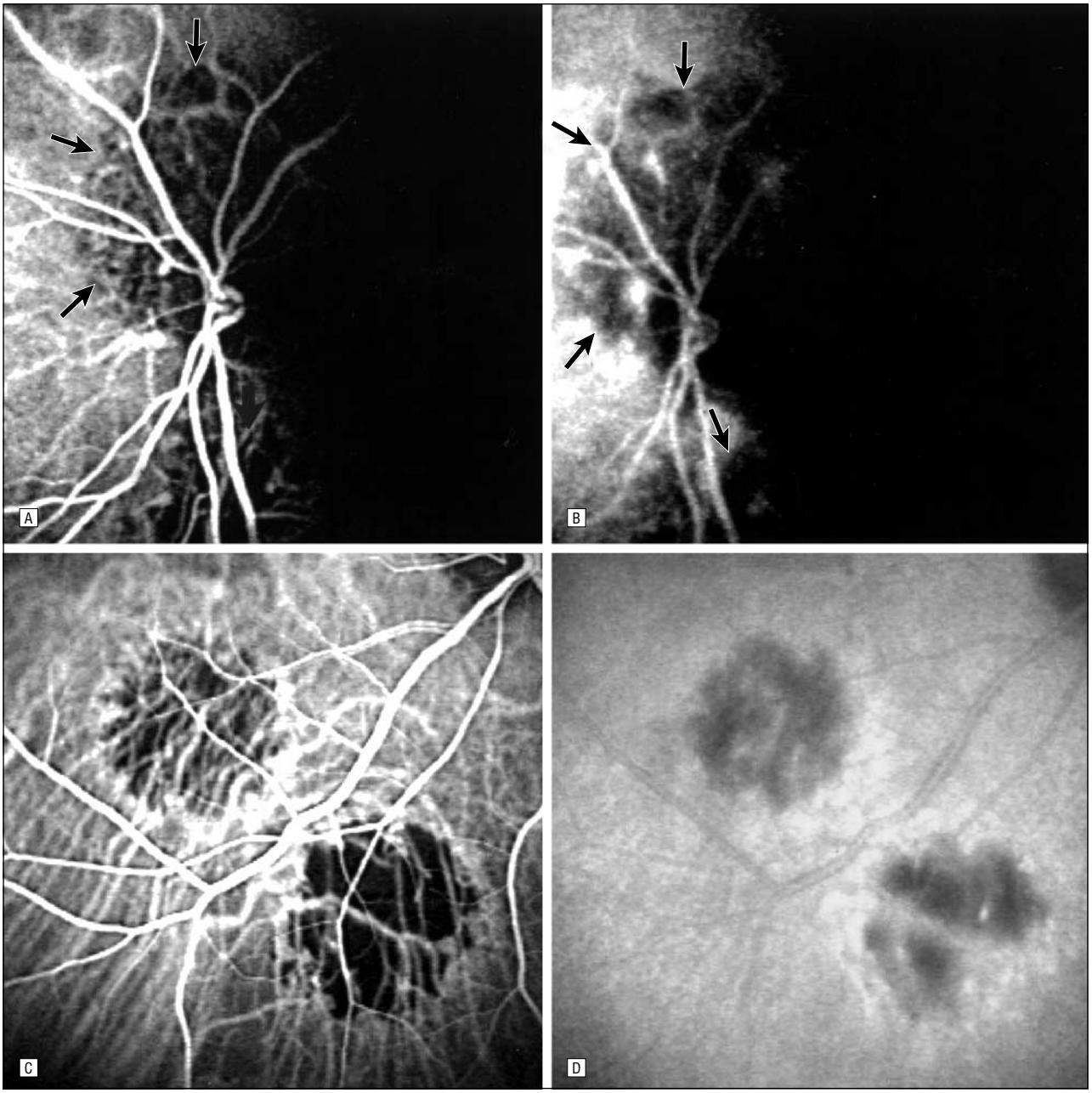

Figure 2. Eye 1. Early (A) and late (B) phases of indocyanine green angiography (ICGA), with demarcation of the 2 spots exposed to 100 J/cm^2 superiorly, including the optic nerve, and 50 J/cm^2 inferiorly. The increasing serous detachment originating from the tumor partially covers the nasal aspect of the image. The arrows indicate the borders of choroidal hypofluorescence. Eye 2. Early (C) and late (D) phases of ICGA, with hypofluorescent areas treated with 50 J/cm^2 of light central and 100 J/cm^2 of light peripheral to the vascular arcade.

and D). Remaining intact endothelial cells appeared to reorganize into smaller capillaries within the degenerated original vessel outline, forming a novel vascular lumen (Figure 6D).

Degenerative changes of deeper (outer) choroidal vessels with extravasation of red blood cells was observed in the 100-J/cm^2, but not in the 50-J/cm^2, treated spots, where those vessels appeared essentially normal with wide open lumina (Figures 4A and B and 5E). Capillaries of the optic nerve head consistently appeared intact after exposure to 100 J/cm^2 of light.

The RPE appeared mostly intact over large areas and showed focal vacuolar degeneration in the 100-J/cm^2 treated areas only; partly, bullous separation of individual pigment epithelial cells from the Bruch membrane could be observed. The overlying photoreceptor layer appeared intact in all PDT-treated areas (Figure 5F). Figures 4A and D and 5C, D, and E show areas treated with 100 J/cm^2 and, therefore, represent rather extensive vacuolization of the RPE cytoplasm and separation from the Bruch membrane. Figure 6, depicting patient 2, is not quite representative because of reembedding from paraffin and a rather poor preservation of the ultrastructure. However, slight alterations of RPE cells, such as intracellular vacuolization indicative of intracellular edema, were also evident in the areas treated with 50 J/cm^2 (**Figure 7**). Retinal pigment

epithelial cells appeared otherwise normal with regard to their plasma membrane, cytoplasmic organelles, nuclei, and melanin granules.

The retinal capillaries appeared generally normal in areas treated with either 50 or 100 J/cm^2 (**Figure 8**).

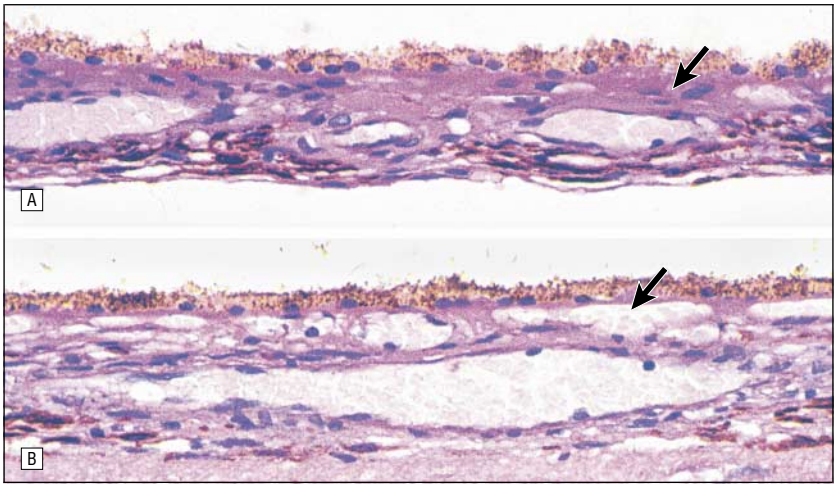

Figure 3. Light microscopy of a choroidal section of eye 2 following photodynamic therapy. A, The superficial portion of the choroid appears condensed, with obliterated vascular lumina within the capillary layer (arrow), while large vessels remain patent. B, Choriocapillary vessels and deeper vessels of an untreated area are open (arrow) and contain red blood cells (original magnification ×450).

Comment. Photodynamic treatments using verteporfin with the procedure recommended for patients with neovascular ARMD were performed in human eyes. The treatment effect was controlled by angiographic imaging, and the areas of interest were identified and subsequently evaluated by light and electron microscopic histologic features, with the aim to qualify structural changes induced by PDT.

The primary effect of PDT seems to be damage of the choriocapillary endothelium, as indicated by swelling, fragmentation, detachment from its basement membrane, and degeneration; however, recanalization of occluded choriocapillaries seems to occur within a short interval. Significant alterations of the RPE and the neural retina do not occur.

Vascular endothelial damage is the major hallmark of photodynamic tissue effects and results from the direct interaction of a singlet of oxygen with the lipids of endothelial cytoplasmic membranes.[8] Additional intracellular photo-oxidation causes a rearrangement of the cytoskeleton, with shrinkage of the endothelial cells and exposure of the basement membrane, an intensive thrombogenic stimulus.[9] Activated platelets release vasoactive mediators (eg, thromboxane, tumor necrosis factor α, and histamine).[8] Blood flow stasis is the result of endothelial swelling, erythrocyte sludging, platelet adhesion, vasoconstriction, and increased vascular permeability. The release of cytokines, such as interleukin 1β, interleukin 2, and tumor necrosis factor α, from attracted macrophages further facilitates vessel closure.[10] The mechanistic sequelae of these phototoxic effects were seen histologically (Figures 5 and 6): vascular endothelial membranes were discontinuous, and cells were fragmented. Cellular swelling and detachment from the basement membrane were common features. Clots consisted of densely packed red blood cells, thrombocytes, and fibrin. Macrophages were found, consistent with an inflammatory stimulus. None of the described mechanisms is selective for neovascular endothelial cells. Hence, intensive damage to physiological vascular structures should be expected.

In animal studies, the only source of histologic features to date, closure of choriocapillaris following verteporfin therapy, was proved by light and electron microscopy.[5,6] A direct dose-response relationship was found with capillary occlusion at lower doses, while higher light doses invariably led to alteration of larger choroidal vessels and RPE.[5] The photothrombotic efficacy of verteporfin clearly depends on the drug and light dose applied, with larger-caliber vessels occluded at an increasing dosage.[11] Accordingly, occlusive effects were also found in deeper layers and in vessels with larger lumina in areas exposed to 100 J/cm^2 of light in human eyes. Occlusive choroidal effects are not specific for verteporfin or liposomal preparations, but have also been described with various other compounds with hydrophilic or amphiphilic character, such as purlytin, lutetium texaphyrin, ATX-S10 (Na), and mono-L-aspartyl chlorin e_6.[12-15]

Intensive controversy was raised by the characteristic hypofluorescence seen regularly after PDT. Hypofluorescence is most pronounced in FA performed 1 week after PDT. Based on the homogeneity and the intensity of hypofluorescence in an angiographic modality using a low wavelength, like FA, masking of the underlying fluorescence was suspected (eg, by hemoglobin or an altered RPE).[16] The fact that hypofluorescence covers precisely the area of the treatment spot and resolves slowly during the following weeks suggests transient choroidal nonperfusion rather than masking—which was substantiated with correlation of angiographic and histopathological features. The consistency of histologic results and ICGA imaging is striking because by ICGA, choriocapillary shutdown was seen in the 50-J/cm^2 treated spot (Figure 3A) and disappearance of larger vessels occurred in the 100-J/cm^2 treated spot (which was supported by the respective extent of vascular obliteration in histopathological features). Indocyanine green angiography may, therefore, be recommended as a useful clinical tool for documentation of photodynamic vascular effects.[7,17,18]

How is obvious choriocapillary occlusion compatible with maintenance of visual function? Histologic features reveal structural integrity of overlying photoreceptors after an interval of hypothetical hypoxia for as long as 1 week. Microperimetry, a sensitive test of photoreceptor function, demonstrates improvement of retinal sensitivity within the treated CNV area in 80% of eyes at 4 weeks.[18] The oxygen supply provided by patent large vessels might guarantee

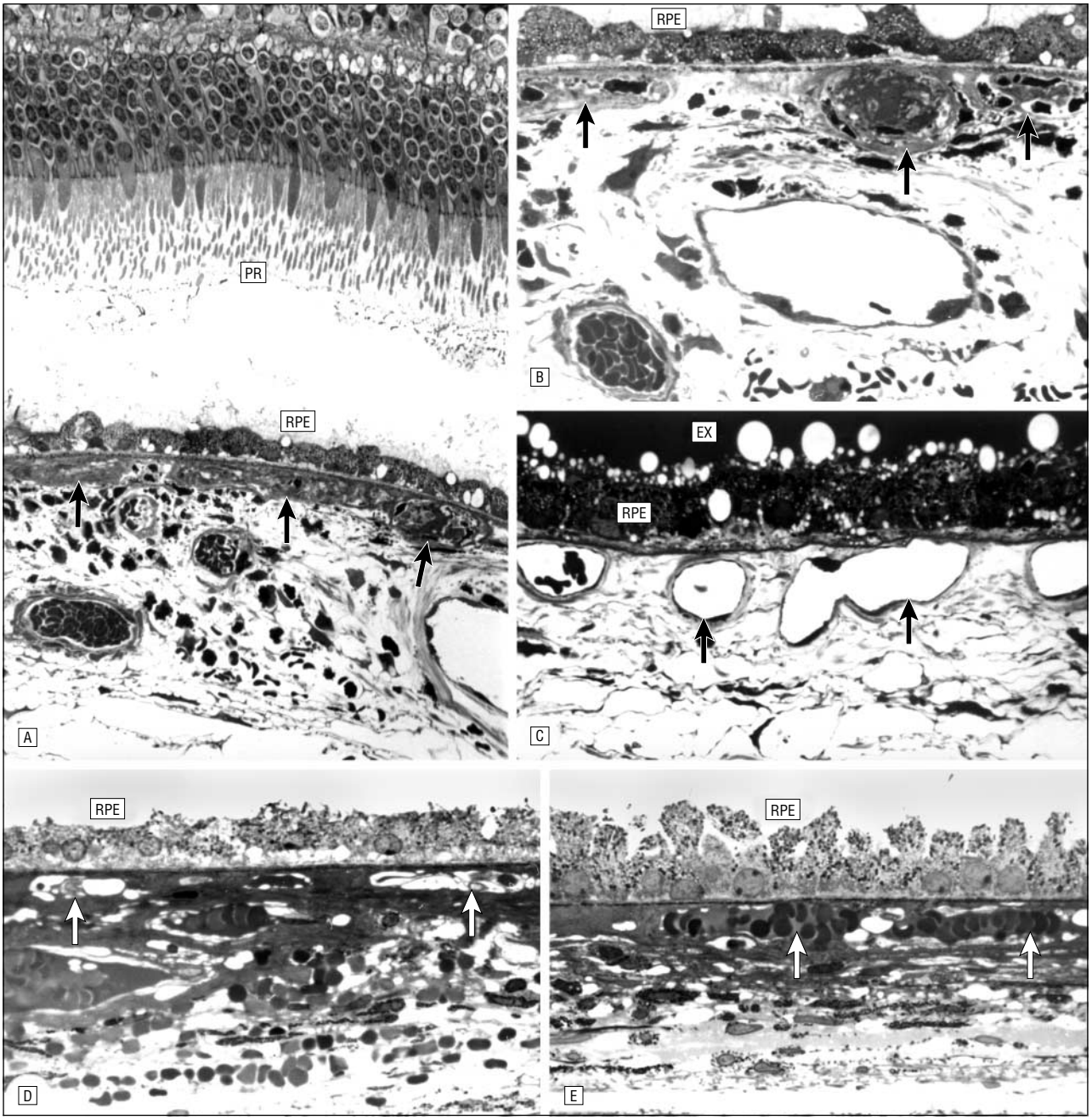

Figure 4. Light microscopic appearance (1-µm semithin sections) of the choroid and the retina of patients 1 (A-C) and 2 (D and E) (toluidine blue O). A, The retina and choroid in the area treated with 100-J/cm^2 spots, showing complete obstruction of the choriocapillaris (arrows) and a slightly vacuolated retinal pigment epithelium (RPE). The deeper choroidal vessels and the overlying photoreceptor layer (PR) appear normal (original magnification ×350). B, The choroid in the area treated with 50-J/cm^2 spots, showing occlusion of the choriocapillaris (arrows), open deeper vessels, and a rather normal RPE (original magnification ×620). There are minor changes in the RPE (ie, rounding up of the apices is the result of retinal detachment). C, The choroid in an untreated area showing choriocapillaries (arrows) with wide-open lumina and a normal-appearing RPE; retinal detachment and accumulation of subretinal exudate (EX) occurred secondary to tumor development (original magnification ×670). D, The choroid in the photodynamic therapy–treated area showing occlusion of the choriocapillaris (arrows) due to swelling of endothelial cells and open deeper vessels (original magnification ×630). E, The choroid in an untreated area with an intact choriocapillaris (arrows) and a normal-appearing RPE (original magnification ×630).

photoreceptor survival. A more convincing argument is the observation that progression of occlusion is extremely slow. Short-term follow-up by ICGA demonstrated that choroidal perfusion is not compromised at all for several hours after PDT. Choroidal darkening only occurs during the following days and reaches its maximal intensity after 3 days to 1 week.[19] Apparently, photoreceptors and RPE are better capable of tolerating a prolonged reduction in oxygen supply than an immediate choroidal thrombosis, which is usually associated with significant visual loss.[20,21] A relative reduction in photoreceptor function, however, defined as a transient visual disturbance, was reported by 18% of the PDT-treated patients in the Treatment of Age-Related Macular Degeneration With Photodynamic Therapy trial.[1] Although the progression of the disease was halted

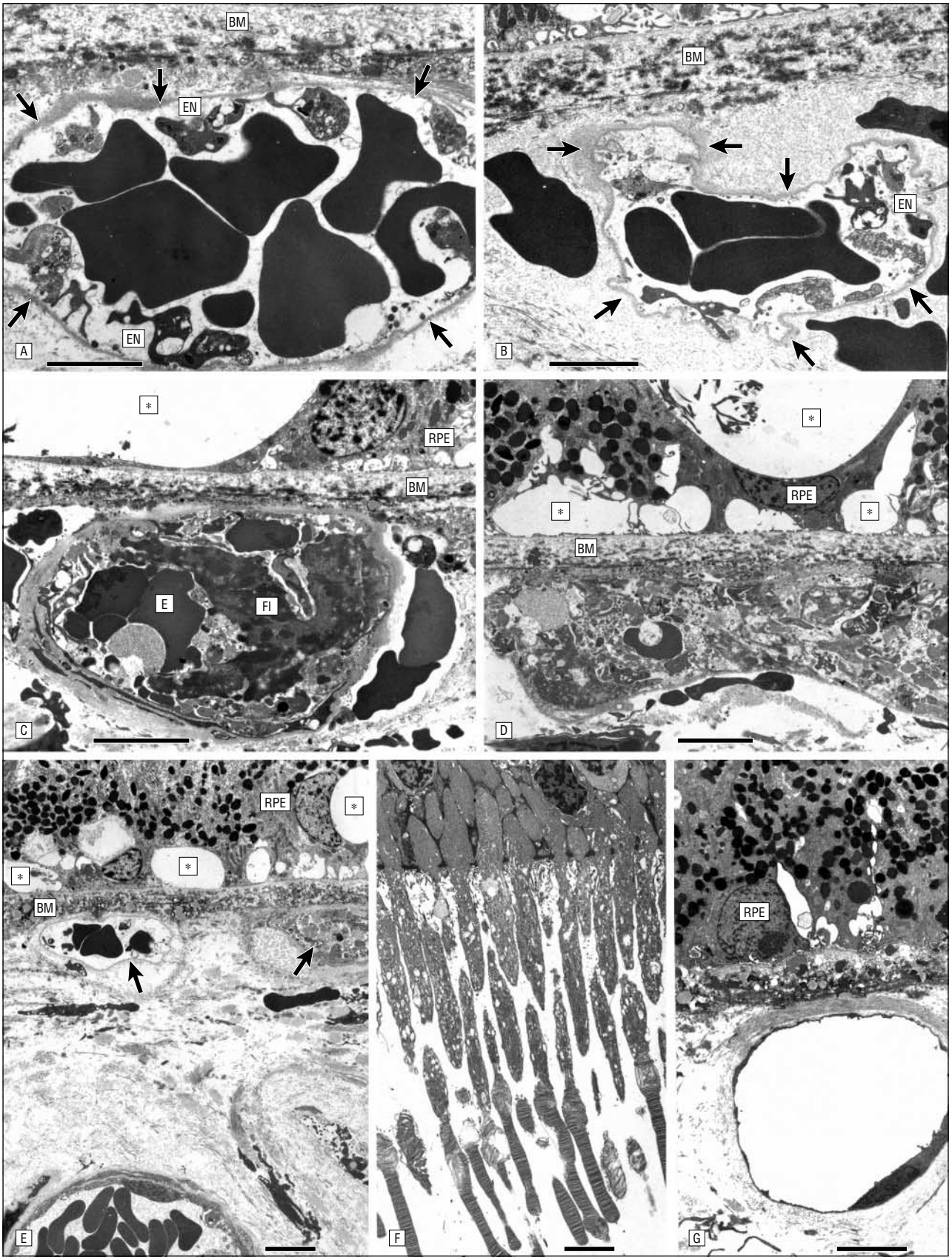

See legend on next page.

Figure 5. Electron microscopic appearance of the choroid and the retina of patient 1 in areas treated with 50 J/cm^2 (A and B) and 100 J/cm^2 (C-F) of light and in untreated areas (G). A, A choriocapillary showing rupture and fragmentation of endothelial cells (ENs) and detachment from their basement membrane (arrows); deformed erythrocytes fill the vessel lumen. B, A choriocapillary with advanced degeneration of ENs, leaving a denuded basement membrane (arrows) and extravasation of erythrocytes. C, A choriocapillary completely obstructed by cell debris, erythrocytes (E), and fibrin (FI); the asterisk indicates large vacuoles that are present in the overlying retinal pigment epithelium (RPE). D, Occlusion of the choriocapillaris and vacuolar degeneration (asterisks) of the RPE. E, The choroid, showing degenerative changes of the choriocapillaries (arrows), vacuolar changes of the RPE (asterisks), and intact deeper vessels. F, Intact photoreceptor cells overlying an area with occluded choriocapillaries. G, An intact choriocapillary and RPE in an adjacent untreated area. BM indicates Bruch membrane; bar, 3 µm (A and B) and 5 µm (C-G).

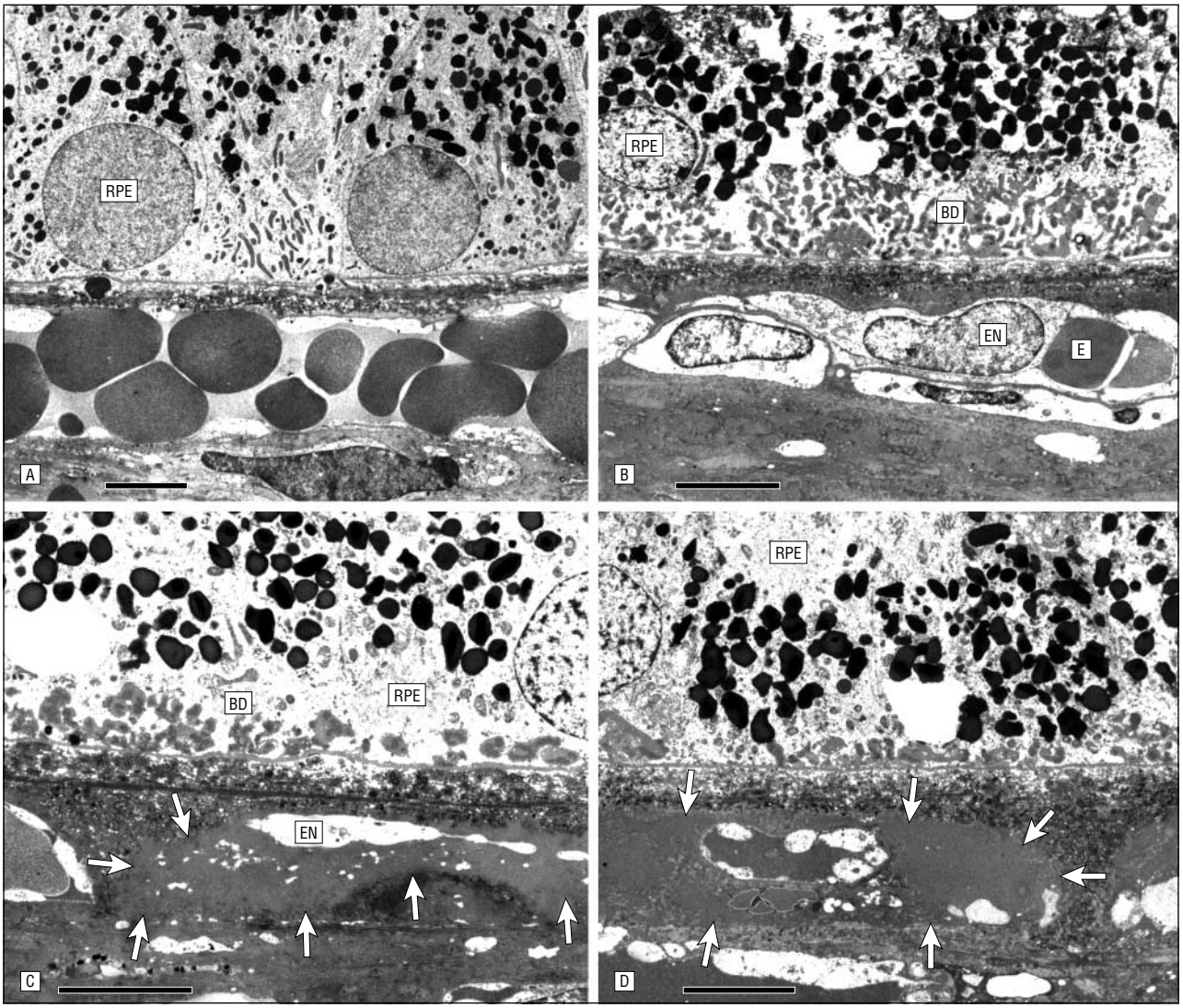

Figure 6. Electron microscopic appearance of the choriocapillaris and retinal pigment epithelium (RPE) of patient 2 in untreated areas (A) and photodynamic therapy–treated areas (B-D). The ultrastructural preservation is suboptimal due to reembedding from paraffin. A, A normal-appearing choriocapillary and RPE in an untreated central area. B, A choriocapillary with a compressed lumen and an immured erythrocyte (E) due to swelling of endothelial cells (ENs); the overlying RPE shows slight vacuolar degeneration. C, Extensive degeneration of vascular ENs. The arrows indicate the original capillary lumen. D, The remaining ENs appear to reorganize into smaller capillaries within the degenerated original capillary outline (arrows). BD indicates basal laminar deposits; bar, 5 µm (all parts).

successfully, patients lost a mean of 2 lines of visual acuity during follow-up, which might reflect a residual choriocapillary alteration.[1]

Recanalization was found in multiple areas of the primarily occluded choriocapillary. Slow progression of photothrombosis over 1 week in concordance with increasing recanalization during the same interval might be a competing mechanism and in summary reduce the extent of ischemia. Recanalization is illustrated histologically by the formation of novel lumina within previously occluded channels. Electron microscopy in experimental models showed duplication of vascular basement membranes indicative of recanalization.[22] An intraluminal reorganization would lead to a reduplication of the vascular wall, potentially with restoration of the vascular barrier. Recanalization processes might play an important role in the observed change in the biological features of the CNV complex as well. Cessation of leakage from classic CNV is the prominent angiographic feature in clinical PDT.[1-4] Typically, CNV nets are still delineated in early FA during follow-up, but become progressively silent with resolution of leakage activity. Histopathological features reveal a possible mechanism of barrier stabilization in those with treated CNV with recanalization. Persistent CNV without extravasation

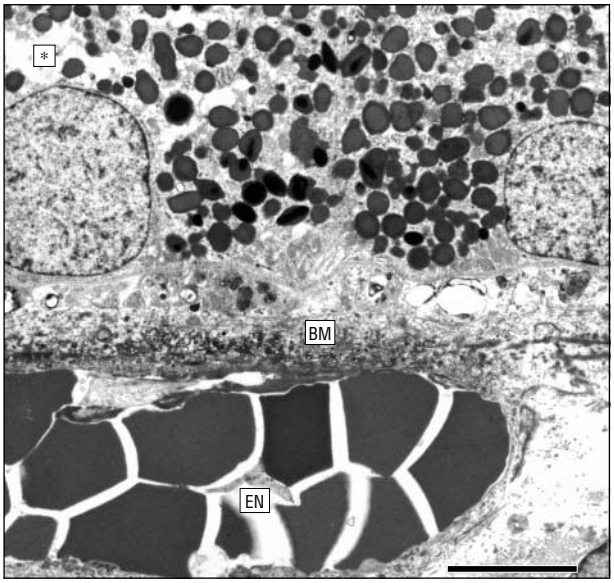

Figure 7. Electron microscopic appearance of the retinal pigment epithelium of patient 1 in the area treated with 50 J/cm^2 of light. The cells show slight intracellular vacuolization (asterisk), but appear rather normal and attached to the Bruch membrane (BM); the underlying choriocapillary shows rupture and fragmentation of its endothelial lining (EN). The bar indicates 5 µm.

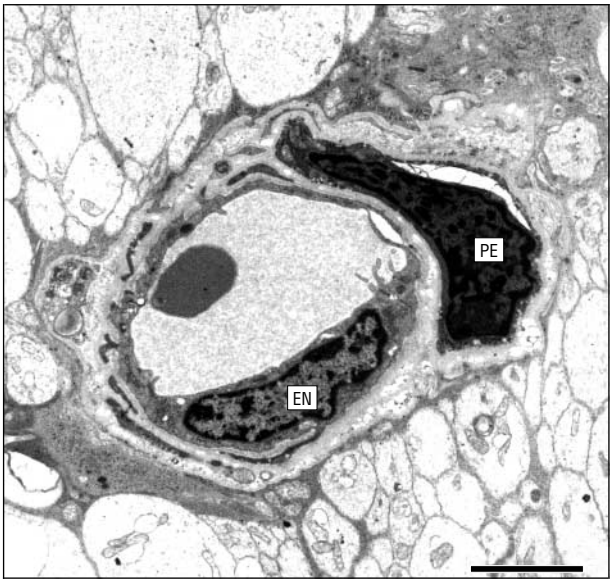

Figure 8. Electron microscopic appearance of a retinal capillary of patient 1 in the area treated with 50 J/cm^2 of light. The vascular endothelial cells (ENs) show no obvious alterations. PE indicates pericyte; bar, 3 µm.

would not further compromise retinal integrity. Such an involutional stabilization is the therapeutic rationale of various interventions, such as radiotherapy, antiangiogenesis, and transpupillary thermotherapy, which do not eradicate CNV but decrease the exudative activity.[23-25] Spontaneously regressed CNV histologically exhibits persistent neovascular channels, however, with lack of exudation due to a restored barrier function either due to RPE or endothelial reproliferation.[26]

Recanalization is most likely an important mechanism of CNV recurrence, particularly because recurrent "growth" and enlargement of CNV occurs at a faster rate than de novo occurrence of CNV.[4] Choroidal ischemia induced by PDT might stimulate growth factor expression (eg, vascular endothelial growth factor), which is recognized as a major stimulator of CNV.[27,28] Repair of choroidal damage might be a challenge in elderly eyes because choroidal density and integrity were compromised with age.[29] A combination therapy of PDT with antiangiogenic agents might, therefore, be promising in respect to CNV recurrence but problematic in respect to choroidal regeneration.

Although verteporfin PDT of CNV does not spare the physiological choroidal capillaries, retinal vessels and neural structures, including photoreceptors and the optic nerve, remained intact even if exposed to a light dose twice as high as conventionally used. Moderate RPE changes could be found. Increased vacuolization was documented, which was partially within normal age-related limits, at 50 J/cm^2 in our patients, who primarily had age-related macular changes. Whether this damage was a direct consequence of the PDT effect or developed secondarily due to choriocapillary occlusion for as long as 1 week is difficult to analyze. Determining the histologic features immediately or shortly after photosensitization is obviously not an option considering the risk of widespread phototoxic damage during the surgical procedure at a time of high sensitizer retention. Retinal pigment epithelial cells also demonstrate a high regenerative potential following structural damage.[30,31]

The histopathological findings of this study identify important mechanisms of PDT in human eyes. The extent of vaso-occlusion with concomitant thrombosis of a normal choriocapillaris is documented, as are active repair mechanisms. In future clinical applications of PDT, the application of a low light dose should be considered to allow for appropriate choroidal regeneration in between treatment intervals and to include choroidal perfusion as a factor for retreatment indication.

Ursula Schmidt-Erfurth, MD
Horst Laqua, MD
Luebeck, Germany
Ursula Schlötzer-Schrehard, MD
Arne Viestenz, MD
Gottfried O. H. Naumann, MD
Erlangen, Germany

The Wellman Laboratories of Photomedicine, Massachusetts General Hospital, Boston, and Dr Schmidt-Erfurth are holders of a patent on the use of verteporfin and have a proprietary interest under the guidelines of Harvard Medical School, Boston.

Corresponding author: Ursula Schmidt-Erfurth, MD, Department of Ophthalmology, University Eye Hospital Luebeck, Ratzeburger Allee 160, D-23538 Luebeck, Germany (e-mail: uschmidterfurth@ophtha.mu-luebeck.de).

1. Treatment of Age-Related Macular Degeneration With Photodynamic Therapy (TAP) Study Group. Photodynamic therapy of subfoveal choroidal neovascularization in age-related macular degeneration with verteporfin: one-year results of 2 randomized clinical trials—TAP report. *Arch Ophthalmol.* 1999;117:1329-1345.
2. Schmidt-Erfurth U, Miller J, Sickenberg M. Photodynamic therapy of subfoveal choroidal neovascularization: clinical and angiographic examples. *Graefes Arch Clin Exp Ophthalmol.* 1998; 236:365-374.
3. Miller JW, Schmidt-Erfurth U, Sickenberg M,

et al. Photodynamic therapy with verteporfin for choroidal neovascularization caused by age-related macular degeneration: results of a single treatment in a phase 1 and 2 study. *Arch Ophthalmol.* 1999;117:1161-1173.
4. Schmidt-Erfurth U, Miller JW, Sickenberg M, et al. Photodynamic therapy with verteporfin for choroidal neovascularization caused by age-related macular degeneration: results of retreatments in a phase 1 and 2 study. *Arch Ophthalmol.* 1999;117:1177-1187.
5. Schmidt-Erfurth U, Hasan T, Gragoudas E, Michaud N, Flotte TJ, Birngruber R. Vascular targeting in photodynamic occlusion of subretinal vessels. *Ophthalmology.* 1994;101:1953-1961.
6. Kramer M, Miller JW, Michaud N, et al. Lysosomal benzoporphyrin derivative verteporfin in photodynamic therapy: selective treatment of choroidal neovascularization in monkeys. *Ophthalmology.* 1996;103:427-438.
7. Schmidt-Erfurth U, Michels S, Hager A, Laqua H. ICG-angiographic analysis of the photodynamic mechanism in the photodynamic treatment of choroidal neovascularization. *Invest Ophthalmol Vis Sci.* 1998;39(suppl): S242.
8. Finger VH. Vascular effects of photodynamic therapy. *J Clin Laser Med Surg.* 1996;14:323-328.
9. Henderson BW, Dougherty TJ. How does photodynamic therapy work? *Photochem Photobiol.* 1992;55:145-157.
10. Gollnick SO, Liu X, Owczarczak B, Musser DA, Henderson BW. Altered expression of interleukin 6 and interleukin 10 as a result of photodynamic therapy in vivo. *Cancer Res.* 1997; 57:3904-3909.
11. Lange N, Ballini JP, Waguieres G, van den Bergh H. A new drug-screening procedure for photosensitizing agents used in photodynamic therapy for CNV. *Invest Ophthalmol Vis Sci.* 2001;42:38-46.
12. Obana A, Gohto Y, Kanas M, Nakajima S, Kaneda K, Miki T. Selective photodynamic effects of the new photosensitizer ATX-S10 (Na) on choroidal neovascularization in monkeys. *Arch Ophthalmol.* 2000;118:650-658.
13. Blumenkranz MS, Woodburn KW, Qing F, Verdooner S, Kessel D, Miller R. Lutetium texaphyrin (LU-Tex): a potential new agent for ocular fundus angiography and photodynamic therapy. *Am J Ophthalmol.* 2000;129: 353-362.
14. Mori K, Yoneya S, Ohta M, et al. Angiographic and histologic effects of fundus photodynamic therapy with a hydrophilic sensitizer (mono-L-aspartyl chlorin e_6). *Ophthalmology.* 1999;106:1384-1391.
15. Thomas EL, Rosen R, Murphy R, et al. Purlytin (SnET2)-photodynamic therapy produces closure of subfoveal choroidal neovascularization in humans. *Invest Ophthalmol Vis Sci.* 1998; 39(suppl):S242.
16. Flower RW, Snyder WJ. Expanded hypothesis on the mechanism of photodynamic therapy action on choroidal neovascularization. *Retina.* 1999;19:365-369.
17. Schmidt-Erfurth U, Michels S, Barbazetto I, Laqua H. Photodynamic effects on choroidal neovascularization and physiological choroid. *Invest Ophthalmol Vis Sci.* 2002;43:830-841.
18. Schmidt-Erfurth U. Indocyanine green angiography and retinal sensitivity after photodynamic therapy of subfoveal choroidal neovascularization. *Semin Ophthalmol.* 1999;14:35-44.
19. Michels S, Schmidt-Erfurth U. Early vascular changes induced by photodynamic therapy using verteporfin. *Invest Ophthalmol Vis Sci.* 2001; 42(suppl):S304.
20. Aug LP, Yap EY, Fam HB. Bilateral choroidal infarction in a patient with antiphospholipid syndrome: a case report. *Clin Exp Ophthalmol.* 2000;28:326-328.
21. Hoerauf H, Schmidt-Erfurth U. Combined choroidal and retinal ischemia during interferon therapy: ICG-angiographic and microperimetric findings. *Arch Ophthalmol.* 2000;118:580-582.
22. Husain D, Kramer M, Kenney AG, et al. Effects of photodynamic therapy using verteporfin on experimental choroidal neovascularization and normal retina and choroid up to 7 weeks after treatment. *Invest Ophthalmol Vis Sci.* 1999;40:2322-2331.
23. Finger PT, Chakravarthy U, Augsburger JJ. Radiotherapy and the treatment of age-related macular degeneration: external beam radiation therapy is effective in the treatment of age-related macular degeneration. *Arch Ophthalmol.* 1998;116:1507-1511.
24. Fung WE. Interferon alpha 2a for treatment of age-related macular degeneration. *Am J Ophthalmol.* 1991;112:349-350.
25. Reichel E, Berrocal A, Ip M, et al. Transpupillary thermotherapy of occult subfoveal choroidal neovascularization in patients with age-related macular degeneration. *Ophthalmology.* 1999;106:1908-1914.
26. Miller H, Miller B, Ryan SJ. The role of retinal pigment epithelium in the involution of subretinal neovascularization. *Invest Ophthalmol Vis Sci.* 1986;27:1644-1652.
27. McLeod DS, Lutty GA. High-resolution histologic analysis of the human choroidal vasculature. *Invest Ophthalmol Vis Sci.* 1994;35:3799-3811.
28. Kvanta A, Algvere B, Berghin L, Seregard S. Subfoveal fibrovascular membranes in age-related macular degeneration express vascular endothelial growth factor. *Invest Ophthalmol Vis Sci.* 1996;37:1929-1934.
29. Kwak N, Okamoto N, Wood J, Campochiaro P. VEGF is major stimulator in model of choroidal neovascularization. *Invest Ophthalmol Vis Sci.* 2000;41:3158-3164.
30. Heriot WJ, Machemer R. Pigment epithelial repair. *Graefes Arch Clin Exp Ophthalmol.* 1992; 230:91-109.
31. Roider J, Michaud N, Flotte TJ, Birngruber R. Response of the retinal pigment epithelium to selective photocoagulation. *Arch Ophthalmol.* 1992;110:1786-1792.

Mushroom-Shaped Choroidal Recurrence of Retinoblastoma 25 Years After Therapy

An important method of conservative therapy for retinoblastoma during the past 50 years has been external beam radiotherapy. In general, this modality offers favorable tumor control, but subsequent monitoring for local recurrence and application of salvage therapy have been emphasized. Several authors have observed that recurrence is usually detected within 1 year of therapy.[1,2] We report late-onset choroidal recurrence of retinoblastoma 25 years following therapy.

Report of a Case. A 25-year-old Latin American woman noticed sudden, painless visual loss in her only eye on awakening. Visual acuity was hand motions OD; the left eye had been enucleated. She gave a history of bilateral sporadic retinoblastoma diagnosed at age 12 months and managed initially with chemotherapy and cryotherapy to the right eye and enucleation of the left eye. One year later, 2 tumor recurrences were detected at the site of previous cryotherapy scars superiorly and inferonasally, measuring $1.5 \times 1.5 \times 1.0$ mm and $12.0 \times 10.5 \times 8.0$ mm, respectively. The inferonasal mass displayed vitreous seeds and the eye was classified as Reese-Ellsworth group Vb. External beam radiotherapy using 3500 rad was delivered through an anterior portal. A cataract was subsequently removed. During the following 24 years, the tumors were followed-up elsewhere and remained regressed. Examination under anesthesia with complete funduscopy was performed for 9 consecutive years and office evaluation for the subsequent 15 years. Radiation complications of maculopathy, dry eye, and corneal opacification combined with photophobia afforded a poor view of the fundus during those 15 years.

At the most recent examination, there was a hyphema and vitreous hemorrhage that precluded a view of the fundus. The patient was referred to the Ocular Oncology Service at Wills Eye Hospital (Philadelphia, Pa) for further management. Results of ocular ultrasound revealed a mushroom-shaped fundus mass measuring 15.0 mm in base and 10.3 mm in thickness. There was a slight suggestion of calcification in the tumor but no acoustic shadowing in the orbit (**Figure 1**). Vascular pulsations were absent. Vitreous echoes suggestive of blood were noted. Based on these findings, the differential diagnosis included late-onset recurrence of retinoblastoma or choroidal melanoma.

The right eye was enucleated. Gross pathology revealed a mushroom-shaped amelanotic choroidal tumor (**Figure 2**). Histopathologic examination results confirmed that the tumor was a poorly differentiated, mitotically active retinoblastoma forming a massive tumor in the ciliary body and peripheral choroid (Figure 2). The tumor cells grew in a confluent fashion without necro-

sis. The cells had scant cytoplasm and showed intense positive immunoreactivity for neuron-specific enolase and were negative for S100 protein, consistent with retinoblastoma. A few calcific foci from a previous scar were noted near the base of the recurrence. There was tumor invasion of the anterior chamber. Chemoprophylaxis for metastatic disease was provided using vincristine, etoposide, and carboplatin for 6 months.

Comment. Whole-eye radiotherapy for retinoblastoma offers tumor control in 41% to 74% of cases.[1-4] When radiotherapy is combined with focal salvage treatments (cryotherapy, laser photocoagulation, and plaque radiotherapy), tumor control improves to 80%.[2] However, tumor control decreases with more advanced retinoblastoma, such as Reese-Ellsworth group V, where stable regression is achieved in 29% to 66% of eyes.[1,2]

Tumor recurrence following external beam radiotherapy generally is detected within 1 year of treatment[2,5] and 96% occurs within 2 years following treatment.[1] In an analysis of 65 eyes treated with external beam radiotherapy, all retinoblastoma recurrences were found within 2.75 years of treatment.[1] Tumor recurrence was more likely in slightly older children (1.8 years in the recurrence group vs 0.9 years in the nonrecurrence group) and in those with larger tumors (16 mm in the recurrence group vs 8.9 mm in the nonrecurrence group).

Recurrence of retinoblastoma beyond 4 years following radiotherapy is extremely rare. Ytteborg and Arnesen[6] observed one case of late-onset recurrence 12 years after radiotherapy. The patient had shown initial poor tumor control for 2 years following 2 courses of external beam radiotherapy and subsequent cobalt plaque radiotherapy and xenon photocoagulation. Recurrence was discovered 10 years after an interval of stable findings. Others have recognized late recurrence at 4.5 and 9 years.[5,7]

An alternative possiblity to tumor recurrence in our case could be new tumor formation in a patient with germinal mutation of the retinoblastoma gene. In most instances, new tumors in bilateral cases occur within 1 to 2 years from initial diagnosis.[8] Late-onset new tumors after 5 years of follow-up in bilateral retinoblastoma have been observed at 8 years[9] and 12 years.[10] Another possibility for the pathogenesis of this tumor is that it represents a radiation-induced second cancer.[11] It seems highly improbable to have retinoblastoma as a second cancer after treatment of retinoblastoma. In our case, it is most likely that choroidal recurrence of retinoblastoma developed after 25 years.

Another interesting facet of this case was the configuration of the recurrence as a mushroom-shaped choroidal mass, suggestive of melanoma with a rupture through the Bruch membrane.[12] The mushroom configuration has rarely been found with nonmelanoma tumors, such as choroidal metastasis[13,14] and choroidal hemangioma,[15] that have broken through the Bruch membrane. To our knowledge, this is the first report of choroidal invasion from retinoblastoma assuming this configuration. However, we have seen another case of retinoblastoma histopathologically that had massive choroidal invasion and had ruptured through the Bruch membrane, assuming a mushroom configuration. Because of the ultrasound findings, melanoma was a

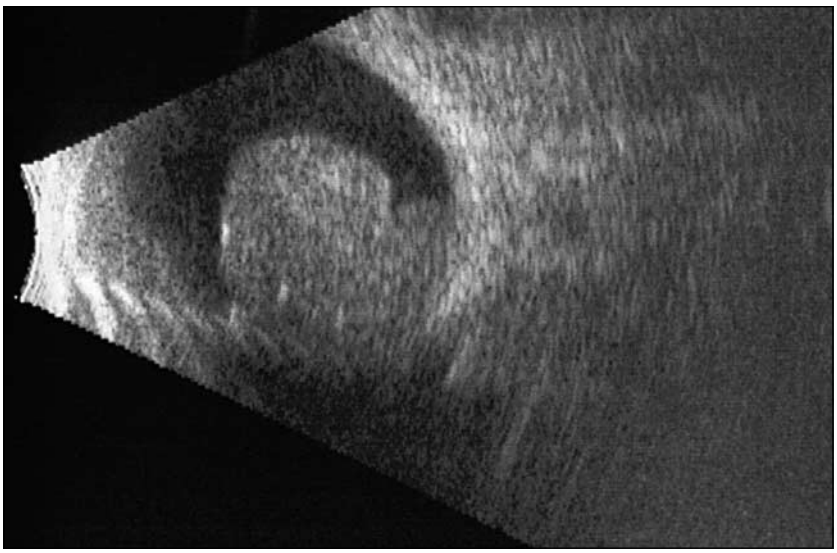

Figure 1. B-scan ocular ultrasound of an eye with no fundus view owing to hyphema and vitreous hemorrhage. Note the echogenic mushroom-shaped fundus mass in the peripheral choroid and ciliary body region.

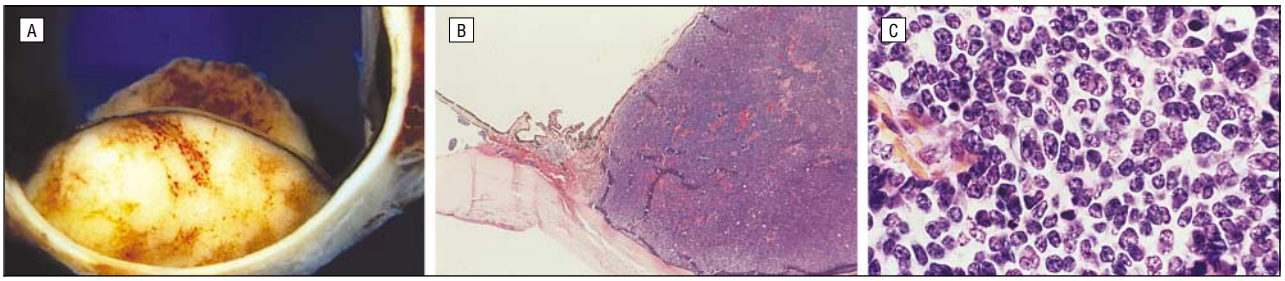

Figure 2. Pathologic examination revealed an amelanotic mushroom-shaped choroidal mass. A, Gross pathologic appearance of the retina and retinal pigment epithelium lining the inner surface of the choroidal mass. B, The choroidal mass is noted with overlying retinal tissue (hematoxylin-eosin, original magnification ×10). C, Poorly differentiated retinoblastoma is shown (hematoxylin-eosin, original magnification ×200).

diagnostic consideration since choroidal melanoma has been reported in association with both unilateral and bilateral retinoblastoma.[11,16]

In summary, we report a remarkable case of choroidal recurrence of retinoblastoma 25 years after radiotherapy, that assumed a mushroom shape, simulating a choroidal melanoma. We advise that patients with retinoblastoma maintain regular monitoring of the affected eye(s) throughout their lifetimes. If difficulty in visualization develops owing to media opacity or patient cooperation, then regular ocular ultrasonography and examination with sedation are warranted.

Carol L. Shields, MD
Michelle R. Piccone, MD
Jerry A. Shields, MD
Ralph C. Eagle, Jr, MD
Philadelphia, Pa
Michael Singer, MD
San Antonio, Tex

This research was supported by the Eye Tumor Research Foundation, Philadelphia, Pa (Dr C. L. Shields), the Paul Kayser International Award of Merit in Retina Research, Houston Tex (Dr J. A. Shields), and the Noel T. and Sara L. Simmonds Endowment for Ophthalmic Pathology, Wills Eye Hospital, Philadelphia (Dr Eagle).

Corresponding author and reprints: Carol L. Shields, MD, Ocular Oncology Service, Wills Eye Hospital, 900 Walnut St, Philadelphia, PA 19107.

1. Abramson DH, Servodidio CA, De Lillo AR, et al. Recurrence of unilateral retinoblastoma following radiation therapy. *Ophthalmol Genet.* 1994;15:107-113.
2. Toma NMG, Hungerford JL, Plowman PN, et al. External beam radiotherapy for retinoblastoma, II: lens sparing technique. *Br J Ophthalmol.* 1995;79:112-117.
3. Schipper J. *Retinoblastoma: A Medical and Experimental Study* [thesis]. the Netherlands: State University of Utrecht; 1980.
4. Foote RL, Garretson BR, Schomberg PJ, et al. External beam irradiation for retinoblastoma: patterns of failure and dose-response analysis. *Int J Radiat Oncol Biol Physics.* 1989;16:823-30.
5. Messmer EP, Sauerwein W, Heinrich T, et al. New and recurrent tumor foci following local treatment as well as external beam radiation in eyes of patients with hereditary retinoblastoma. *Graefes Arch Ophthalmol.* 1990;228:426-431.
6. Ytteborg J, Arnesen K. Later recurrence of retinoblastoma. *Acta Ophthalmol.* 1972;50:367-374.
7. Paterson MW, Charteris AA. Retinoblastoma: report of 19 patient treated with radiotherapy. *Br J Ophthalmol.* 1965;49:347-358.
8. Salmonsen P, Ellsworth RM, Kitchin FD. The occurrence of new retinoblastomas after treatment. *Ophthalmology.* 1965;86:837-843.
9. Stallard HB. The conservative treatment of retinoblastoma. *Trans Ophthalmol Soc UK.* 1962; 82:473-534.
10. Skeggs D, Williams J. The treatment of advanced retinoblastoma by means of external irradiation combined with chemotherapy. *Clin Radiol.* 1966;17:169-172.
11. Wong FL, Boice JD, Abramson DH, et al. Cancer incidence after retinoblastoma: radiation dose and sarcoma risk. *JAMA.* 1997;278:1262-1267.
12. Shields JA, Shields CL. *Ultrasonography of Posterior Uveal Melanoma: Atlas of Intraocular Tumor.* Philadelphia, Pa. Lippincott Williams & Wilkins; 1999:109.
13. Shields CL, Shields JA, Gross N, et al. Survey of 520 uveal metastases. *Ophthalmology.* 1997; 104:1265-1276.
14. Ward SD, Byrne BJ, Kincaid MC, Mann ES. Ultrasonographic evidence of a mushroom-shaped choroidal metastasis. *Am J Ophthalmol.* 2000;130:681-682.
15. Spraul CW, Kim D, Fineberg E, Grossniklaus HE. Mushroom-shaped choroidal hemangioma. *Am J Ophthalmol.* 1996;122:434-436.
16. Singh AD, Shields CL, Shields JA, Sternberg P. Occurrence of retinoblastoma and uveal melanoma in the same patient. *Retina.* 2000;20:305-306.

Cosmetically Significant Proptosis Following a Tube Shunt Procedure

A 16-year-old boy was hit in the right eye with a paint ball, resulting in a dislocated lens, prolapsed iris, and a vitreous hemorrhage. He had a lensectomy, vitrectomy, and complete iridectomy. Subsequent visual acuity was hand movements OD and a right afferent pupillary defect with no identifiable anterior segment structures.The visual acuity in was 20/20 OS. One month following surgery, the patient developed elevated intraocular pressure (IOP) ranging between 40 and 50 mm Hg. The patient was referred for management of his glaucoma.

Report of a Case. When we first saw the patient, the optic disc of the right eye had a cup-disc ratio of 0.6. In contrast, the left optic disc had almost no cup. It was believed that marked glaucoma damage had already occurred. Visual acuity was too poor to permit a meaningful visual field examination. It was believed that surgery was necessary to control the IOP, and because of the extensive scarring caused by the previous surgery and the absence of vitreous, a tube shunt procedure was considered appropriate.

An Ahmed (New World Medical Inc, Cucamonga, Calif) tube shunt with a Tutoplast (Tutogen Medical Inc, Clifton, NJ) patch graft was implanted superotemporally without complication, and the tube was placed into the anterior chamber. The IOP postoperatively was consistently lower than 21 mm Hg. However, there was gradually increasing proptosis, and by 2 months postoperatively, he had developed 6 mm of proptosis, with marked displacement of the right globe inferiorly. There was significant limitation of elevation, restriction of abduction, and exposure keratitis of the right eye. The patient and his parents were notably unhappy with the cosmetic result. Magnetic resonance imaging results revealed a large, focal collection of fluid superolaterally to the globe. The tube shunt could be identified within the fluid collection (**Figure**). The diagnosis was proptosis caused by the cyst surrounding the Ahmed tube shunt.

It was elected to follow up the patient conservatively. The exposure keratitis was treated with intensive lubrication and it gradually cleared. The IOP remained between 12 and 15 mm Hg. There was no symptomatic diplopia, presumably because of the poor vision in the right eye. After 6 weeks of follow-up, the proptosis had decreased to a 1-mm difference between the 2 globes and there continued to be mild limitation of elevation of the right eye. One year later, the eye remained slightly proptosed and inferiorly displaced, but the cosmetic defect was considered tolerable by the patient and his parents.

Comment. To our knowledge, this is the first reported case of proptosis following implantation of a drainage device. Oculomotility problems secondary to tube shunts are known complications of Ahmed, Krupin (Hood Laboratories, St Pembroke, Mass), Baerveldt (Pharmacia & Upjohn, Bridgewater, NJ), and Molteno (OP Inc, Costa Mesa, Calif) drainage implants.[1-5] There has been 1 reported case of extraocular muscle restriction with the Ahmed tube shunt. The tube shunt was placed superonasally and resulted in an ac-

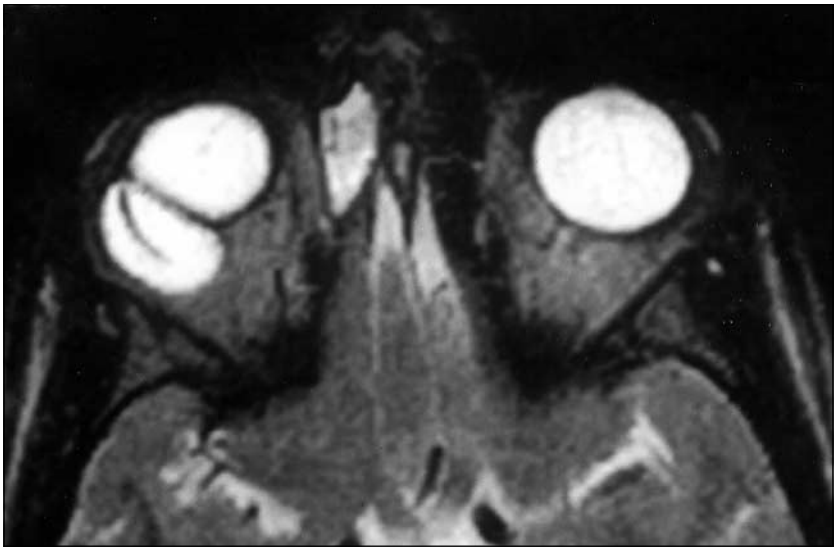

Magnetic resonance imaging shows the tube shunt within a collection of fluid superolaterally to the globe.

quired pseudo-Brown syndrome on the first postoperative day.

Oculomotility disturbances may result from several factors. First, when an implant placed under the rectus muscles is responsible for producing diplopia, the limitation of movement is in the direction of the implant, eg, a superotemporal quadrant implant produces a hypotropia that increases in upgaze, an esotropia that increases in abduction, or a combination of both. This is thought to be related to a posterior fixation effect induced by scarring between the muscle belly and the sclera. Scarring posterior to the widest portion of the implant will weaken the function of the muscle in its field of action. Second, a large bleb produced by aqueous expansion of the capsule that forms around the reservoir may result in a crowding-effect that limits the movement of the eye and in mechanical displacement of muscles.[3] The most common factor that results in oculomotility disturbances is the large size of the implant and its location or extension under a muscle belly. Many patients with motility disturbance secondary to drainage device placement require surgical intervention to correct the misalignment. In our case, the proptosis and motility disturbance appeared 2 months after the placement of the Ahmed device and resolved partially 6 weeks following the initial visit.

This case highlights the motility disturbance that may be a complication of drainage devices, emphasizing the need for an appropriate discussion with the patient prior to surgery. It also reports, to our knowledge, the first case of proptosis following the placement of an Ahmed tube shunt. Finally, it suggests that a period of observation may be useful before embarking on surgical correction for motility disturbances following implantation of drainage devices.

Helen V. Danesh-Meyer, MD, FRACO
Auckland, New Zealand
George L. Spaeth, MD
Marlan Maus, MD
Philadelphia, Pa

Corresponding author: Helen V. Danesh-Meyer, MD, FRACO, Department of Ophthalmology, University of Auckland, Auckland, New Zealand (e-mail: h.daneshmeyer@auckland.ac.nz).

1. Topouzis F, Coleman AL, Choplin N, et al. Follow-up of the original cohort with the Ahmed glaucoma valve implant. *Am J Ophthalmol.* 1999; 128:198-204.
2. Huang MC, Netland PA, Coleman AL, et al. Intermediate-term clinical experience with the Ahmed glaucoma valve implant. *Am J Ophthalmol.* 1999;127:27-33.
3. Ball SF, Ellis GS, Harrington RG, et al. Brown's superior oblique tendon syndrome after Baerveldt glaucoma implant [letter]. *Arch Ophthalmol.* 1992;110:1368.
4. Coats DK, Paysse EA, Orenga-Nania S. Acquired pseudo-Brown's syndrome immediately following Ahmed valve glaucoma implant. *Ophthalmic Surg Lasers.* 1999;30:396-397.
5. Christmann LM, Wilson ME. Motility disturbances after Molteno implants. *J Pediatr Ophthalmol Strabismus.* 1992;29:44-48.

Paradoxical Intraocular Pressure Elevation After Combined Therapy With Latanoprost and Bimatoprost

Latanoprost is a prostaglandin F_{2a} analogue prodrug that is used in the management of ocular hypertension and glaucoma. Latanoprost is widely prescribed and has displayed ocular hypotensive efficacy greater than that exhibited by timolol maleate in controlled comparative studies.[1-4] The effect on intraocular pressure (IOP) seems to be caused by increased uveoscleral outflow.[5,6]

Bimatoprost is a new ocular compound that appears to mimic the prostamides. Prostamides are the most recently described members of the fatty-acid amide family and are potent ocular hypotensive agents. Bimatoprost also has been shown to have superior hypotensive efficacy compared with timolol.[7,8] Bimatoprost seems to work by enhancing pressure-independent aqueous outflow, presumably corresponding to uveoscleral outflow and conventional outflow through the trabecular meshwork. Bimatoprost has also been noted to increase aqueous production.[9]

We have recently noted 3 patients who have demonstrated marked paradoxical IOP elevation after adding bimatoprost to the treatment regimen of an eye already being treated with latanoprost, and we present those cases.

Report of Cases. *Case 1.* A 61-year-old African American man had been diagnosed as having open-angle glaucoma 6 months previously. When he was first evaluated by one of us (L.W.H.) a month after his diagnosis, he was noted to have a Goldmann applanation IOP of 22 mm Hg OD and 19 mm Hg OS. He had been using timolol 0.5% in both eyes twice daily until discontinuing this medication 1 week before the visit. For compliance reasons and as a trial in 1 eye, he began applying timolol maleate ophthalmic gel-forming solution (Timoptic XE; Merck & Co, Inc, West Point, Pa)

0.5% in the right eye once daily in the morning. A horseshoe retinal tear was incidentally found in the right eye, and the patient underwent prophylactic laser treatment of the tear at the same visit.

At follow-up 3 weeks later, the IOP was 24 mm Hg OD and 21 mm Hg OS. Because he required a lower target IOP, timolol maleate ophthalmic gel-forming solution was replaced with latanoprost in the right eye once daily in the evening. Two months following his initial visit, the IOP was 25 mm Hg OD and 15 mm Hg OS, and bimatoprost was added to the treatment regimen in the right eye once daily in the morning. At follow-up 5 weeks later, the IOP was 48 mm Hg OD and 21 mm Hg OS. Bimatoprost was discontinued, and the IOP 1 week later (following use of latanoprost alone in the right eye) was 33 mm Hg OD and 20 mm Hg OS. The patient reported compliance with therapy at every follow-up visit, and the anterior segment remained stable. The IOP was measured in the early to late afternoon at each visit and by the same person (L.W.H.) each time.

Case 2. A 70-year-old white man was diagnosed as having pigmentary glaucoma, more severe in the right eye than in the left, in 1988. He had undergone trabeculectomy in the right eye and had received an Ahmed valve implantation in the left eye in February 2000. Medications in the right eye had been discontinued since the trabeculectomy. However, the condition of the left eye required that glaucoma medications be resumed. By March 2001, the IOP was 10 mm Hg OU, with the patient applying latanoprost once daily in the evening in the left eye and a combination of dorzolamide hydrochloride and timolol maleate ophthalmic solution (Cosopt; Merck & Co, Inc) twice daily in the left eye, with a stable anterior segment in both eyes. At follow-up in May 2001, the dorzolamide hydrochloride–timolol maleate ophthalmic solution was replaced with dorzolamide hydrochloride twice daily, as the patient was noted to have bradycardia. He continued using latanoprost in the left eye. The IOP at that visit measured 8 mm Hg OD and 20 mm Hg OS. Dorzolamide hydrochloride was replaced with bimatoprost once daily in the morning in the left eye. At the next follow-up visit in 2 weeks, the IOP was 7 mm Hg OD and 35 mm Hg OS. Bimatoprost was discontinued, with resumption of dorzolamide hydrochloride–timolol maleate ophthalmic solution twice daily with the patient applying nasolacrimal duct occlusion. At the follow-up visit 2 weeks later, the IOP was 6 mm Hg OD and 13 mm Hg OS. The IOP was measured in the late morning or early afternoon at each visit and was measured by the same person (L.W.H.) each time. The patient reported compliance with the medical regimen at each visit.

Case 3. A 62-year-old white woman was diagnosed as having acute-angle closure in the left eye in 1974 and underwent surgical peripheral iridectomy. She had laser peripheral iridotomy performed on the right eye in 1982. She had been using treatment drops for glaucoma in both eyes since the 1970s, with some recent difficulty in controlling the IOP in the left eye. During the past year, the IOP had remained in the midteens in the right eye, but had ranged between 16 and 23 mm Hg OS. By May 2001, the IOP was 13 mm Hg OD and 19 mm Hg OS using 1 drop of latanoprost daily in both eyes in the evening and 1 drop of brimonidine tartrate twice daily in the left eye. One drop of bimatoprost in the left eye every evening was added to the regimen. Four weeks later, the IOP was 42 mm Hg OS, although the patient had discontinued the bimatoprost 4 days before this visit because of irritation and redness of the left eye. The IOP in the right eye was 16 mm Hg at that visit. Timolol maleate ophthalmic gel-forming solution 0.5% once daily in the morning in the left eye was added to the current regimen of latanoprost and brimonidine, and 3 days later the IOP was 15 mm Hg OU.

Comment. Glaucoma is a chronic, progressive disease characterized by visual field loss and optic nerve damage, often in the presence of elevated IOP.[10] Patients with glaucoma are usually treated initially with monotherapy to reduce their IOP; however, many patients eventually require more than 1 medication.[11] Recent studies[12,13] have shown the importance of lowering the IOP in the management of glaucoma, perhaps to lower levels than were thought necessary in the past. With the development of newer glaucoma medications and combinations thereof, lower target IOPs are more readily achieved. Because many patients with glaucoma require combination therapy, the combination of the 2 powerful hypotensive agents latanoprost and bimatoprost may become a popular treatment option. In addition, latanoprost and bimatoprost offer convenient once daily dosing.

Latanoprost and bimatoprost seem to work by increasing uveoscleral outflow, so combining 2 drugs that facilitate outflow may not be the most optimal approach, although these 2 agents presumably work on different receptors. Woodward et al[14] showed that bimatoprost has no significant affinity for prostaglandin receptors or for several other receptors in a feline iris sphincter preparation. This finding, albeit in a feline model, supports the concept that the target receptor for bimatoprost is pharmacologically unique.

It is also known that the use of latanoprost twice daily is less effective than once daily application,[15-18] and an early study[7] also shows that bimatoprost twice daily is less effective than bimatoprost once daily. In a study of 40 healthy volunteers who received latanoprost once daily in one eye and twice daily in the fellow eye, Linden and Alm[18] showed that once daily dosing resulted in a significantly lower IOP compared with twice daily dosing on day 15, but not on day 2. They believed that a twice daily regimen of latanoprost leads to desensitization at the level of the FP-receptor. In monkeys, treatment with large dosages of prostaglandin F_{2a} for 4 to 8 days induces loss of extracellular material between the ciliary muscle bundles.[19,20] In their 6-month comparison of the effects of bimatoprost vs timolol, Sherwood et al[7] reported a 33% reduction of IOP from baseline with bimatoprost once daily, compared with a 26% reduction with bimatoprost twice daily. They speculated that twice daily dosing of bimatoprost may give concentrations

that are past the peak of the dose-response curve, resulting in reduced efficacy. Commercially available latanoprost and bimatoprost are near the top of their dose-response curves, so using them together results in excessive dosages (Carl Camras, MD, written communication, March 12, 2001). Brubaker et al[9] demonstrated that bimatoprost also causes an increase in aqueous production. Perhaps the increased aqueous flow in the face of compromised conventional outflow is the reason for the elevated IOP. Interestingly, the combination of latanoprost and unoprostone isopropyl, another hypotensive lipid, has been reported to have an additive pressure-lowering effect on diurnal curve characteristics.[21]

Each of our patients demonstrated marked IOP elevation within 2 to 5 weeks after adding bimatoprost to the treatment regimen of an eye being treated with latanoprost. There are possible mitigating factors other than the combination therapy that could have contributed to the pressure rises in our patients. Although each patient claimed compliance with medical therapy, missed doses of the eyedrops could have led to rebound elevation in IOP. In case 2, the patient had a diagnosis of pigmentary glaucoma. Wide swings of IOP have been demonstrated with secondary glaucomas, such as pigmentary and pseudoexfoliative glaucoma, although this possibility would be unlikely in this patient, as there was no evidence of active pigment dispersion. In case 3, the patient had a diagnosis of combined mechanism glaucoma after peripheral iridectomy. Certainly, variability of IOP control is notorious in this setting; however, this patient had undergone iridectomy many years previously, and gonioscopic findings were unchanged. Although this patient had discontinued bimatoprost 4 days before the follow-up visit, she had used the medication for 3 weeks before discontinuing it, so it is likely that there was a lingering effect of the bimatoprost. The effect on diurnal IOP of latanoprost applied once daily in the evening has been shown to be superior to that of latanoprost applied once daily in the morning.[1] The IOP-lowering advantage of applying bimatoprost in the evening has not been demonstrated (Achim Krauss, PhD, oral communication, March 24, 2001), so bimatoprost was applied in the morning in 2 of the 3 patients for convenience.

In summary, latanoprost and bimatoprost are powerful ocular hypotensive lipids that have shown efficacy superior to that of timolol in controlled clinical trials. Using these 2 medications together may lead to marked IOP elevation in some patients, and close surveillance is advised whenever combined therapy is prescribed. Further study is indicated to determine more clearly which patients might be at risk for this paradoxical reaction.

Leon W. Herndon, MD
Sanjay G. Asrani, MD
Gayle H. Williams, MD, PhD
Pratap Challa, MD
Paul P. Lee, MD
Durham, NC

Corresponding author: Leon W. Herndon, MD, Duke University Eye Center, PO Box 3802, Durham, NC 27710 (e-mail: hernd012@mc.duke.edu).

1. Alm A, Stjernschantz J, for the Scandinavian Latanoprost Study Group. Effects on intraocular pressure and side effects of 0.005% latanoprost applied once daily, evening or morning: a comparison with timolol. *Ophthalmology*. 1995;102:1743-1752.
2. Camras CB, the United States Latanoprost Study Group. Comparison of latanoprost and timolol in patients with ocular hypertension and glaucoma: a six-month, masked, multicenter trial in the United States. *Ophthalmology*. 1996; 103:138-147.
3. Watson P, Stjernschantz J, the Latanoprost Study Group. A six-month, randomized, double-masked study comparing latanoprost with timolol in open-angle glaucoma and ocular hypertention. *Ophthalmology*. 1996;103:126-137.
4. Mishima HK, Masuda K, Kitazawa Y, et al. A comparison of latanoprost and timolol in primary open-angle glaucoma and ocular hypertension. *Arch Ophthalmol*. 1996;114:929-932.
5. Alm A, Villumsen J. PhXA34, a new potent ocular hypotensive drug: a study on dose-response relationship and on aqueous humor dynamics in healthy volunteers. *Arch Ophthalmol*. 1991;109: 1564-1568.
6. Ziai N, Dolan JW, Kacere RD, Brubaker RF. The effects on aqueous dynamics of PhXA41, a new prostaglandin $F_{2\alpha}$ analogue, after topical application in normal and ocular hypertensive human eyes. *Arch Ophthalmol*. 1993;111:1351-1358.
7. Sherwood M, Brandt J, for the Bimatoprost Study Groups 1 and 2. Six-month comparison of bimatoprost once-daily and twice-daily with timolol twice-daily in patients with elevated intraocular pressure. *Surv Ophthalmol*. 2001;45 (suppl 4):S361-S368.
8. Brandt JD, VanDenburgh AM, Chen K, for the Bimatoprost Study Group. Comparison of once- or twice-daily bimatoprost with twice-daily timolol in patients with elevated IOP: a 3-month clinical trial. *Ophthalmology*. 2001; 108:1023-1032.
9. Brubaker RF, Schoff EO, Nau CB, et al. Effects of AGN 192024, a new ocular hypotensive agent, on aqueous dynamics. *Am J Ophthalmol*. 2001;131:19-24.
10. Shields MB. *Textbook of Glaucoma*. 3rd ed. Baltimore, Md: Williams & Wilkins; 1992:172-188.
11. Everitt D, Avorn J. Systemic effects of medications used to treat glaucoma. *Ann Intern Med*. 1990;112:120-125.
12. AGIS Investigators. The Advanced Glaucoma Intervention Study (AGIS), 7: the relationship between control of intraocular pressure and visual field deterioration. *Am J Ophthalmol*. 2000; 130:429-440.
13. Collaborative Normal-Tension Glaucoma Study Group. Comparison of glaucomatous progression between untreated patients with normal-tension glaucoma and patients with therapeutically reduced intraocular pressures. *Am J Ophthalmol*. 1998;126:487-497.
14. Woodward DF, Krauss AH, Chen J, et al. The pharmacology of bimatoprost (Bimatoprost). *Surv Ophthalmol*. 2001;45(suppl 4):S337-S345.
15. Alm A, Villumsen J, Tornquist P, et al. Intraocular pressure-reducing effect of PhXA41 in patients with increased eye pressure: a one-month study. *Ophthalmology*. 1993;100:1312-1317.
16. Nagasubramanian S, Sheth GP, Hitchings RA, et al. Intraocular pressure-reducing effect of PhXA41 in ocular hypertension: comparison of dose regimens. *Ophthalmology*. 1993;100:1305-1311.
17. Alm A, Widengard I, Kjellgren D, et al. Latanoprost administered once daily caused a maintained reduction of intraocular pressure in glaucoma patients treated concomitantly with timolol. *Br J Ophthalmol*. 1995;79:12-16.
18. Linden C, Alm A. Latanoprost twice daily is less effective than once daily: indication of receptor subsensitivity? *Curr Eye Res*. 1998;17:567-572.
19. Lutjen-Drecoll E, Tamm E. Morphological study of the anterior segment of cynomolgus monkey eyes following treatment with prostaglandin $F_{2\alpha}$. *Exp Eye Res*. 1988;47:761-769.
20. Tamm E, Rittig M, Lutjen-Drecoll E. Elektronenmikroskopische und immunhistochemische untersuchungen zur augendrucksenkenden wirkung von prostaglandin $F_{2\alpha}$ [in German]. *Fortschr Ophthalmol*. 1990;87:623-629.
21. Stewart WC, Sharpe ED, Stewart JA, et al. Additive efficacy of unoprostone isopropyl 0.12% to latanoprost 0.005%. *Am J Ophthalmol*. 2001; 131:339-344.

Orbital Cellulitis as a Late Complication of Glaucoma Shunt Implantation

Orbital cellulitis is a rare complication of glaucoma tube shunt implantation. We describe a patient who developed orbital cellulitis 15 months after placement of a Baerveldt tube shunt (Pharmacia Corporation, Peapack, NJ). The proximal portion of the Baerveldt tube shunt had eroded through the conjunctiva, presumably serving as a portal of entry for microorganisms. The cellulitis was

Figure 1. Computed tomographic scan of the orbits with contrast (axial section) demonstrates preseptal soft tissue swelling surrounding and extending from the region of the left Baerveldt tube shunt (long arrow). Infiltration of the orbital fat is also apparent (short arrow). Of note is that Baerveldt tube shunts are impregnated with barium and therefore are radio-opaque.

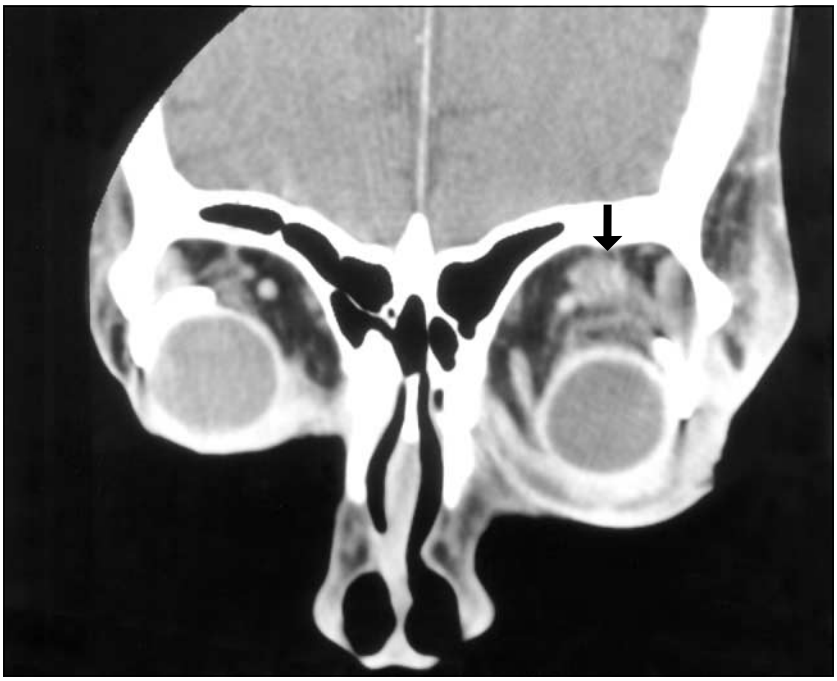

Figure 2. Computed tomographic scan of the orbits with contrast (coronal section) demonstrates inferior displacement of the globe, as well as inflammation around the levator–superior rectus complex (arrow).

successfully treated with intravenous antibiotics and subsequent removal of the glaucoma tube shunt.

Report of a Case. A 78-year-old African American woman was seen with a 3-day history of left eye pain, eyelid swelling, and decreased vision in her left eye. According to the referring ophthalmologist, the left intraocular pressure had become elevated to the 40–mm Hg range and vision had worsened from counting fingers to no light perception over the preceding 3 days. She had been treated with oral acetazolamide, timolol maleate, dorzolamide hydrochloride, and brimonidine tartrate.

The patient had an extensive medical and ocular history. She had hypertension, gout, and hypothyroidism and had undergone aortic valve replacement and bilateral knee replacements. In the right eye, she had undergone multiple penetrating keratoplasties for Fuchs endothelial dystrophy and graft failure. She also had placement of a Baerveldt tube shunt (350 mm^2) for chronic angle-closure glaucoma. In the left eye, she had undergone penetrating keratoplasty with cataract extraction and intraocular lens implantation. Three years later, she underwent implantation of a Baerveldt tube shunt (350 mm^2) for chronic angle-closure glaucoma. Four months following insertion of the glaucoma tube shunt, she underwent repeated penetrating keratoplasty, anterior synechialysis, and shunt revision for iris incarceration of the tube. Subsequently, she required surgical drainage of peripheral choroidal effusions and scleral patch graft reinforcement for tube erosion through the conjunctiva 11 months prior to initial examination.

She was afebrile at clinical examination. Visual acuity was light perception in the right eye and hand motions temporally in the left eye (her visual acuity was 20/400 OS 1 year previously). The intraocular pressures were 19 mm Hg OD and 12 mm Hg OS. She had a right relative afferent pupillary defect with 50% light desaturation. Ocular ductions were full in the right eye. In the left eye she had severe limitation of motility in all directions. There was swelling, erythema, tenderness, and warmth of the left upper eyelid, and the globe was inferiorly displaced. The left conjunctiva also had diffuse hyperemia and was chemotic. On computed tomography of the orbits, preseptal soft tissue swelling was extended from the region of the glaucoma tube shunt, with some infiltration of the intraconal fat (**Figure 1** and **Figure 2**). Biomicroscopic and fundus examination findings did not reveal any evidence of endophthalmitis or panophthalmitis.

The patient was admitted and started receiving intravenous ampi-

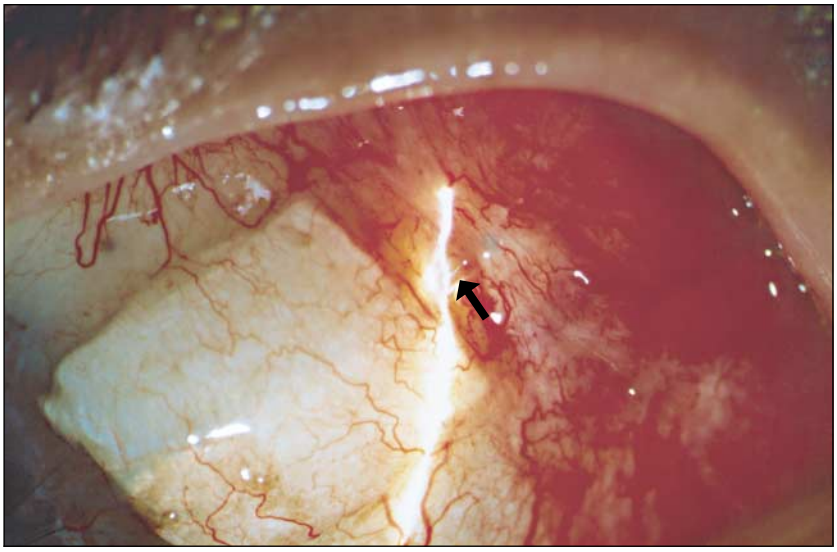

Figure 3. Anterior segment biomicroscopy reveals erosion of the Baerveldt tube through the conjunctiva (arrow).

cillin sodium/sulbactam sodium. The ocular motility and eyelid swelling improved dramatically within 24 hours. Intravenous methylprednisolone sodium succinate (Solu-Medrol; Pharmacia Corporation) was then added. Following several more days of intravenous antibiotics, the left conjunctival hyperemia became localized to the superotemporal quadrant region. There was conjunctival erosion and exposure of the proximal portion of the Baerveldt tube with negative Seidel test results (**Figure 3**). The bleb over the tube shunt appeared convex (indicative of a functional shunt implant).

Given the persistent ocular pain and redness, the glaucoma tube shunt was surgically removed. No growth was observed from any of the bacterial cultures. The patient's ocular symptoms resolved and her visual acuity improved to counting fingers range. Moreover, the left intraocular pressure remained stable with antiglaucoma medication.

Comment. Orbital cellulitis is a rare complication of glaucoma tube shunt implantation. To our knowledge, this is the first case of orbital cellulitis reported in a patient with a functioning tube shunt. A case of orbital cellulitis was reported in a child 1 month following a stage 1 Molteno shunt procedure.[1] The tube had been tucked under the conjunctiva and was found to have slipped out, presumably creating a portal of entry for infection. The patient was treated with systemic antibiotics and required removal of the shunt. In contrast, our case involved a functional glaucoma tube shunt of over 1 year's duration that eroded through the conjunctiva. The differential diagnosis also included an orbital inflammatory syndrome. Indeed, myositis has been reported to be associated with Baerveldt tube shunt surgery.[2] This case occurred in a patient with a history of ocular myositis before glaucoma tube shunt surgery. However, our patient's rapidly progressive course, her dramatic improvement with intravenous antibiotics, and the computed tomographic scan findings in the left orbit are consistent with an infectious process.

Orbital cellulitis has occurred in patients with other periocular implants, including scleral buckles.[3] Infections with scleral buckles have usually been associated with exposure of the implant or explant. The treatment of these infections almost invariably requires removal of the element, as well as treatment with antibiotics.[4]

We believe that exposure of the Baerveldt tube through the conjunctiva allowed entry of microorganisms into the subconjunctival space and secondarily into the orbit. Given the lengthy duration between the scleral reinforcement surgery and the development of cellulitis, it is unlikely that residual buried epithelium from the reinforcement surgery could have caused the delayed glaucoma tube shunt exposure. Exposure of glaucoma tube shunts may be managed successfully with anterior surgical revision[5] and/or pars plana vitrectomy and repositioning the tube into the vitreous cavity.[6] However, in the setting of active orbital cellulitis, immediate treatment with intravenous antibiotics is necessary. Subsequent removal of the glaucoma tube shunt implant may be required for complete resolution of the infection.

Adrian M. Laviña, MD
Jeffrey L. Creasy, MD
Nashville, Tenn

James C. Tsai, MD
New York, NY

This work was supported in part by the Homer McK Rees Scholar Award (Dr Tsai) and an unrestricted grant from Research to Prevent Blindness Inc, New York, NY.

The authors have no proprietary interest in any of the products mentioned.

Corresponding author and reprints: James C. Tsai, MD, Harkness Eye Institute, 635 W 165th St, New York, NY 10032 (e-mail: jct2002@columbia.edu).

1. Karr DJ, Weinberger E, Mills RP. An unusual case of cellulitis associated with a Molteno implant in a 1-year-old child. *J Pediatr Ophthalmol Strabis*. 1990;27:107-110.
2. Kean OT, Alward WLM, Kardon RH. Myositis associated with a Baerveldt glaucoma implant. *Am J Ophthalmol*. 1999;128:375-376.
3. Kanski JJ, Gregor Z. *Retinal Detachment: A Colour Manual of Diagnosis and Treatment*. 2nd ed. Oxford, England: Butterworth-Heinman Ltd; 1994:128-129.
4. Smiddy WE, Miller D, Flynn HW. Scleral buckle removal following retinal reattachment surgery: clinical and microbiologic aspects. *Ophthalmic Surg*. 1993;24:440-445.
5. Tsai JC, Grajewski AL, Parrish RK II. Surgical revision of glaucoma shunt implants. *Ophthalmic Surg Lasers*. 1999;30:41-46.
6. Joos K, Laviña AM, Agarwal A, Tawansy K. Successful repositioning of glaucoma shunt implants after pars plana vitrectomy for anterior segment complications. *Ophthalmology*. 2001;108:279-284.

Retinitis Pigmentosa Associated With Ectopia Lentis

Retinitis pigmentosa (RP) is characterized by night blindness, visual field loss, and reduced or extinguished electroretinogram results. Retinitis pigmentosa may be associated with a wide variety of ocular and systemic disorders. Ectopia lentis, a dislocation of the crystalline lens, may cause visual disturbances depending on the type and degree of dislocation and may be associated with a variety of ocular and systemic abnormalities. When associated with systemic disorders, ectopia lentis may be an important diagnostic sign.[1] An association between RP and ectopia lentis has rarely been reported. We describe 2 siblings exhibiting RP and ectopia lentis with an autosomal recessive inheritance pattern.

Report of Cases. *Case 1.* A 42-year-old Japanese woman was brought in for a consultation in 1999 because her mother noticed that the patient's visual acuity was gradually decreasing. She was born under asphyxial conditions after an 8-month pregnancy. She began walking at age 7 years, talking at age 10 years, and began menses at age 17 years. Microcephaly was pointed out at age 5 years. She did not have a history of convulsions or ocular trauma, and could speak and understand only a few words. She was 140.8 cm tall, weighed 53.6 kg, had an arm span of 135 cm, and a head circumference of 48 cm (less than the third percentile). No other systemic disorders were observed.

Her visual acuity was 20/470 OD and 20/710 OS using Teller acuity cards but nystagmus was not observed. Slitlamp biomicroscopy revealed normal corneas and anterior chambers but iridodonesis associated with ectopia lentis was detected bilaterally. The lens was dislocated inferiorly and showed mild opacities in both eyes (**Figure 1**).

Results of fundus examination showed macular degeneration associated with pigmentary retinal degeneration in the pericentral region in both eyes. The retinal arteries were attenuated and the optic disc was somewhat pale (**Figure 2**). Fluorescein angiography showed hyperfluorescence of the posterior lesions associated with a hypofluorescence in the peripapillary region bilaterally (Figure 2).

The amplitudes of the a-waves on the results of dark-adapted standard electroretinograms were severely reduced and the b-waves were extinguished. The rod-isolated responses were extinguished while the cone-isolated responses were markedly reduced (**Figure 3**).

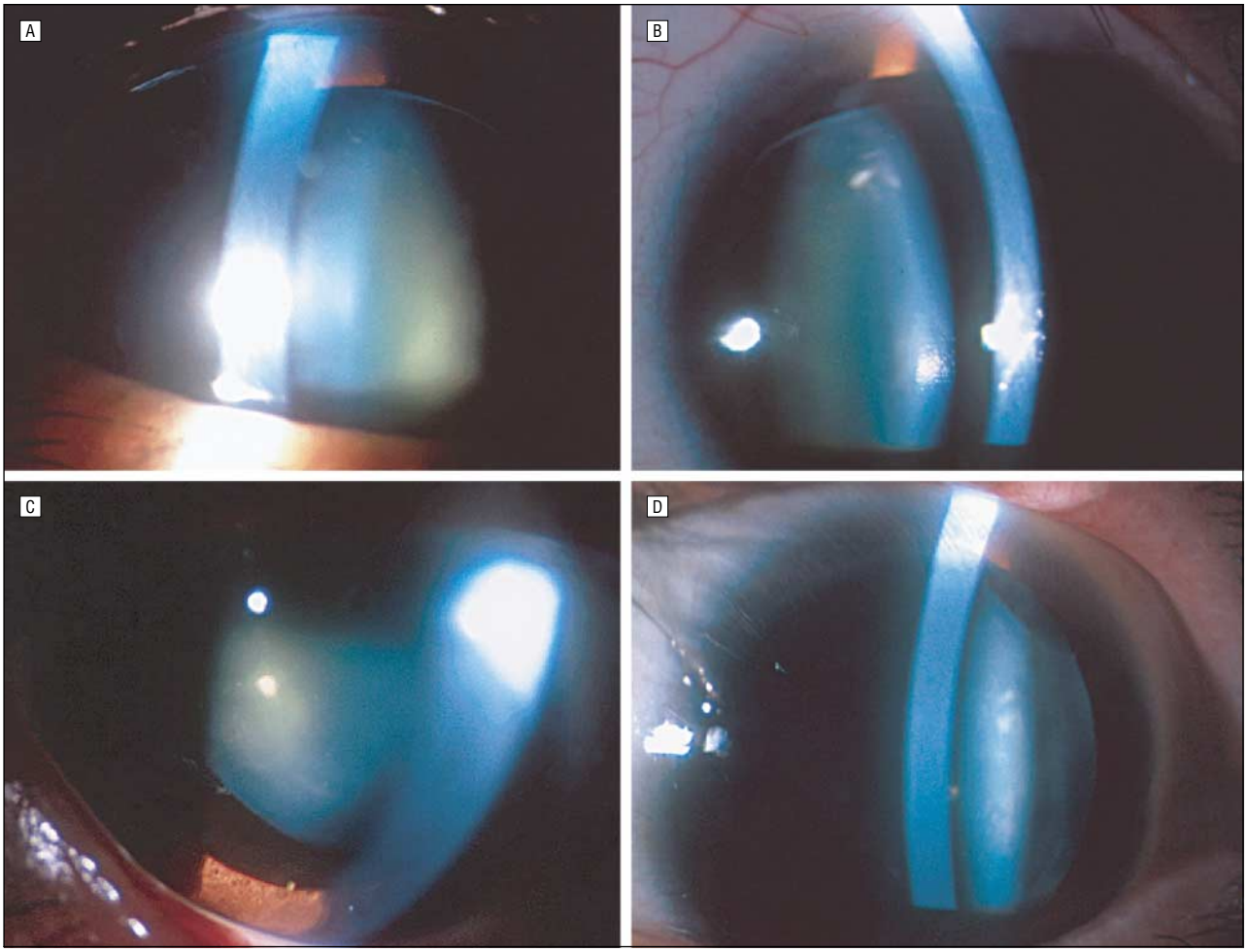

Figure 1. Slitlamp photographs showing dislocation of the lens inferiorly in the right (A) and left (B) eyes of case 1. In case 2, the lens in the right (C) and left (D) eyes were dislocated superiorly and nasally, respectively.

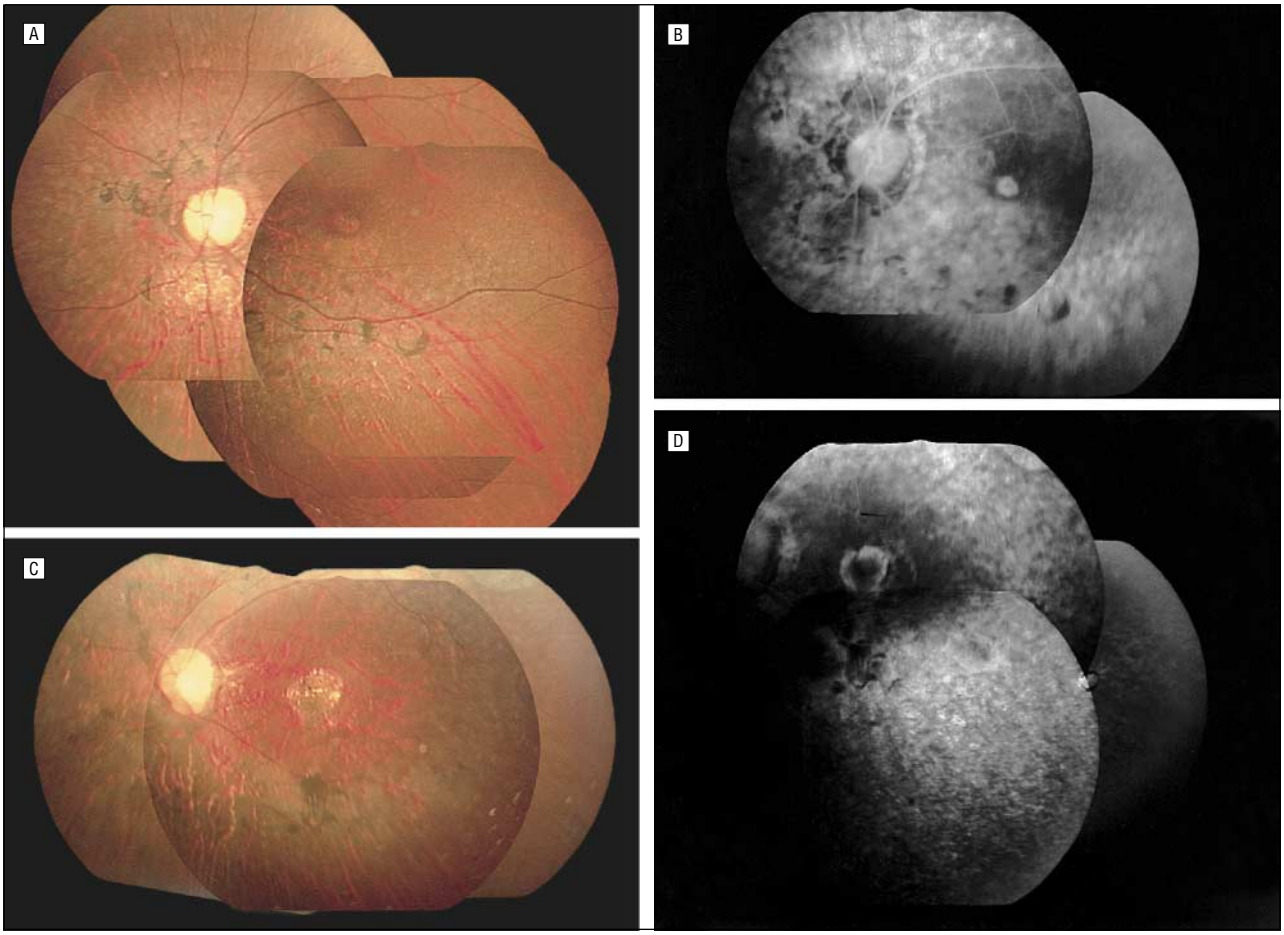

Figure 2. A and C, Fundus photographs of the left eye showing pigmentary retinal degeneration in the pericentral region and macular degeneration. B and D, Fluorescein angiograms showing diffuse hyperfluorescence of the posterior lesions. A and B, case 1. C and D, case 2.

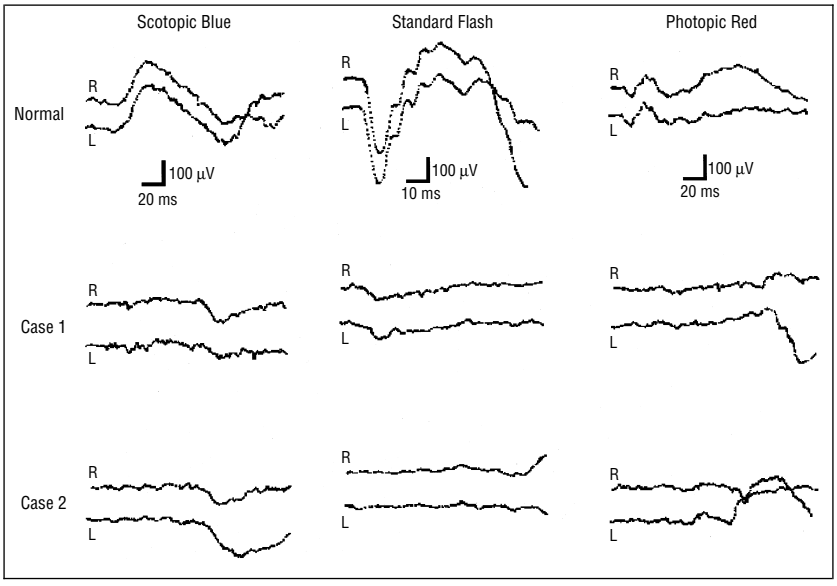

Figure 3. Electroretinograms (ERGs) of cases 1 and 2. The standard and cone-isolated responses were severely reduced while the rod-isolated responses were nonrecordable in case 1. All ERGs of case 2 were nonrecordable.

Case 2. The 37-year-old brother of case 1 was also born under asphyxial conditions after a full-term pregnancy. He began to walk at age 2 years and abnormal electroencephalogram results were detected at age 5 years. However, he had no history of convulsions or ocular trauma. He could speak and understand only a few words and had been our patient since 1990 because his mother noticed that he had impaired visual acuity and night blindness.

The initial visual acuity was 20/200 OU using Teller acuity cards. Slit-lamp examination showed ectopia lentis in the right eye. Fundus examination results disclosed macular degeneration associated with pigmentary retinal degeneration bilaterally. Neuronal ceroid lipofuscinosis was suspected because of both pigmentary retinal degeneration and mental retardation; however, there were neither vacuolated lymphocytes nor inclusion bodies specific for the disease. Results of computed tomography and magnetic resonance imaging showed microcephaly but no abnormality in the brain.

In 1999, he was 159.5 cm tall, weighed 56.0 kg, had an arm span

Clinical Characteristics of the Family Members*

Family Member/Age, y	Refraction	Visual Acuity	Lens in Both Eyes	Funduscopic Appearance in Both Eyes	Other Abnormalities
Patient 1/42	–4.50, –4.25 A180 OD –7.75, –5.00 A20 OS	20/470 OD 20/710 OS	Subluxated	Retinitis pigmentosa	Microcephaly, mental retardation
Patient 2/37	–5.25, –1.50 A90 OD –3.00, –3.50 A10 OS	20/630 OD 20/630 OS	Subluxated	Retinitis pigmentosa	Microcephaly, mental retardation
Father/68	+1.25, –3.00 A90 OD +1.25, –3.00 A90 OS	20/25 OD 20/25 OS	Cataract	Normal	. . .
Mother/72	+2.5 OD +2.0 OS	20/25 OD 20/32 OS	Cataract	Normal	. . .

*Ellipses indicate not applicable.

of 145 cm, and a head circumference of 49 cm (less than the third percentile). His visual acuity was 20/630 OU using Teller acuity cards. He was exotropic but nystagmus was not observed. Slitlamp biomicroscopy revealed that the corneas and anterior chambers were normal but iridodonesis associated with ectopia lentis was observed in both eyes. The lens in the right eye was dislocated upward while that in the left eye was dislocated nasally (Figure 1). The lenses had mild opacities. Fundus examination and fluorescein angiography results disclosed a similar appearance to those of his sister (Figure 2). All electroretinograms were nonrecordable (Figure 3).

Comment. Our 2 patients are members of a Japanese family with RP, ectopia lentis, microcephaly, and mental retardation with no history of consanguinity (**Table**). They had twin brothers who died soon after birth for unknown reasons. Results of ocular examination of the parents exhibited only cataractous lenses that were considered to be caused by age-related changes and the lenses were not dislocated. They had no complaints of night blindness although the patients' father had congenital dyschromatopsia. There was no exposure to toxic substances or infectious organisms during pregnancy. We conclude that some of the disorders associated with our patients were congenital and were inherited in an autosomal recessive fashion.

From a review[1] of the ocular findings and systemic disorders associated with patients with ectopia lentis, we were able to exclude the most common syndromes, such as Marfan syndrome, homocystinuria, Weil-Marchesani syndrome, hyperlysinemia, and sulfite oxidase deficiency because both patients had neither the characteristic skeletal features nor the abnormal amino acid levels in the plasma and/or urine. Furthermore, Refsum syndrome, in which both RP and ectopia lentis can be present, was excluded because of the absence of peripheral neuropathy and the normal plasma levels of phytanic acid. Serologic testing ruled out lues. Chromosomal study revealed normal karyotype in both patients, and they had no sign of hyperextensibility of the joints and skin, polydactyly, and cardiovascular disorders. None of the syndromes or eye diseases in the literature matched the signs and symptoms of our patients.

Although microcephaly with chorioretinopathy has been found as a hereditary disorder (OMIM [online mendelian inheritance in man] 251270), the mental retardation and microcephaly observed in our patients may have resulted from the asphyxial condition because perinatal asphyxia associated with hypoxic-ischemic brain injury is an important cause of neurodevelopmental impairments, such as motor disabilities, visual and/or hearing impairments, and cognitive and learning disabilities.[2] The degree of visual impairment depends on the extent of damage of the optic radiations and/or visual cortex.

To the best of our knowledge, only 3 cases of hereditary chorioretinal disorders associated with ectopia lentis have been reported.[3-5] Although these patients also showed autosomal recessive inheritance, they had dense or posterior subcapsular cataracts. Our patients showed mild nuclear and cortical cataracts. Thus, chorioretinal disorders associated with ectopia lentis may be a new clinical entity although subclinical and genotypic classification will be necessary.

Hajime Sato, MD, PhD
Yuko Wada, MD, PhD
Toshiaki Abe, MD, PhD
Miyuki Kawamura, MD
Ryosuke Wakusawa, MD
Makoto Tamai, MD, PhD
Sendai, Japan

Corresponding author and reprints: Hajime Sato, MD, PhD, Department of Ophthalmology, Tohoku University School of Medicine, 1-1 Seiryo-machi, Aoba-ku, Sendai 980-8574, Japan (e-mail: hasato@oph.med.tohoku.ac.jp).

1. Nelson LB, Maumenee IH. Ectopia lentis. *Surv Ophthalmol*. 1982;27:142-160.
2. Simon NP. Long-term neurodevelopmental outcome of asphyxiated newborns. *Clin Perinatol*. 1999;26:767-778.
3. Guillaumat L, Lemaitre M. Myopie forte, retinite pigmentaire, luxation congenitale des deux cristallins chez une jeune fille issue d'un mariage consaguin: probleme pathogenique. *Bull Soc Ophthalmol Fr*. 1948;3:90-92.
4. Noble KG, Bass S, Sherman J. Ectopia lentis, chorioretinal dystrophy and myopia. *Doc Ophthalmol*. 1993;83:97-102.
5. Simonelli F, Crecchio GD, Testa F, et al. Retinal degeneration associated with ectopia lentis. *Ophthalmic Genet*. 1999;20:121-126.

Pigmentary Retinopathy Associated With Intravitreal Fomivirsen

Cytomegalovirus (CMV) retinitis is the leading cause of visual loss in patients with acquired immunodeficiency syndrome (AIDS). Treatment modalities include intravenous ganciclovir sodium, cidofovir, or foscarnet sodium; oral ganciclovir or

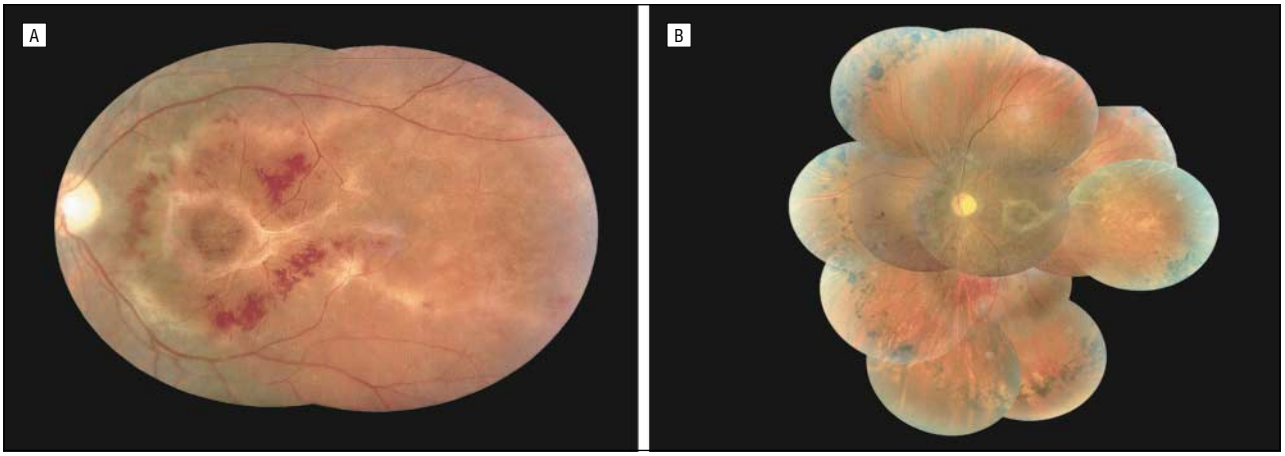

Figure 1. Case 1. A, Left fundus composite photograph of active cytomegalovirus (CMV) in the macula prior to fomivirsen sodium injection. No peripheral photographs were taken. B, New pigmentary changes in the 360° midperipheral retina. The CMV retinitis in the macula is inactive.

valganciclovir hydrochloride; intravitreal (IV) injections of ganciclovir, cidofovir, or foscarnet; and ganciclovir implants. Foscarnet, ganciclovir, and cidofovir selectively inhibit viral DNA polymerase. Fomivirsen sodium (Vitravene, ISIS 2922; ISIS Pharmaceuticals, Carlsbad, Calif) is the latest addition to the armamentarium of local CMV retinitis treatment options. A phosphorothioate oligonucleotide administered intravitreally, fomivirsen inhibits CMV replication through an antisense mechanism, binding to viral messenger RNA and blocking its transcription.[1,2] The Food and Drug Administration approved fomivirsen in August 1998 as highly active antiretroviral therapy (HAART) began to dramatically decrease the incidence of CMV retinitis.[3]

Clinical experience with IV fomivirsen is limited. Reported adverse effects with the approved dosage include transient and reversible inflammation in the anterior chamber (19%), increase in intraocular pressure (19%), vitreitis (11%), and uveitis (5%). Cataract (9%) has also been reported.[2] Isolated case reports describe foveal retinal pigment epithelial (RPE) stippling with reversible bull's-eye maculopathy,[4] peripheral RPE stippling[3,6] associated with visual field loss,[6] and marked retinal toxic side effects after 495 µg doses.[7] Bull's-eye maculopathy was diagnosed after five 330-µg doses in one case and after 15 injections bilaterally in another. In both cases, fomivirsen was administered every other week; RPE stippling was diagnosed after weekly injections of 165 µg for 3 weeks. We report 2 additional cases of peripheral pigmentary changes accompanied by electroretinogram (ERG) abnormalities following IV injection of fomivirsen.

Report of a Case. *Case 1.* A 34-year-old African American man with AIDS had failed HAART. His CD4 cell count was 20 cells/µL. The patient had human immunodeficiency virus (HIV) retinopathy in the right eye and CMV retinitis in zones 1 and 2 of the left eye in May 2000 (**Figure 1**A). The fovea was involved and vision had decreased to 20/400 OS. Cytomegalovirus retinitis was initially treated with intravenous ganciclovir followed by IV fomivirsen. Fomivirsen was used owing to a shortage of ganciclovir. The patient received a 2-dose induction regimen consisting of 330 µg of IV fomivirsen sodium injections every other week. His retinitis progressed when he failed to return for follow-up during the next 7 weeks. The induction regimen was repeated when the patient returned. He then received a maintenance dose of 330 µg 1 month after the second induction, totaling 5 injections of fomivirsen. There was no elevated intraocular pressure. Mild anterior chamber inflammation and mild vitreitis improved while he was receiving topical steroids. The patient was subsequently readministered intravenous ganciclovir for CMV colitis. No additional intraocular injections were given. Six months following the initial IV injection, findings from examination of the left eye revealed new pigmentary changes in the 360° midperipheral retina previously unaffected by CMV retinitis (Figure 1B). The ERG revealed an absent rod response, 40% reduction in cone amplitude, and normal implicit times (**Figure 2**). Visual field testing was not performed because the patient was too debilitated. No cataract was found at a follow-up examination 3 months after the last injection.

Case 2. A 41-year-old white man had AIDS and a CD4 cell count below 50 cells/µL. He was also failing HAART, and his left eye CMV retinitis was controlled with a ganciclovir implant. The right eye had HIV retinopathy and lattice degeneration in the superior and inferior periphery at initial examination (**Figure 3**A). Cytomegalovirus retinitis involving zone 3 of the superotemporal quadrant developed in the right eye at 4 months' follow-up in January 2001. The right eye received one 330-µg IV fomivirsen sodium injection while he awaited surgery for an IV ganciclovir implant. There was no ocular hypertension or inflammation in the eye following the injection. Retinitis became inactive, and he underwent surgery to receive the implant 3 weeks later. During a follow-up examination 1 month after the injection, new RPE pigmentary changes were found in the inferior quadrants previously unaf-

fected by retinitis (Figure 3B). The ERG revealed an absent rod response, 50% decrease in cone response, and a normal implicit time. Goldmann visual field testing of the right eye showed an absolute scotoma in the area corresponding to the previous CMV-affected superotemporal retina. Visual field testing results were normal in the area corresponding to the inferior retina. His vision remained 20/20 OD with no cataract formation at the last follow-up examination 3 months after fomivirsen injection.

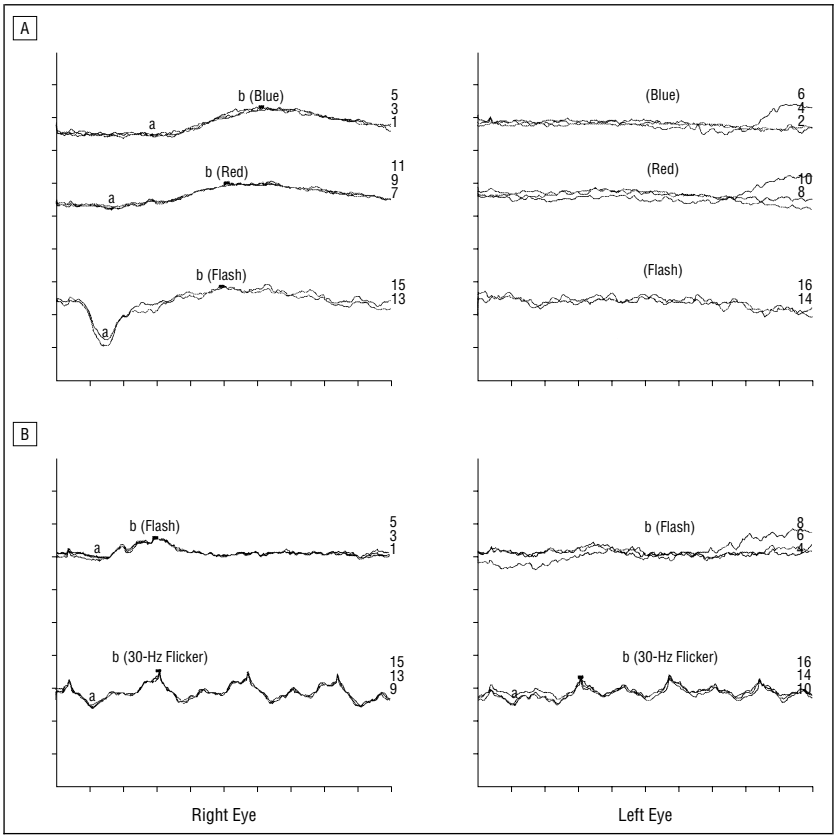

Figure 2. Case 1. Findings from electroretinogram (ERG) performed following intravitreal injection of fomivirsen sodium in the left eye. A, Scotopic flash ERG. B, Photopic flash ERG. The right eye results show normal scotopic and photopic responses. The left eye results show absent scotopic responses; absent flash photopic response; and decreased cone response to a 30-Hz stimulus with normal implicit time. a Indicates a wave and b, b wave. (Electroretinogram test manufacturer information: Nicolet Biomedical, Madison, Wis.)

Comment. Treatment of CMV retinitis with IV ganciclovir or foscarnet requires weekly injections. Intravitreal cidofovir is associated with prolonged ocular hypotony. Fomivirsen requires less frequent injections. The recommended induction dose of IV fomivirsen sodium is one 330-µg injection every other week for 2 doses. Subsequent maintenance doses are administered every 4 weeks after induction. In vitro studies have shown that fomivirsen is active against clinical isolates of human CMV and drug-resistant mutants of the virus.[8] In clinical trials, fomivirsen significantly delayed the progression of CMV retinitis in previously untreated patients and decreased CMV activity in patients with refractory CMV retinitis.[1] In the United States, fomivirsen is reserved as a second-line treatment for CMV retinitis in patients who are intolerant or unresponsive to other forms of treatment.

The only published toxicity profile study, to our knowledge, found that high concentrations of fomivirsen in the vitreous caused total retinal destruction in rabbit eyes.[9] However, even at lower concentrations equivalent to human eye injection doses, destruction of the photoreceptor outer segments and RPE cell changes were noted.[9,10]

Retinal pigment changes are among the ocular adverse reactions listed on the fomivirsen package label.[11] Frequency of retinal pigment changes is unknown. We used IV fo-

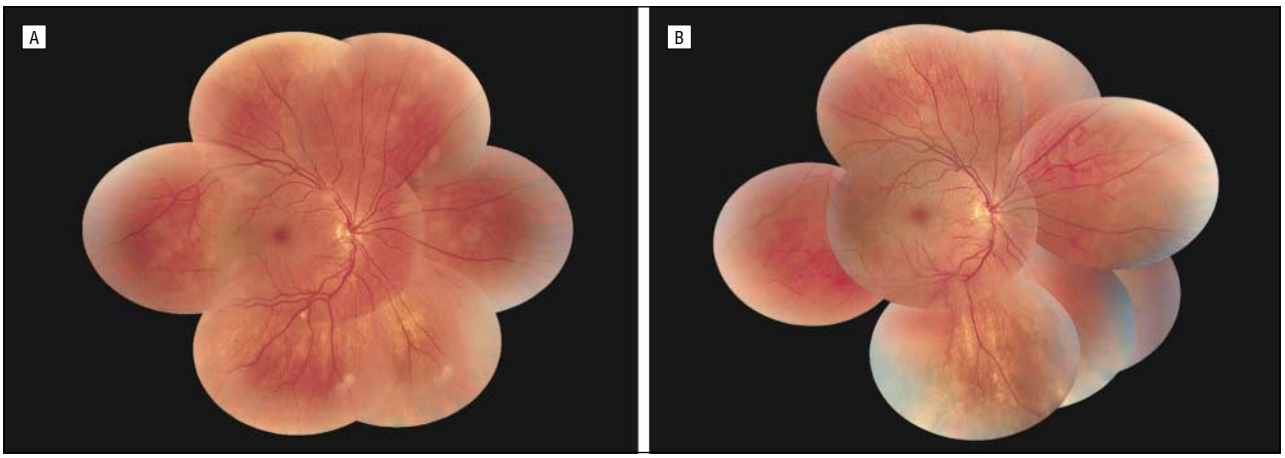

Figure 3. Case 2. A, Right fundus composite photograph prior to cytomegalovirus retinitis and prior to fomivirsen sodium injection. B, New pigmentary changes in inferior quadrants 1 month after 1 intravitreal fomivirsen injection.

mivirsen in 10 eyes of 9 patients from 1999 to 2001 as follows:

Eyes, No.	Injections, No.
6	1
1	2
1	3
1	5
1	23

Most of these patients are now deceased. Over 2 years, we noted pigmentary changes in only the 2 patients reported herein. Neither patient reported nyctalopia. Both patients died within a few months after diagnosis of retinal toxicity. Their pigmentary changes persisted until last follow-up. Electrophysiologic testing could not be repeated to evaluate for reversibility as our patients' systemic status progressively worsened. Abnormal ERG findings have been noted in patients with HIV, AIDS, and CMV retinitis.[1,2] In our patients, the reduction in ERG amplitudes of the treated eye is consistent with photoreceptor dysfunction affecting mainly the rod system. This reduction may have been induced by fomivirsen given that ERG responses in fellow eyes were normal. Case 2 developed pigmentary changes and photoreceptor dysfunction after only 1 injection. Neither patient had ever been treated with didanosine. Unlike the study by Amin et al,[6] visual field in our patient (case 2) was not constricted. His unaffected visual field and normal ERG testing implicit time may be consistent with relative sparing of the peripheral cones. The patient receiving 23 injections (Table) had no pigmentary changes. This eye underwent 2 ganciclovir implant procedures prior to our fomivirsen injections. Liquefied vitreous in this eye may have had more even diffusion of fomivirsen compared with other eyes with formed vitreous. Our case reports support the view that IV fomivirsen has a narrow therapeutic index[10] for retinal toxicity and should be used judiciously.

Sami H. Uwaydat, MD
Helen K. Li, MD
Galveston, Tex

This article was supported by an unrestricted grant from Research to Prevent Blindness Inc, New York, NY.

Corresponding author: Helen K. Li, MD, University of Texas Medical Branch, Department of Ophthalmology and Visual Sciences, 301 University Blvd, Galveston, TX 77555-1106 (e-mail: hli@utmb.edu).

1. Perry CM, Balfour JAB. Fomivirsen. *Drugs*. 1999;57:375-380.
2. de Semet MD, Meenken C, van den Horn GJ. Fomivirsen: a phosphorothioate oligonucleotide for the treatment of CMV retinitis. *Ocul Immunol Inflamm*. 1999;7:189-198.
3. Jalali S, Reed JB, Mizogushi M, et al. Effect of highly active antiretroviral therapy on the incidence of HIV-related cytomegalovirus retinitis and retinal detachment. *AIDS Patient Care STDS*. 2000;14:343-346.
4. Stone TW, Jaffe GJ. Reversible bull's-eye maculopathy associated with intravitreal fomivirsen therapy for cytomegalovirus retinitis. *Am J Ophthalmol*. 2000;103:242-243.
5. Hudson HL, Boyer DS, Kupperman BD. Future trends and experimental modalities in the therapeutics of cytomegalovirus retinitis. *Ophthalmol Clin North Am*. 1997;10:61-71.
6. Amin HI, Ai E, McDonald HR, Johnson RN. Retinal toxic effects associated with intravitreal fomivirsen. *Arch Ophthalmol*. 2000;188:426-427.
7. Hutcherson SL, Palestine AG, Cantrill HL, et al. Antisense oligonucleotide safety and efficacy for CMV retinitis in AIDS patients. Paper presented at: 35th Interscience Conference on Antimicrobial Agents and Chemotherapy; September 17, 1995; San Francisco, Calif. Abstract 204.
8. Anderson KP, Fox MC, Brown-Driver V, et al. Inhibition of human cytomegalovirus immediate-early gene expression by an antisense oligonucleotide complementary to immediate-early RNA. *Antimicrob Agents Chemother*. 1996;40:2004-2011.
9. Flores-Aguilar M, Besen G, Vuong C, et al. Evaluation of retinal toxicity of anti-cytomegalovirus and anti-herpes simplex virus antiviral phosphorothioate oligonucleotides ISIS 2922 and 4015. *J Infect Dis*. 1997;175:1308-1316.
10. Freeman WR. Retinal toxic effects associated with intravitreal fomivirsen [letter]. *Arch Ophthalmol*. 2001;119:458.
11. Vitravene [package insert]. Carlsbad, Calif: ISIS Pharmaceuticals, 1998.
12. Latkany PA, Holopigian K, Lorenzo-Latkany M, et al. Electroretinographic and psychophysical findings during early and late stages of human immunodeficiency virus infection and cytomegalovirus retinitis. *Ophthalmology*. 1997;104:445-453.

Sequential Branch Retinal Artery Occlusions Following Embolization of an Intracranial Meningioma

Therapeutic embolization is an accepted component in the management of vascular tumors, arteriovenous malformations, and active bleeding sites.[1] Complications are rare, but include infarction by unintended occlusion of vessels.[1] This occurs either when particles are injected from a proximally placed catheter or when they reflux from distal vessels during flushing.

Inadvertent occlusion of the ophthalmic or central retinal artery during external carotid artery embolization has been reported in 4 cases,[2-4] with immediate loss of vision. We report a case in which stepwise decline of vision related to

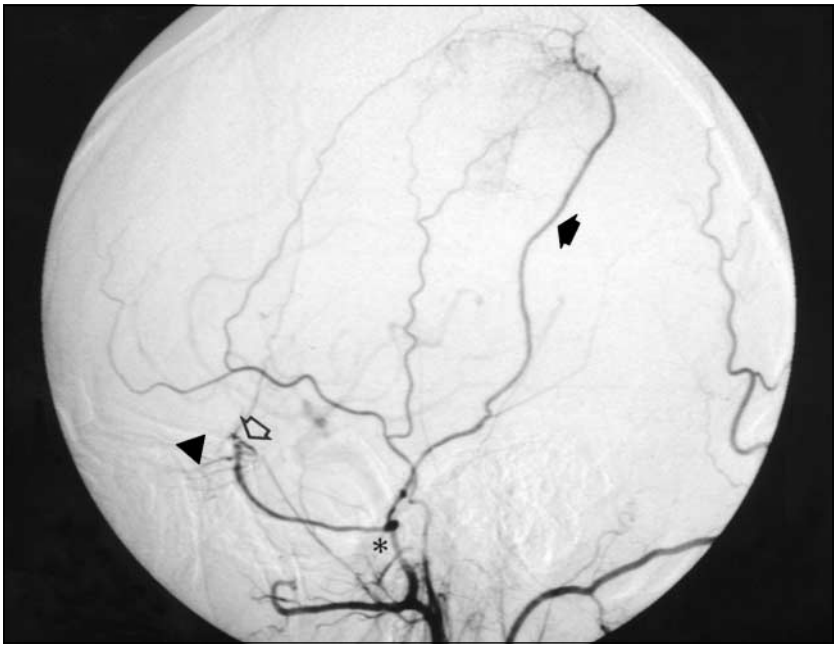

Figure 1. Preembolization left external carotid arteriogram showing middle meningeal artery (asterisk), parietal branch (solid arrow) to tumor (blush of small vessels), sphenoidal artery (open arrow), and ophthalmic artery (arrowhead).

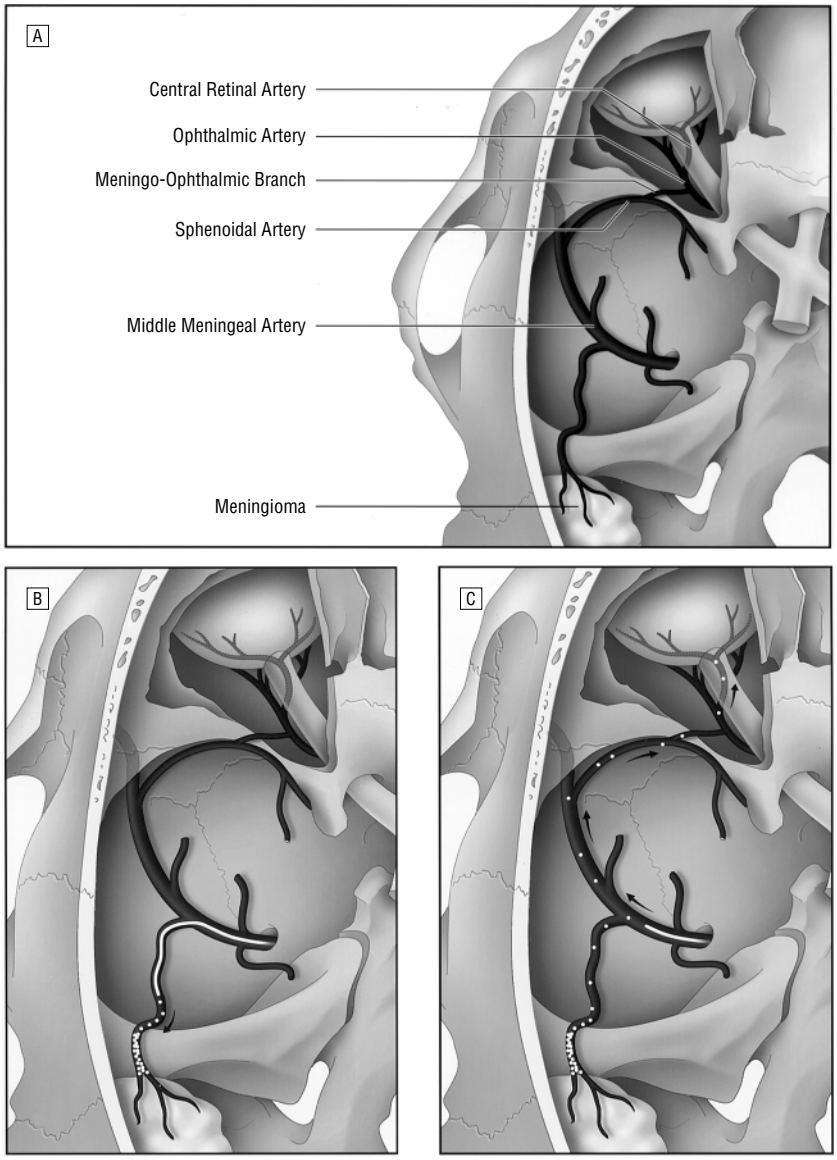

Figure 2. Schematic view of tumor and retinal embolization. A, Left middle meningeal branches, including supply to convexity meningioma, and anastomosis to ophthalmic artery. B, Catheter injecting polyvinyl alcohol (PVA) particles to occlude vessels in the tumor bed. It is positioned in a meningeal branch distal to the branch that leads to the sphenoidal artery. C, Catheter has been pulled back to proximal meningeal artery in preparation for postembolization arteriogram. The pull-back is done to avoid reflux of loose PVA particles lying in tumor vessels. Those PVA particles residing in the microcatheter are inadvertently flushed into meningeal branches that anastomose to sphenoidal, ophthalmic, and retinal arteries. These particles occlude retinal arterioles and, as they swell, sequentially infarct the retina.

progressive swelling of polyvinyl alcohol (PVA) particles lodged in retinal arterioles occurred throughout a period of 8 days.

Report of a Case. A 39-year-old woman underwent preresection embolization of a left-posterior frontal convexity meningioma. A preembolization arteriogram visualized the middle meningeal branches to the tumor, as well as an anastomosis to the ophthalmic artery via the sphenoidal artery (**Figure 1** and **Figure 2**A).

A 5F catheter was positioned in the left external carotid artery, and through this catheter, a 2F microcatheter was advanced into the middle meningeal artery supplying the lesion. The patient was systemically heparinized during the procedure. The catheter was positioned distal to the take-off of the sphenoidal artery (Figure 2B). To confirm that the catheter was beyond all dangerous anastomoses, provocative testing was performed by injecting amobarbital and lidocaine through the microcatheter.[5] When this testing produced no visual or other neurological deficits, 45- to 150-µm PVA particles suspended in radiographic contrast were slowly injected under fluoroscopic guidance into the tumor (Figure 2B). After slowed flow to the tumor was seen, the microcatheter was flushed with heparinized saline to evacuate any remaining particles in the catheter. To prevent reflux of emboli that had been deposited in the distal vessels supplying the tumor, the catheter was then pulled back proximal to the sphenoidal artery take-off (Figure 2C), and contrast was injected to confirm devascularization of the meningioma. As the contrast was injected, the patient reported a sudden flash of light in the left eye, and she soon developed an inferior scotoma on that side. Polyvinyl alcohol particles retained within the catheter had evidently been flushed into the ophthalmic artery anastomosis and reached the retinal arterioles (Figure 2C).

Ophthalmic examination performed 3 hours after the procedure disclosed visual acuities of 20/25 OD and 20/25 OS, and a left afferent pupil defect. Ophthalmoscopy revealed ischemic clouding of the retina superotemporally. Small, yellow-white particles were visible in retinal arterioles of the superior and inferior arcades, including the vessel that was occluded in the superior arcade (**Figure 3**A). A formal visual field test (Humphrey Field Analyzer Program 24-2; Humphrey Instruments, San Leandro, Calif) disclosed a corresponding inferonasal scotoma (Figure 3B). Seven days later, the patient reported a further decline in vision in her left eye. Ophthalmoscopy revealed enlargement of the superior retinal infarct (**Figure 4**A) and of the corresponding scotoma (Figure 4B). The particle in the proximal inferior temporal arteriole had enlarged. Despite 4 mg of oral dexamethasone taken 3 times daily, she developed loss of the superior field one day later. Visual acuity had fallen to 20/400; ophthalmoscopy showed that the particle in the inferior temporal artery had further

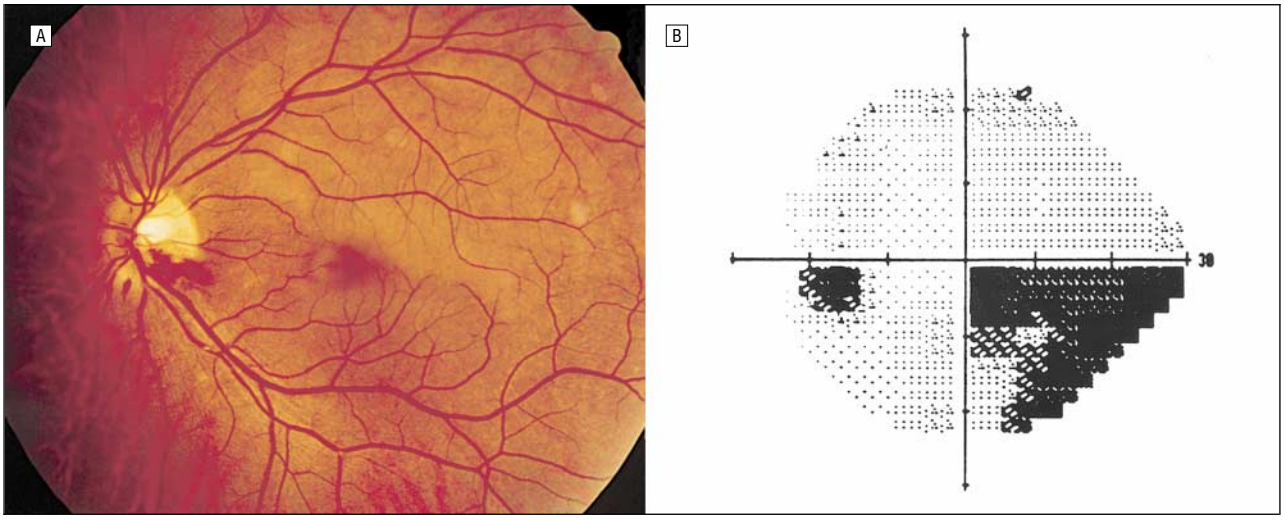

Figure 3. Fundus photographs and visual fields of the left eye on the day of procedure. A, Superior branch retinal artery occlusion as ischemic whitening. Several yellow-white polyvinyl alcohol particles are impacted within proximal retinal arterioles. B, Corresponding inferior nerve fiber bundle defect.

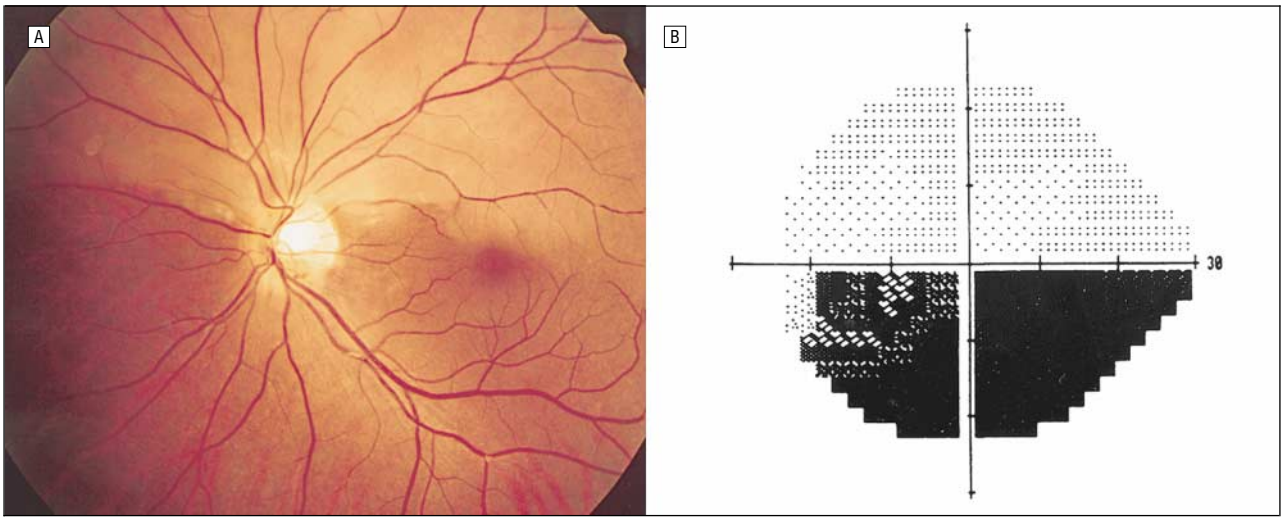

Figure 4. Fundus photographs and visual fields of the left eye 7 days after the procedure. A, Retinal infarction has extended nasally. B, Enlargement of visual field defect, corresponding to enlarged area of infarction.

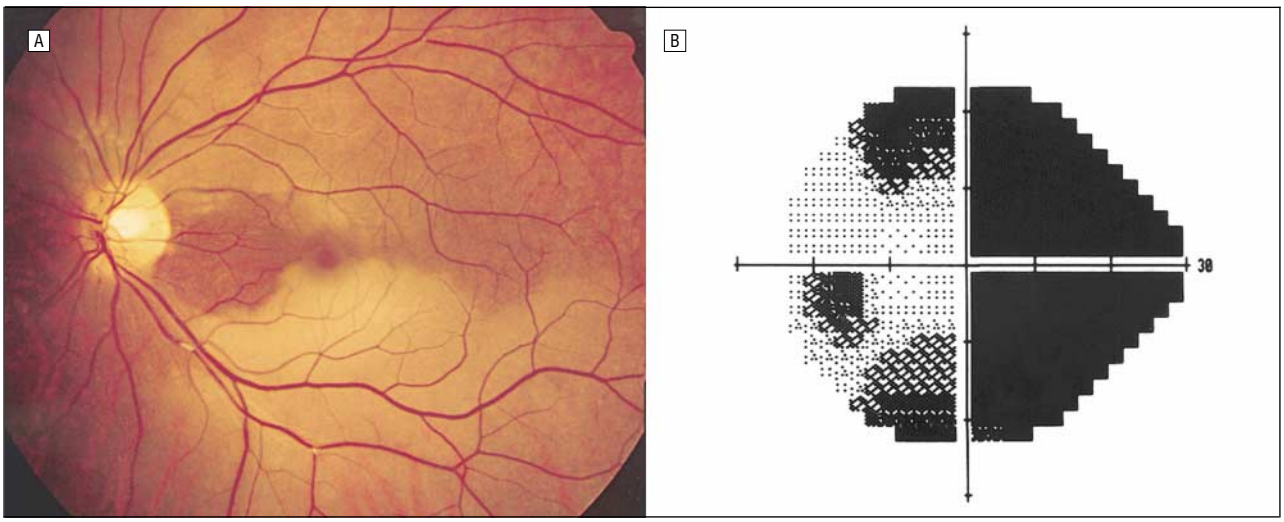

Figure 5. Fundus photographs and visual fields of the left eye 8 days after the procedure. A, Retinal infarction now also involves the inferior branch artery. The particle lodged in the proximal inferior temporal retinal arteriole has enlarged. B, Visual field defect now involves the upper field, corresponding to new infarction of the inferior retina.

enlarged, that the inferior retina was now infarcted (**Figure 5**A), and that the scotoma involved most of the visual field (Figure 5B). Follow-up examination 2 months later showed a pale left optic disc and no change in visual function.

Comment. Our patient had a rare complication of therapeutic PVA embolization, namely, inadvertent occlusion of branches of the central retinal artery. This complication is based on known anastomoses between the external carotid circulation and the ophthalmic artery.[6-8] External carotid branches may replace the internal carotid artery as the predominant supply of the ophthalmic artery in 5% of patients with otherwise normal cephalic vessels[7] and in a much higher proportion in those with arteriosclerosis, which preferentially affects the internal carotid system.

Aware that this anastomosis might cause a serious problem, our interventional neuroradiologist (J.P.D.) positioned the catheter far distal to it, performed preembolization pharmacologic provocative testing, embolized gently without repositioning the catheter, and flushed the catheter after embolization. However, these techniques failed to prevent errant emboli from reaching the retinal vessels. Some particles were undoubtedly present in the catheter even after careful flushing with saline, suggesting that it may not be possible to completely remove all particles from the microcatheter.

Four additional measures might have prevented this complication. First, embolization could have been performed with particulate agents too large to enter the anastomotic pathway, but there are 2 drawbacks to this maneuver. The first is that the size of anastomoses and particles vary, making it impossible to be sure that some particles will not enter the anastomosis. The second drawback is that large particles are less effective in devascularizing the tumor bed.[9] The second measure would have been to selectively occlude the anastomosis with a microcoil prior to embolization of the tumor bed. This would have prevented small particles from entering the anastomosis, but this is not feasible if the anastomosis is too small or tortuous to be selectively catheterized. A third preventive measure would have been to remove the microcatheter used for injecting emboli, and to then introduce a new microcatheter to perform the postembolization arteriographic studies. The drawback to this measure is that if further embolization of the tumor through a distal site is found to be necessary, additional time and risk would be added to the procedure. Fourth, we could have injected contrast dye during the follow-up arteriogram through the guiding catheter positioned in the external carotid artery, rather than through the microcatheter. This would have avoided the need to manipulate the microcatheter and would have virtually eliminated the risk of injecting retained PVA emboli. The main disadvantage of this otherwise practical solution is that a guiding catheter must have a large enough inner lumen to allow passage of the inner microcatheter and leave enough room around it to inject viscous contrast material. Perhaps a larger 6F guiding catheter would have been preferable in this case.

An unusual aspect of our case is the sequential nature of the branch retinal artery occlusions occurring throughout a period of 8 days. We attribute this phenomenon, (not previously reported) to progressive swelling and/or thrombus formation in these vessels. Swelling is a feature that makes PVA a useful agent for therapeutic embolization, but that increases the possibility that errant PVA particles will cause neurological deficits. Unfortunately, there is no antidote to reverse the swelling of the particles.

Although our case has unusual features, we doubt that inadvertent occlusion of the retinal artery during preoperative embolization via the external carotid system is as rare as the published literature would suggest. An authoritative textbook[10] describes 2 unpublished cases. In presenting this case to gatherings of ophthalmologists and neuroradiologists, many members of our audiences have told us of similar experiences.

Tina Turner, MD
Jonathan D. Trobe, MD
John P. Deveikis, MD
Ann Arbor, Mich

Corresponding author: Jonathan D. Trobe, MD, Kellogg Eye Center, 1000 Wall St, Ann Arbor, MI 48105 (e-mail: jdtrobe@umich.edu).

1. Taylor W, Rodesch G. Recent advances: interventional neuroradiology. *BMJ*. 1995;311:789-792.
2. Soong HK, Newman SA, Kumar AAJ. Branch artery occlusion: an unusual complication of external carotid embolization. *Arch Ophthalmol*. 1982;100:1909-1911.
3. Mames RN, Snady-McCoy L, Guy J. Central retinal and posterior ciliary artery occlusion after particle embolization of the external carotid artery system. *Ophthalmology*. 1991;98:527-531.
4. Shimizu Y, Kiyosawa M, Miura T, Takahashi A, Tamai M. Acute obstruction of the retinal and choroidal circulation as a complication of interventional angiography. *Graefes Arch Clin Exp Ophthalmol*. 1993;231:43-47.
5. Deveikis JP. Sequential injections of amobarbital sodium and lidocaine for provocative testing in the external carotid circulation. *AJNR Am J Neuroradiol*. 1996;17:1143-1147.
6. Gillilan LA. The collateral circulation of the human orbit. *Arch Ophthalmol*. 1961;65:684-694.
7. Hayreh SS. Arteries of the orbit in the human being. *Br J Surg*. 1963;50:938-953
8. Ahn HS, Kerber CW, Deeb ZL. Extra- to internal arterial anastomoses in therapeutic embolization: recognition and role. *AJNR Am J Neuroradiol*. 1980;1:71-75.
9. Wakhloo AK, Juengling FD, Velthoven W, Schumacher M, Hennig J, Schwechheimer K. Extended preoperative polyvinyl alcohol microembolization of intracranial meningiomas: assessment of two embolization techniques. *AJNR Am J Neuroradiol*. 1993;14:571-582.
10. Kupersmith MJ, Berenstein A. Embolic and noninflammatory occlusive vascular disease of the visual and ocular motor system. In: Kupersmith MJ, Berenstein A. *Neurovascular Neuroophthalmology*. Berlin,Germany: Springer-Verlag; 1993:126, 358.

Bilateral Vasoproliferative Retinal Tumors With Identical Localization in a Pair of Monozygotic Twins

Vasoproliferative retinal tumors are benign vascular tumors of unknown origin that are usually located in the periphery of the lower ocular fundus. They became a clinical entity in 1995 when Shields et al[1] coined the term "vasoproliferative tumors of the ocular fundus." Before then, these lesions were called presumed acquired hemangiomas, angioma-like lesions, or peripheral retinal telangiectasis. Histological examinations of vasoproliferative retinal tumors have demonstrated glial and vascular proliferation.[2,3] These tumors can develop idiopathically or can be secondary to other retinal disorders. Concomitant phenomena, such as exudative retinal detachment, lipid exudates, and macular

Figure 1. A fundus photograph shows vasoproliferative retinal tumors in the right eye of patient 1. The tumors are located in the inferior part of the fundus and show marked exudation.

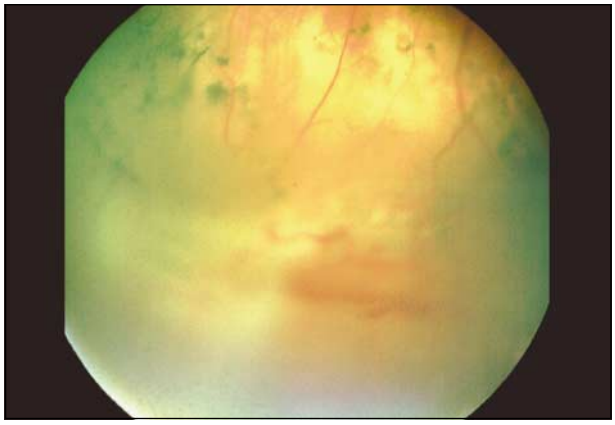

Figure 2. A fundus photograph shows a vasoproliferative retinal tumor with concomitant retinal detachment in the left eye of patient 2.

edema or hemorrhages, can lead to the deterioration of vision.

Report of Cases. A pair of 58-year-old monozygotic female twins sought care because of visual deterioration. Both sisters had bilateral multiple peripheral vasoproliferative retinal tumors (**Figure 1** and **Figure 2**) of nearly identical spread and localization in the inferior part of the ocular fundus. Fluorescein angiography demonstrated extensively vascularized tumors that were filling from the retinal vessels in the early phase and consecutive marked fluorescein leakage in the late phase.

Because of the relatively low thickness of the tumors (1.5 mm and 2.0 mm), patient 1 was treated with bilateral cryotherapy. Her sister, who had thicker tumors (4.6 mm and 2.5 mm), underwent ruthenium 106 brachytherapy in both eyes. Both cryotherapy and ruthenium 106 brachytherapy led to regression of the vasoproliferative retinal tumors. Subsequent examination of the twins' DNA band-sharing rates confirmed monozygosity.

Comment. To our knowledge, this is the first description of vasoproliferative retinal tumors in a pair of monozygotic twins. Although vasoproliferative retinal tumors usually develop unilaterally, our 2 patients showed the typical clinical picture.[1,2] This consists of retinal tumors characterized by a pink to yellow appearance on funduscopy that are associated with intraretinal hemorrhage, intraretinal or subretinal exudate, and hyperpigmentation of the retinal pigment epithelium. Fluorescein angiography shows rapid filling of the tumors through a nondilated retinal-feeding arteriole and diffuse leakage in the venous and late phase of the angiogram. Our patients showed no abnormalities in the lipid metabolism and no underlying systemic diseases.

During the differential diagnosis, von Hippel–Lindau disease was excluded based on its not being present in the family history, the absence of additional clinical features of von Hippel-Lindau disease, and a negative molecular genetic test for a mutation of the *VHLD* gene.[4] In addition, the age of onset in our patients was inappropriate for von Hippel–Lindau disease.

Although some similarities to familial exudative retinopathy may exist, the former includes a family history for this with autosomal dominant or X-linked inheritance, which was not the case in our patients. Moreover, familial exudative retinopathy is not associated with retinal tumors, and the age of onset is much younger.

Coats disease also develops at a much younger age, rarely occurs bilaterally, usually affects boys, and is characterized in advanced cases by massive exudation at the posterior pole. Similar tumorous lesions rarely occur in this disease, even in very advanced stages.

The pathogenesis of vasoproliferative retinal tumors has yet to be explained. A study by Shields et al[1] in 103 patients showed that about three quarters of vasoproliferative retinal tumors are primary and about one quarter are secondary to other diseases. In our patients, no other eye disease was evident.

Irvine et al[3] suggested renaming vascular retinal tumors as "reactionary retinal glioangiosis." This suggestion reflects the hypothesis that the vessel proliferation is caused by the release of vasoproliferative factors from the proliferating neuroglial tissue. However, the actual trigger and stimulus for this proliferation remain unclear. Moreover, we do not know whether the neuroglial proliferation is already present, nor do we know what triggers it in primary cases, such as the ones described here.

The tumors in our patients were unusually similar in localization and extension and had also developed bilaterally in a pair of monozygotic, and thus genetically similar, twins. The absence of underlying systemic diseases leads us to assume that these are primary cases. This suggests, however, that the pathogenesis could be genetically determined, to a certain degree, and not entirely dependent on reactive changes.

Joachim Wachtlin, MD
Heinrich Heimann, MD
Claudia Jandeck, MD
Klaus M. Kreusel, MD
Nikolaos E. Bechrakis, MD
Ulrich Kellner, PhD
Michael H. Foerster, PhD
Berlin, Germany

This study was presented in part at the 10th International Congress of Ocular Oncology, Amsterdam, the Netherlands, June 19, 2001.

We thank Martin Digweed, PD, for performing the DNA analysis for monozygosity and Hartmut P. H. Neuman, PhD, for screening for a mutation in the VHLD *gene.*

Corresponding author and reprints: Joachim Wachtlin, MD, Department of Ophthalmology, University Medical Center Benjamin Franklin, Free University of Berlin, Hindenburgdamm 30, 12200 Berlin, Germany (e-mail: wachtlin@ukbf.fu-berlin.de).

1. Shields CL, Shields JA, Barrett J, De Potter P. Vasoproliferative tumors of the ocular fundus: classification and clinical manifestations in 103 patients. *Arch Ophthalmol.* 1995;113:615-623.
2. Heimann H, Bornfeld N, Vij O, et al. Vasoproliferative tumours of the retina. *Br J Ophthalmol.* 2000;84:1162-1169.
3. Irvine F, O'Donnell N, Kemp E, Lee WR. Retinal vasoproliferative tumors: surgical management and histological findings. *Arch Ophthalmol.* 2000;118:563-569.
4. Stolle C, Glenn G, Zbar B, et al. Improved detection of germline mutations in the von Hippel-Lindau disease tumor suppressor gene. *Hum Mutat.* 1998;12:417-423.

Figure 1. Case 1. Left fundus photograph taken at 7 months' gestation showing a large inferior exudative detachment overlying the circumscribed choroidal hemangioma.

Choroidal Hemangiomas With Exudative Retinal Detachments During Pregnancy

We describe the clinical course of 3 cases of circumscribed, choroidal hemangiomata that were associated with progressive exudative detachments during pregnancy.

Report of Cases. *Case 1.* A 31-year-old woman, gravida 1, visited our affiliation when 7 months pregnant with a 4-week history of blurred vision in the left eye. She had a cutaneous hemangioma of the left eyelid, dilated episcleral vessels, and amblyopia. Her visual acuity was 20/13 OD and 20/1200 OS. Left fundoscopy revealed an inferior temporal, orange choroidal mass with some subretinal fibrosis. Overlying the mass was a large inferior retinal detachment with shifting fluid (**Figure 1**). The mass (excluding the overlying fluid) was 12.0×12.0 mm wide and 7.4 mm high; it demonstrated high internal reflectivity on ocular ultrasound. Right fundoscopy results were unremarkable.

The diagnosis was a circumscribed choroidal hemangioma in Sturge-Weber syndrome associated with an exudative detachment. One month later, the exudative detachment had significantly increased in size. The patient's visual acuity subsequently deteriorated to light perception. She was at risk for developing a total retinal detachment, and therefore underwent an elective cesarean section at 37 weeks' gestation.

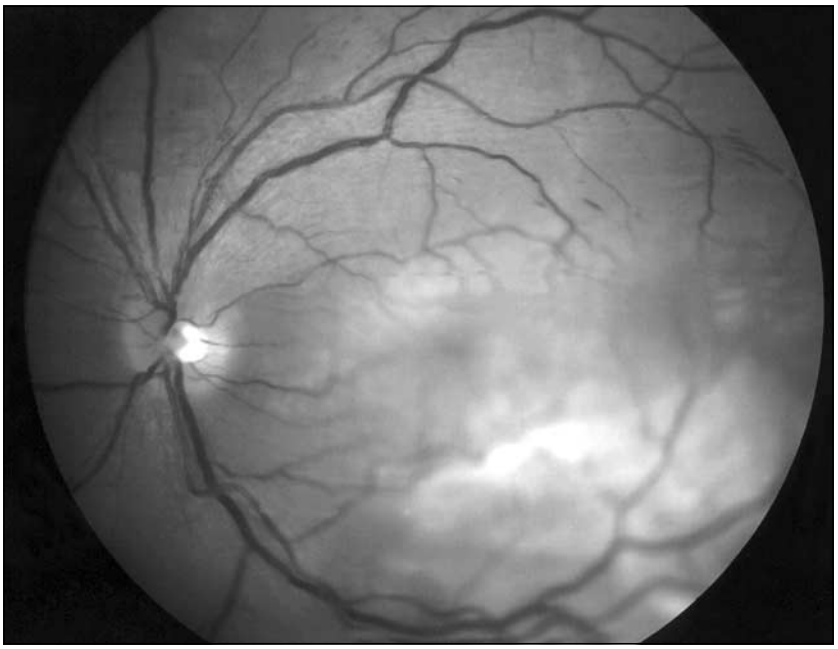

Figure 2. Case 1. Left fundus photograph taken at 5 weeks' post partum, prior to any thermotherapy. There is a marked reduction in the subretinal fluid in this eye, which had clinical evidence of a choroidal hemangioma with some subretinal fibrosis.

Five weeks' post partum, there was a marked reduction in the size of the retinal detachment (**Figure 2**), and her visual acuity improved to hand motions. She had one treatment of transpupillary diode thermotherapy. Five months later, the retinal detachment had completely resolved, and the hemangioma was replaced by scar tissue. Her pin-

Figure 3. Case 2. Right fundus photograph taken at 31 weeks' gestation showing a large dome-shaped detachment at the posterior pole, which is associated with retina striae and cystoid macular edema.

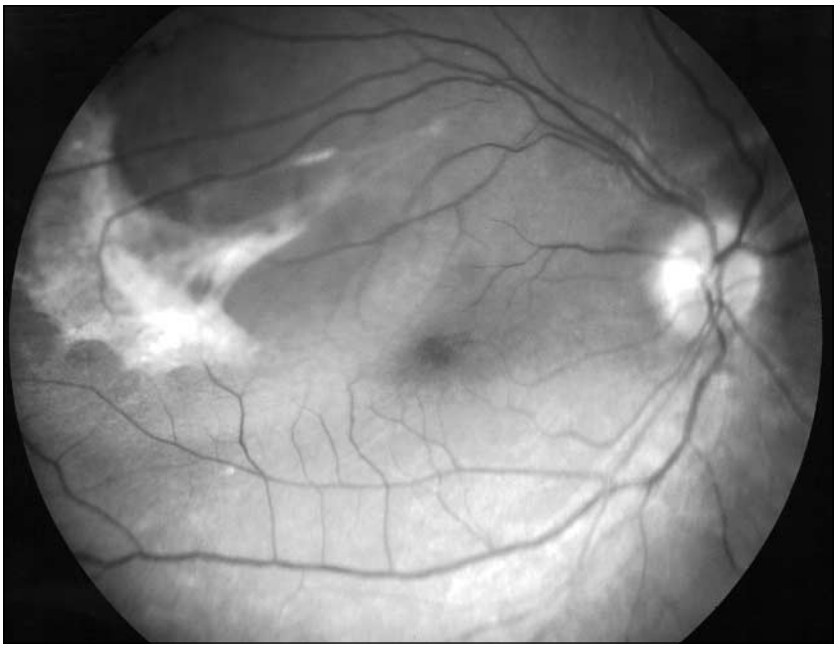

Figure 4. Case 2. Right fundus photograph taken at 9 months' post partum with no treatment. The retinal detachment has resolved; subretinal fibrosis is seen associated with the circumscribed choroidal hemangioma.

hole corrected acuity improved to 20/80 OS.

Case 2. A 26-year-old woman, gravida 1, was referred when 31 weeks pregnant. She had a congenital cutaneous angioma along the first division of the right trigeminal nerve involving the right upper eyelid, with dilated episcleral veins on the same side. Her visual acuity was 20/220 OD and 20/60 OS. Fundoscopy revealed a large dome-shaped detachment at the posterior pole associated with cystoid macular edema (**Figure 3**).

She had no visual symptoms because the right eye was amblyopic. Underlying the exudative detachment was a circumscribed, orange choroidal mass that showed high internal reflectivity on B-scan.

The diagnosis was a circumscribed choroidal hemangioma in Sturge-Weber syndrome associated with an exudative detachment. Two weeks later, her acuity deteriorated to counting fingers as the subretinal fluid extended beyond the posterior pole to detach the inferior retina.

No intervention was undertaken during her pregnancy, but the intention was to treat the patient with radiotherapy after the delivery. She was examined 4 months after childbirth. When visual acuity started to improve to 20/400 OD, the subretinal fluid was resolving spontaneously. At 9 months' post partum, visual acuity returned to 20/120 OD, and the retina was entirely flat. An isolated circumscribed choroidal hemangioma was seen at the right posterior pole with associated subretinal fibrosis (**Figure 4**). Four years later, the retina remains flat. During the course of follow-up the choroidal hemangioma has not changed in size. The patient has not had any further pregnancies.

Case 3. A 19-year-old woman visited our affiliation 10 months after the birth of her first child. She complained of blurred vision and micropisa in the right eye, which started when she was 8 months pregnant. Her vision had not improved following delivery. Her visual acuity at initial visit was 20/60 OD and 20/20 OS. She had a dome-shaped, orange choroidal mass at the posterior pole and a large inferior exudative detachment. She did not have a facial angioma or any episcleral abnormality.

The diagnosis was a solitary, circumscribed choroidal hemangioma with an associated exudative detachment. The patient was treated with argon laser photocoagulation. One month later, her vision improved, but on fundal examination, the hemangioma had not responded, and the inferior detachment remained unchanged. Two further applications of argon laser photocoagulation were administered, but the retinal detachment did not resolve. The patient was lost to follow-up.

Five years after delivery, the patient returned with an acuity of no light perception, as there was a total retinal detachment. Eight months later, the eye became painful as the intraocular pressure rose to 41 mm Hg. A right enucleation was subsequently performed for uncon-

trolled secondary glaucoma. The pathology report confirmed the diagnosis of a choroidal hemangioma.

Comment. Little is known about the behavior of choroidal hemangioma in pregnancy. There is one previous report of leakage from a circumscribed choroidal hemangioma in pregnancy, and the fluid resolved following full-term normal delivery.[1]

In our case series, exudative retinal detachments developed during the third trimester of pregnancy. All the mothers were primigravida, but none had symptoms or signs of pre-eclampsia. Blood pressure was monitored during the pregnancies. Cases 1 and 2 had Sturge-Weber syndrome. The most frequently described ocular manifestation in this syndrome is a flat diffuse choroidal hemangioma, giving the fundus the typical "tomato ketchup" appearance, but recently circumscribed elevated choroidal hemangiomatas have been described.[2,3]

Isolated hemangiomas are known to grow very slowly.[4] Shields et al[5] compared ultrasound measurements of an enlarging circumscribed choroidal hemangioma with histology reports at enucleation. They demonstrated that enlargement was the result of venous congestion and was not due to cell multiplication.[5] The altered hemodynamic state in pregnancy may result in engorgement of the vascular networks within a hemangioma, resulting in increased transudation of fluid into the subretinal space. This could explain the observed leakage from a choroidal hemangioma in the late stages of pregnancy. There may also be hormonal influence on the growth of vascular malformations; however, this remains speculative.

This series demonstrates that following delivery, the subretinal fluid tends to reabsorb, and the hemangioma ceases to leak. The retina was flat at 5 months' post partum following one episode of thermotherapy in case 1. The retina was flat at 9 months' post partum with no treatment in case 2. However, resolution of an exudative detachment after delivery is not always the rule, even following the supplementary argon laser photocoagulation treatment. The third patient suffered from a total retinal detachment and secondary glaucoma, and she finally required enucleation.

In summary, the effect of pregnancy on choroidal hemangiomas is unknown, although in select situations, there may be an apparent increased exudation and enlargement of the lesion. While 2 of these 3 cases stabilized during the postpartum timeframe, the clinical course may be quite variable.

Victoria M. Cohen, MRCOphth
Paul A. Rundle, FRCOphth
Ian G. Rennie, FRCS, FRCOphth
Sheffield, England

No grants or sponsors were used for this study.

The authors have no commercial interest or conflicting relationship.

Corresponding author: Victoria Cohen, MRCOphth, Department of Ophthalmology, Addenbrooke's Hospital, Hills Road, Cambridge, England CB2 2QQ (e-mail: victoria@victoriac.freeserve.co.uk).

1. Pitta C, Bergen R, Littwin S. Spontaneous regression of a choroidal haemangioma following pregnancy. *Ann Ophthalmol*. 1979;11:772-774.
2. Scott IU, Alexandrakis G, Cordahi GJ, Murray TG. Diffuse and circumscribed choroidal hemangiomas in a patient with Sturge-Weber syndrome. *Arch Ophthalmol.* 1999;117:406-407.
3. Cheung D, Grey R, Rennie IG. Circumscribed choroidal hemangioma in a patient with Sturge Weber Syndrome. *Eye*. 2000;14:238-239.
4. Medlock RD, Augsburger JJ, Wilkinson CP, et al. Enlargement of circumscribed choroidal hemangiomas. *Retina.* 1991;11:385-388.
5. Shields JA, Stephens RF, Eagle RC, et al. Progressive enlargement of a circumscribed choroidal hemangioma. *Arch Ophthalmol.* 1998;110:1276-1278.

Microsporidia-Induced Sclerouveitis With Retinal Detachment

Microsporidia are a rare but increasingly important group of protozoa that cause infections in vertebrates and invertebrates. Ocular involvement affecting mostly the cornea and conjunctiva in otherwise healthy patients has only occasionally been described.[1-4] To the best of our knowledge, posterior segment involvement has not been described to date. We report a case of microsporidia-induced sclerouveitis with retinal detachment.

Report of a Case. A 66-year-old woman with a 6-year history of psoriasis had a progressive loss of vision in her right eye during the previous 6 months. Her visual acuity was hand motions OD. The conjunctiva showed moderate chemosis and increased redness (**Figure 1**A). The cornea was clear with a moderate amount of pigmented endothelial precipitates inferiorly. The anterior chamber was shallow, with trace cells and flare. The pupil was round and miotic with a reduced response to bright light. The lens had a dense cataract that prevented visualization of the posterior segment of the eye. Measurement with applanation tonometry was 30 mm Hg. An ultrasonographic B-scan examination showed a superior serous choroidal detachment and complete retinal detachment without funnel formation (Figure 1B).

A diagnostic vitrectomy was performed, and the lens with cataract was removed. On examination of the posterior segment of the eye, a complete serous retinal detachment was noted. The diagnosis of infection with microsporidia was made 3 days following surgery, and the patient was prescribed a systemic medication with albendazole at a dose of 400 mg twice a day. Eight months following the initial surgery, the eye was completely quiet; the silicone oil was removed, and an anterior chamber lens was implanted. Four months later the eye was still quiet, and the patient's best-corrected visual acuity was 20/200 OD.

Examinations of the vitreous aspirate included detection of the level of antibodies in both the vitreous humor and serum against varicella-zoster virus, herpes simplex virus, cytomegalovirus, and toxoplasmosis. In all instances, the antibody levels of the serum and vitreous were similar, so an intraocular synthesis of antibodies was ruled out.

Examination of the slides stained with hematoxylin-eosin and periodic acid–Schiff revealed erythrocytes, a few lymphocytes, and neutrophilic cells. A few lytic cells and free-melanin pigment granules were observed. No abnormal lymphocytes were present, and no bacteria or fungi were seen. One slide contained several spores that had features consistent with microsporidia

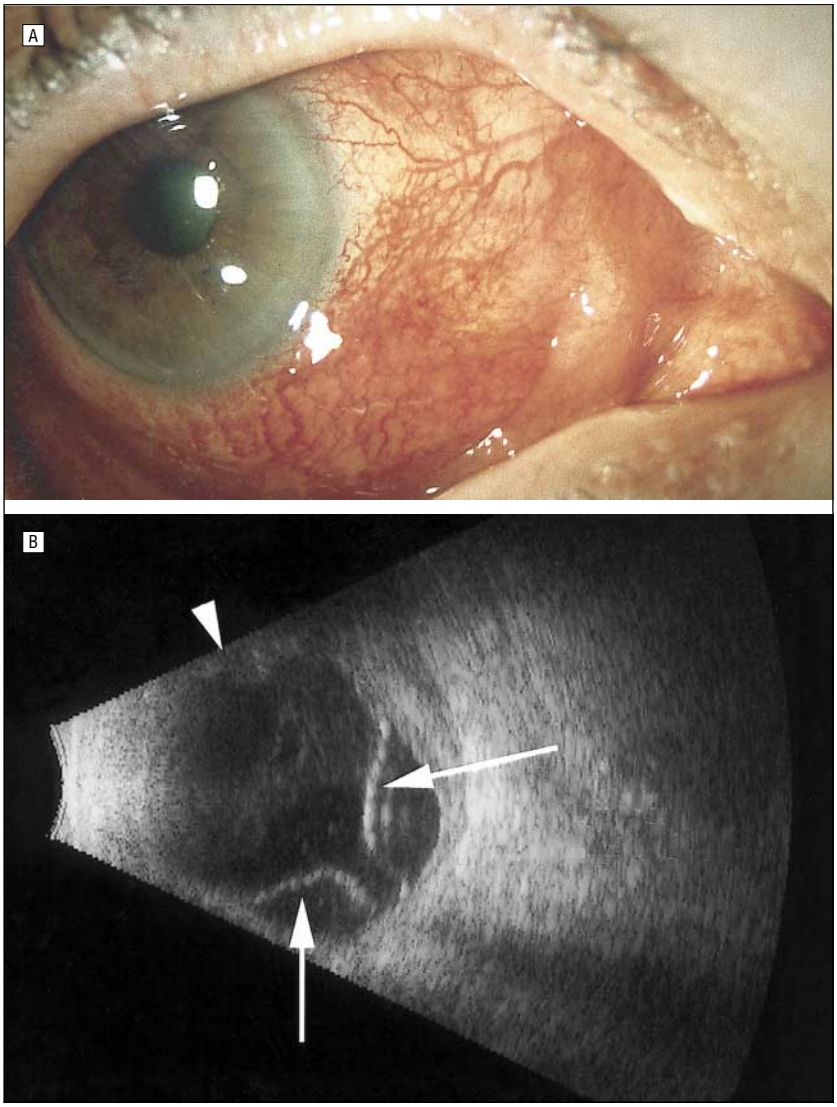

Figure 1. A, Slitlamp photograph of the right eye, with a history of progressive loss of vision for the past 6 months. The nasal conjunctiva is swollen and shows an increased redness. The cornea is clear with only a few endothelial precipitates. The visual acuity is hand motions OD because of a cataractous lens and complete retinal detachment. B, Ultrasonographic B-scan of the right eye. A complete retinal detachment is present (arrows), and there is an anterior serous detachment of the choroid (arrowhead).

(**Figure 2**A). The positive results of staining with Uvitex 2B further confirmed the diagnosis (Figure 2B).

Comment. To date, 4 cases of stromal keratitis have been reported, all of which occurred in immunocompetent patients.[1-4] The genera found include *Encephalitozoon*[1] and *Nosema*.[2-4] The number of reports of keratoconjunctivitis are increasing and generally relate to patients who are immunoincompetent, most of whom have acquired immunodeficiency syndrome. Specific microsporidia identified in these cases include *Encephalitozoon hellum*, *Trachipleistophora* species, *Microsporidium ceylonensis*, *Microsporidium africanum*, *Encephalitozoon intestinalis*, and *Encephalitozoon cuniculi*.

To our knowledge, this is the first report of severe sclerouveitis with retinal detachment caused by microsporidia. It is interesting that no such cases have previously been reported. One may speculate that thorough cytopathologic examinations of vitreous aspirates are infrequently performed in cases of uveitis of unknown origin. Fluorescent staining with Uvitex 2B clearly showed that the responsible organism in this case was a microsporidium.

Physicians confronted with a case of uveitis of unknown origin should include the possibility of microsporidia in their differential diagnosis.

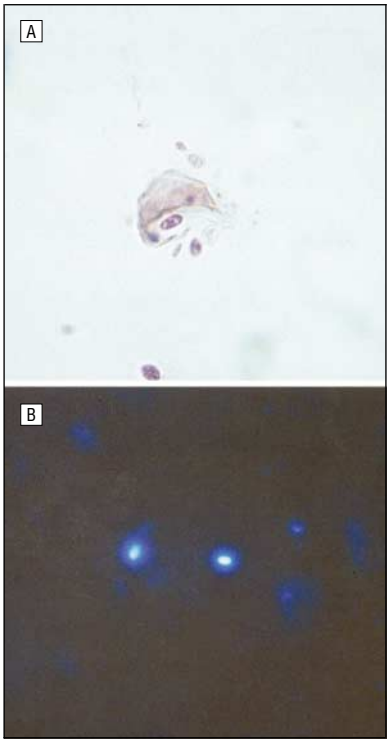

Figure 2. A, Light microscopy of the protozoan revealed by examination of the vitreous aspirate. According to its morphologic characteristics, this protozoan is from the *Nosema* genus (hematoxylin-eosin, original magnification ×250). B, Fluorescent stain with Uvitex 2B of a slide from the diagnostic vitrectomy. The slide was examined under a UV microscope at a wavelength of 395 to 415 nm. The bright white spots represent the chitin in the spore walls of the microsporidia (fluorescence, original magnification ×250).

Holger Mietz, MD
Caspar Franzen, MD
Thomas Hoppe, MD
Cologne, Germany
K. Ulrich Bartz-Schmidt, MD
Tübingen, Germany

Corresponding author: Holger Mietz, MD, Department of Ophthalmology, University of Cologne, 50924 Koeln, Germany (e-mail: h.mietz@uni-koeln.de).

1. Ashton N, Wirasinha PA. Encephalitozoonosis (nosematosis) of the cornea. *Br J Ophthalmol*. 1973;57:669-674.
2. Pinnolis M, Egbert PR, Font RL, Winter FC. Nosematosis of the cornea: case report, including electron microscopic studies. *Arch Ophthalmol*. 1981;99:1044-1047.
3. Font RL, Samaha AN, Keener MJ, Chevez-Barrios P, Goosey JD. Corneal microsporidiosis: report of case, including electron microscopic observations. *Ophthalmology*. 2000;107:1769-1775.
4. Davis RM, Font RL, Keisler MS, Shadduck JA. Corneal microsporidiosis: a case report including ultrastructural observations. *Ophthalmology*. 1990; 97:953-957.

Unilateral Manifestation of Melanoma-Associated Retinopathy

A rare complication of cutaneous melanoma is the development of melanoma-associated retinopathy (MAR), a condition characterized by the acute onset of night blindness, persistent pulsating photopsias, and constriction of the visual field.[1] The pathogenetic mechanisms of the syndrome have been clarified by the detection of immunoglobulins directed against bipolar cells of the retina.[2] The symptoms generally spread to the other eye within an interval of 4 days to 2 months.[3,4] We report a case of MAR that remained unilateral during an observation period of 18 months.

Report of a Case. A cutaneous malignant melanoma was removed from the left leg of a 45-year-old woman in 1992. Because a systematic search revealed no metastasis, no further therapy was administered.

One evening in January 2000, she suddenly experienced difficulty seeing in dark conditions through her right eye, which greatly interfered with her stereovision. She also reported shimmering lights that fluctuated in brightness.

Because an ophthalmological examination demonstrated good visual acuity and no fundus alterations, the patient's complaints were judged to be of psychic origin. Four months later, a metastatic cutaneous melanoma was removed from her left leg. She underwent chemotherapy and was referred to our electrophysiological laboratory because of her persisting visual complaints.

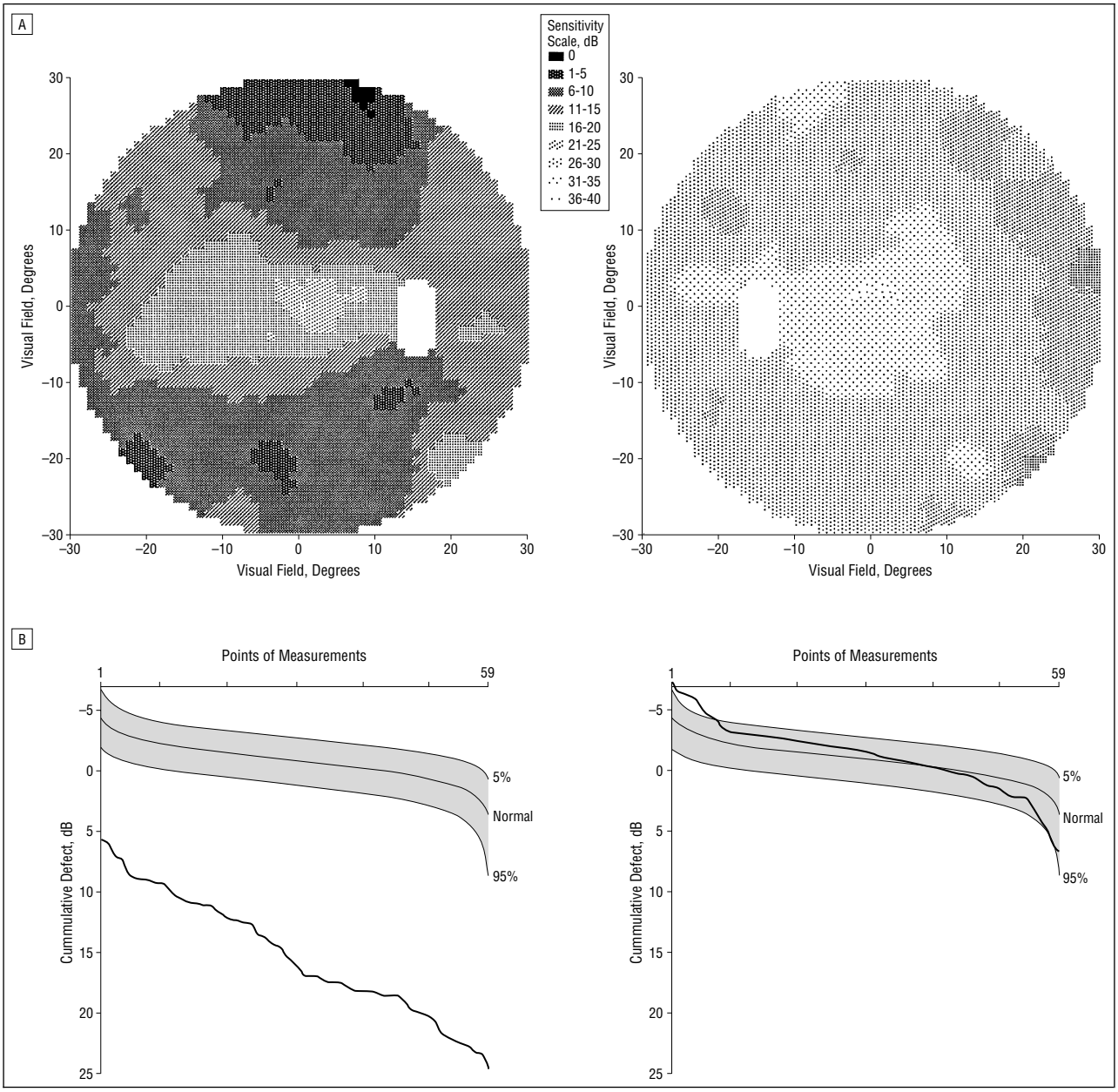

Figure 1. A, Visual field of the right eye (left) and left eye (right) estimated using Octopus equipment. The x- and y-axes represent dimensions of the visual field in degrees. B, Cumulative defect curves (Bebie curve) from the 59 central points in rank order cumulative sensitivity distribution.

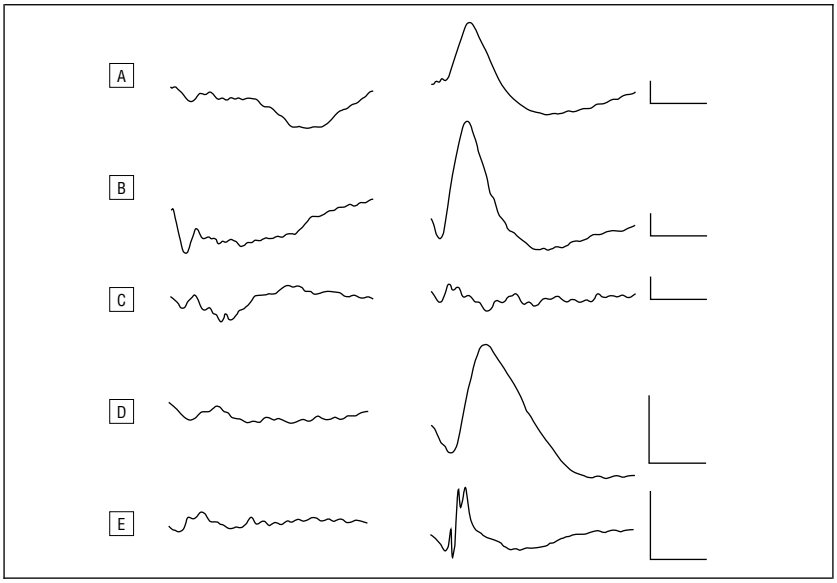

Figure 2. Electrophysiological recordings from the right eye (left) and left eye (right) of the patient. A, Scotopic, rod-isolated response. B, Maximal, dark-adapted response. C, Electroretinographic (ERG) response to red flash. D, Averaged ERG response to 50 blue flashes. E, Averaged oscillatory potentials to 50 blue flashes. Calibrations: 50 μV; 100 milliseconds.

She still had a best-corrected visual acuity of 20/20 OU. Although an ophthalmoscopy consistently showed no alterations in the right eye, a previously unknown uveal nevus was detected in the macular area of the left eye. Computerized perimetry (Octopus) revealed a marked visual field constriction and a general depression of light sensitivity in the right eye. The left eye exhibited no perimetric alterations (**Figure 1**).

Full-field electroretinograms (ERGs) were recorded with gold-foil electrodes in both eyes after maximal pupil dilatation and a 30-minute period of dark adaptation. A stroboscopic lamp placed behind the patient provided flashing lights on a Ganzfeld screen. Scotopic, maximal, and photopic responses were recorded according to the International Society for Clinical Electrophysiology of Vision recommendations. The single-flash, rod-dominant ERG showed a markedly decreased scotopic response in the right eye, whereas maximal-intensity stimulation elicited a typical ERG that showed no abnormalities, a selective b-wave depression with a preserved a wave (**Figure 2**). Both the scotopic rod-isolated response and the maximal response in the left eye were in the normal range. Fifty individual ERG and oscillatory potential responses to blue light flashes were averaged. The averaged ERG and oscillatory potentials were greatly impaired in the right eye but normal in the left eye.

In the immunocytochemistry test, the patient's serum displayed strong binding to retinal bipolar cells, similar to that of a known patient with MAR.

Five control electrophysiological examinations together with perimetry and ophthalmoscopy demonstrated no changes during the following 15-month observation period. Unfortunately, the patient developed agranulocytosis in July 2001 and died of pulmonary metastases and respiratory failure 1 month later. The family did not allow an autopsy.

Comment. In our case, the acute night blindness, sensations of shimmering lights, normal ERG results, and constricted visual field, together with the normal appearance of the retina and the preserved visual acuity, were diagnostic of MAR. The positive immunological reaction of the serum substantiated the diagnosis. The case is peculiar because the condition failed to spread to the other eye during an 18-month observation period. Until recently, all reported MAR cases were bilateral with some interocular latency difference in the appearance of symptoms.[3,4] Although cases with unilateral normal-appearing ERGs have been reported, no evidence of melanoma-related immune activity was found.[5] In our case, some damage to the other eye might have remained undetected by the electrophysiological tests, or the tragic outcome may have prevented a late manifestation of the disease in that eye. Nonetheless, the relatively long observation period raises the possibility that MAR manifests unilaterally in some patients.

Márta Janáky, MD, PhD
Andrea Pálffy, MD
Lajos Kolozsvári, MD, PhD
György Benedek, MD, PhD
Szeged, Hungary

This work was supported by ETT/Hungary grants 56411 and 57404.

We thank Ann Milam, PhD (University of Pennsylvania, Philadelphia), for performing the immunochemistry test.

Corresponding author and reprints: György Benedek, Department of Physiology, Faculty of Medicine, University of Szeged, H-6720 Szeged, POB 427, Hungary (e-mail: benedek@phys.szote.u-szeged.hu).

1. Berson EL, Lessell S. Paraneoplastic night blindness with malignant melanoma. *Am J Ophthalmol*. 1988;106:307-311.
2. Milam AH, Saari JC, Jacobson SG, et al. Autoantibodies against retinal bipolar cells in cutaneous melanoma-associated retinopathy. *Invest Ophthalmol Vis Sci*. 1993;34:91-100.
3. Kellner U, Bornfeld N, Foerster MH. Severe course of cutaneous melanoma associated paraneoplastic retinopathy. *Br J Ophthalmol*. 1995; 79:746-752.
4. Boeck K, Hofmann S, Klopfer M, et al. Melanoma-associated paraneoplastic retinopathy: case report and review of the literature. *Br J Dermatol*. 1997;137:457-460.
5. Fishman GA, Alexander KR, Milam AH, et al. Acquired unilateral night blindness associated with a negative electroretinogram waveform. *Ophthalmology*. 1996;103:96-104.

A Child With Venous Sinus Thrombosis With Initial Examination Findings of Pseudotumor Syndrome

A child with venous sinus thrombosis whose initial clinical findings

Magnetic resonance venous imaging demonstrates complete lack of flow through the right transverse venous sinus (short arrow) and sluggish flow through the left transverse sinus (long arrow).

were consistent with an isolated pseudotumor syndrome without any predisposing factors is described.

Report of a Case. A 6-year-old white girl was seen at the emergency department of a children's hospital with complaints of headaches for 3 weeks and diplopia for 2 days. Three weeks prior to examination, she had 2 episodes of emesis. Findings from systemic review were negative for fever, neck stiffness, ear pain, or upper respiratory symptoms. There was no history of tick bites, skin rashes, or recent travel. She lived in an urban community in Pennsylvania. The remainder of her medical history was unremarkable.

On examination she was afebrile with normal vital signs, alert, and cooperative. Visual acuity was 20/20 OU, and color plate test results from Ishihara plates was normal in each eye. Ocular motility revealed 10% bilateral abduction deficits. Anterior segment examination results were normal. Fundus examination findings revealed mild bilateral disc edema. The remainder of her general and neurologic examination was unremarkable; specifically, no other cranial nerve deficits were present.

Magnetic resonance imaging scans of the head were normal. Lumbar puncture disclosed an opening pressure of 450 cm H_2O. Cerebrospinal fluid composition showed a red blood cell count of 2 cells/μL; white blood cell count, 20 cells/μL (85% lymphocytes, 13% monocytes); and normal protein and glucose levels. An initial diagnosis of a pseudotumor syndrome was entertained. However, magnetic resonance venous imaging showed complete occlusion of right and partial occlusion of left transverse sinus (**Figure**) revealing the diagnosis of venous sinus thrombosis.

The following laboratory investigation findings were normal: complete blood cell count, coagulation profile, cardiolipin antibody, antinuclear antibody, rheumatoid factor, and homocysteine. Serum Lyme titers were positive for IgG and IgM at 4.1 mg/dL (<0.9 mg/dL, negative; >1.1 mg/dL, positive). Cerebrospinal fluid polymerase chain reaction and Western immunoblot were positive for *Borrelia burgdorferi*.

The child was treated with acetazolamide, low-molecular-weight heparin, and 3 weeks of intravenous ceftriaxone sodium. One month later, the headaches had resolved and the child had normal ocular motility and normal optic discs.

Comment. The incidence of venous sinus thrombosis is estimated to be 3 to 5 new cases per year at a single hospital.[1] The clinical findings at initial examination may be similar to pseudotumor cerebri.[1-3] In children, however, most cases of venous thrombosis have been associated with evidence of infection, otitis media, mastoiditis, systemic lupus erythematosus, use of oral contraceptives, or signs of dehydration.[4] Our case demonstrates that even in the absence of identifiable risk factors, venous sinus thrombosis may occur with only signs of increased intracranial pressure in children. The outcome is unpredictable with a 10% to 30% mortality rate; however, anticoagulation may improve neurologic outcome and reduce mortality in select cases.[1]

Our patient had positive results on Lyme serologic analysis. Lyme disease as a possible cause of venous sinus thrombosis has not been previously reported to our knowledge. Our case suggests that there may be an association between neuroborreliosis and venous sinus thrombosis.

In conclusion, our case illustrates the necessity of performing magnetic resonance venous imaging in the presence of normal findings on magnetic resonance imaging and emphasizes the importance of excluding venous sinus thrombosis as a cause of a pseudotumor syndrome in children.

Irfan Ansari, MD
Brian Crichlow, MD
Kammi B. Gunton, MD
Gary R. Diamond, MD
Joseph Melvin, MD
Philadelphia, Pa

Corresponding author and reprints: Kammi B. Gunton, MD, Department of Ophthalmology, St Christopher's Hospital for Children, Erie Avenue at Front Street, Philadelphia, PA 19134-1095.

1. Broderick JP. Cerebral venous thrombosis. MedLink Web site, Neurology section. 2nd 2001 ed. Available at: http://www.medlink.com. Accessed January 31, 2002.
2. Lam BL, Schatz NJ, Glaser JS, Bowen BC. Pseudotumor cerebri from cranial venous obstruction. *Ophthalmology*. 1992;99:706-712.
3. Biousse V, Ameri A, Bousser M-G. Isolated intracranial hypertension as the only sign of cerebral venous thrombosis. *Neurology*. 1999;53:1537-1542.
4. Lessell S. Pediatric pseudotumor cerebri (idiopathic intracranial hypertension). *Surv Ophthalmol*. 1992;37:155-166.

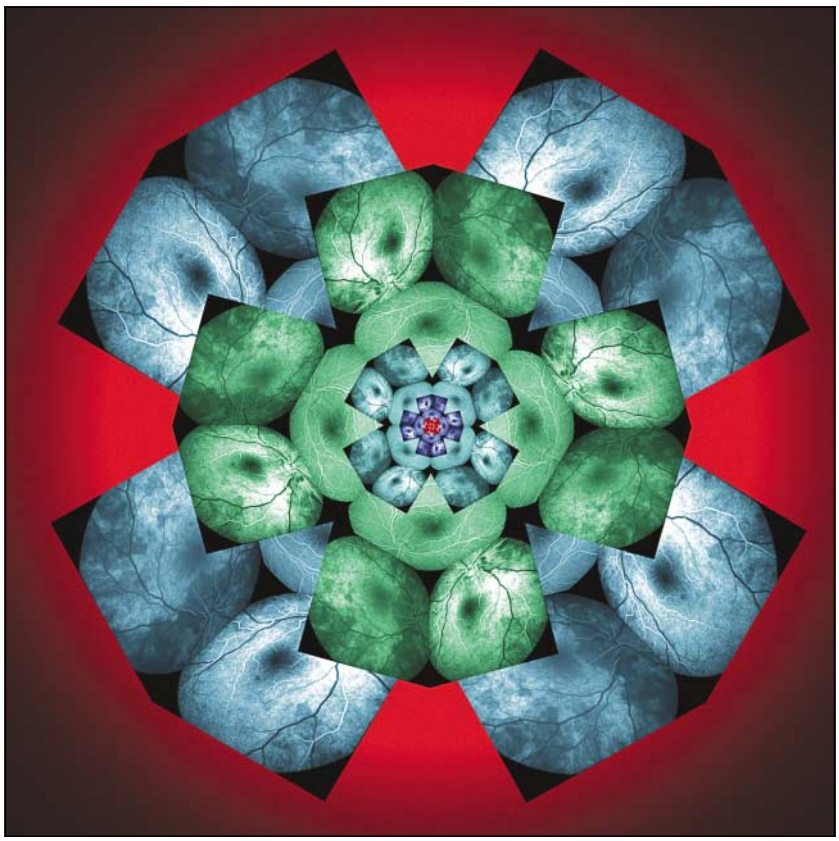

Unfolding Fundus. Created by Patrick J. Saine, MEd, CRA, Dartmouth-Hitchcock Medical Center, Lebanon, NH.